MICROALGAE BIOMASS CULTIVATION FOR PRODUCTION AND QUALITY TESTING OF BIODIESEL

Ph.D. Thesis

By

DESHMUKH SUCHIT ASHOKRAO

DISCIPLINE OF MECHANICAL ENGINEERING

INDIAN INSTITUTE OF TECHNOLOGY INDORE

MAY 2022

MICROALGAE BIOMASS CULTIVATION FOR PRODUCTION AND QUALITY TESTING OF BIODIESEL

A THESIS

Submitted in partial fulfillment of the
requirements for the award of the degree
of
DOCTOR OF PHILOSOPHY

by
DESHMUKH SUCHIT ASHOKRAO

DISCIPLINE OF MECHANICAL ENGINEERING
INDIAN INSTITUTE OF TECHNOLOGY INDORE
MAY 2022

INDIAN INSTITUTE OF TECHNOLOGY INDORE

I hereby certify that the work which is being presented in the thesis entitled **MICROALGAE BIOMASS CULTIVATION FOR PRODUCTION AND QUALITY TESTING OF BIODIESEL** in the partial fulfillment of the requirements for the award of the degree of **DOCTOR OF PHILOSOPHY** and submitted in the **DEPARTMENT OF MECHANICAL ENGINEERING, Indian Institute of Technology Indore**, is an authentic record of my own work carried out during the time period from July 2015 to May 2022 under the supervision of Dr. Ritunesh Kumar, Professor, Department of Mechanical Engineering, IIT Indore and Dr. Kiran Bala, Associate Professor, Department of Biosciences and Biomedical Engineering, IIT Indore.

The matter presented in this thesis has not been submitted by me for the award of any other degree of this or any other institute.

22-12-23

(DESHMUKH SUCHIT ASHOKRAO)

This is to certify that the above statement made by the candidate is correct to the best of our knowledge.

Ritunesh Kumar 22/12/2023

Signature of Thesis Supervisor #1 with date

(Dr. RITUNESH KUMAR)

22/12/23

Signature of Thesis Supervisor #2 with date

(Dr. KIRAN BALA)

DESHMUKH SUCHIT ASHOKRAO has successfully given his Ph.D. Oral Examination held on **20/12/2023**.

Ritunesh Kumar 22/12/2023

Signature of Thesis Supervisor #1 with date

(Dr. RITUNESH KUMAR)

22/12/23

Signature of Thesis Supervisor #2 with date

(Dr. KIRAN BALA)

ACKNOWLEDGEMENTS

First and foremost, I would like to thank God for his blessings.

I would like to express my sincere gratitude to my supervisors, Dr. Ritunesh Kumar and Dr. Kiran Bala, for providing me the opportunity to work under their invaluable guidance and helping me during every stage of my thesis work. I also thank them for being patient with me and encouraging me to complete the work.

I am immensely thankful to my PSPC committee members, Dr. Devendra Deshmukh and Dr. Shaikh Mobin, for their timely suggestions to improve the quality of my work. I would also like to thank faculty members of Mechanical Engineering department, central workshop staff, and SIC facility staff for providing me with the facilities to carry out the research work. I am grateful to the administrative department personnel who have helped me during this research. I am thankful to ministry of education, Govt. of India, for providing me fellowship to pursue my studies. I am indebted to lab managers Mr. Ashwin Wagh and Mr. Mahesh Jhade for their cooperation and for maintaining discipline in the lab. I am truly thankful to my lab mates Dr. Sambhaji Kadam, Dr. Digvijay Patil, Dr. Vikas Yadav, Dr. Gurjeet Singh, Dr. Rehan Khan, and junior research fellows for their support and making this journey joyful. I would also like to thank colleagues from Dr. Kiran's lab for helping me understand the biotechnology aspect of my research and colleagues from Dr. Deshmukh's lab Dr. Vasudev, Devashish and Vishal. I will not forget the time spent with my fellow researchers, Dr. Anirudh, Dr. Vijay Babu, Dr. Debashish and Dr. Ajinkya.

Finally, I would like to thank my wife, Namrata, for being there with me through thick and thin times and encouraging me to move forward. I would like to thank my parents, Mr. Ashokrao Deshmukh and Mrs. Vandana Deshmukh, for all their love and support throughout my life.

Suchit Deshmukh

Dedicated to my family and friends

LIST OF PUBLICATIONS

Publications from PhD thesis work

In referred journals:

1. S. Deshmukh, R. Kumar, K. Bala, Microalgae biodiesel : A review on oil extraction, fatty acid composition, properties and effect on engine performance and emissions, Fuel Process. Technol. 191 (2019) 232–247. https://doi.org/10.1016/j.fuproc.2019.03.013 (Impact Factor **4.507)**.
2. S. Deshmukh, K. Bala, R. Kumar, Selection of microalgae species based on their lipid content, fatty acid profile and apparent fuel properties for biodiesel production, Environ. Sci. Pollut. Res. (2019) 1–12. https://doi.org/10.1007/s11356-019-05692-z (Impact Factor **2.80**).
3. S. Deshmukh, R. Kumar, K. Bala, R. Chandra, Comparison and testing of cerium oxide nanoparticle added Pongamia and Scenedesmus microalgae biodiesel blends, Chem. Eng. Res. Des. (Accepted 2023). (Impact Factor **3.9**).
4. S. Deshmukh, R. Kumar, K. Bala, Inspecting the impact of Scenedesmus sp. biodiesel blends on performance, combustion, and emission attributes of diesel engine, Biotechnol. Genet. Eng. Rev. (Accepted 2023). (Impact Factor **3.2**).

Manuscript ready to be submitted:

- Effect of microalgae and Pongamia biodiesel mix-fuel blend on performance and emission characteristics of a diesel engine.
- Comparison of ethanol and nanoparticles as additives to biodiesel-diesel blend for performance improvement and emission reduction.

Other publications during PhD

Book chapter

- Rehan Khan, Suchit Deshmukh, Ritunesh Kumar. Energy Needs for Sustainable Buildings and Transportation. Sustainability: Fundamentals and Applications. Wiley Online Library, ISBN:9781119434016, DOI:10.1002/9781119434016

ABSTRACT

The global warming and climate change challenge has forced us to reassess the current energy generation and utilization methods. Fossil fuels still fulfill more than 80% of the global annual energy need. The urgency to move towards environmental friendly renewable sources of energy is now more than ever, considering the rapidly rising pollution level and leaping energy demand. Biodiesel has been assessed and recommended as one such alternative fuel for diesel engines. It has an additional benefit of production from locally available resources. Microalgae have been identified as a source of biodiesel that can efficiently fulfill the future transport energy demand of the human population.

In the current research work, microalgae biodiesel has been explored as an alternate fuel for an indirect injection compression ignition engine. Initially, six microalgae strains were isolated using wastewater from the Kabitkhedi sewage treatment plant, Indore, India. The selection of microalgae strains for further study is finalized by analyzing their lipid composition and estimating their thermo-physical properties. Relevant thermo-physical properties (related to fuel spray and combustion modeling) are even calculated for extended temperature ranges, justifying the exposure of liquid fuel to the adverse atmospheric conditions to which the fuel is exposed. *Scenedesmus* sp. is found to be the best among six different microalgae strains. It is selected for outdoor cultivation in raceway ponds with ordinary tap water and urea-DAP as nutrient media. An adequate daily growth rate of microalgae was observed under sufficient light conditions. Despite the high growth rate, around 3.07 kg/month of dried biomass and 14.2% of oil could be obtained only due to simple gravity sedimentation for harvesting and soxhlet for oil extraction. This clearly shows that the technologies for harvesting, and oil extraction need to be scaled to the industrial level for increased, cost-effective production. The *Scenedesmus* sp. biodiesel is analyzed for its fatty acid composition and predicted properties. Even though it had high poly-

unsaturated fatty acid content (mostly linolenic acid) at 29.75%, the saturated fatty acid content is also 38.43%, limiting its thermo-physical properties within the range proposed by international standards. To study the viability of using microalgae biodiesel in a diesel engine, prepared biodiesel's 20% (A20) and 30% (A30) blends were studied in a four-stroke, four-cylinder IDI diesel engine. The slightly poor thermal performance of the engine was found: 3.1% and 6.3% lower brake thermal efficiency (BTE) than diesel for A20 and A30, respectively. However, a tremendous reduction in emissions was provided by microalgae biodiesel blends compared to pure diesel. The NOx emissions were lowered by 13.1% and 10.7%, whereas smoke emissions were reduced by 36.7% and 58.9% for A20 and A30 blends, respectively. Subsequently, the nanoparticle (cerium oxide) addition to the biodiesel blend has been explored to improve the engine's performance (100 ppm concentration in A30 blend). For comparison with contemporary options, 30% Pongamia biodiesel blend was also used in the study. The application of nanoparticles as a fuel additive improved the BTE (average increase of 4.2%) for A30, but it increased NOx emissions. It was also observed that the cost and stability of the nanoparticle-added blend need to be addressed further. Finally, a mix-fuel blend with an equal amount of *Scenedesmus* and Pongamia biodiesel has also been tested. A slight improvement in the engine's performance without any corresponding deterioration in emissions parameters has been observed compared to the A20 and P20 blends. Overall, *Scenedesmus* sp. biodiesel can be satisfactorily used as an alternative fuel to diesel with some advances in biodiesel production steps.

TABLE OF CONTENTS

LIST OF FIGURES

LIST OF TABLES

NOMENCLATURE

D	number of double bonds
D_{AB}	diffusion coefficient (cm^2/s)
DU_m	modified degree of unsaturation
G_{ij}	interaction parameter between component i and j
M	molecular weight (g)
N	percentage of FAME present in biodiesel (%)
P	pressure (bar)
T	temperature (K)
V	volume (cm^3/mol)
y	mole fractions of methyl esters
Z_{RA}	constant to calculate liquid density
ΔHv	latent heat of vaporization (J/mol)

Abbreviations

A10P10	10% *Scenedesmus* sp. biodiesel + 10% Pongamia biodiesel + 80% diesel
A20	20% *Scenedesmus* sp. biodiesel + 80% diesel
A30	30% *Scenedesmus* sp. biodiesel + 70% diesel
A30C100	100 ppm CeO_2 nanoparticles in A30
BTE	brake thermal efficiency
BSFC	brake-specific fuel consumption
CFPP	cold filter plugging point (°C)
CO	carbon monoxide
CR	compression ratio
EGT	exhaust gas temperature
FA	fatty acid
FAME	fatty acid methyl ester
FFA	free fatty acid
GC	gas chromatography
HC	hydrocarbon
HHV	higher heating value (MJ/kg)
HRR	heat release rate
IDI	indirect injection
IV	iodine value (g/100g)

LCSF	long chain saturation factor
LHV	latent heat of vaporization
MCDA	multi-criteria decision aid
MUFA	monounsaturated fatty acid
NOx	oxides of nitrogen
OS	oxidation stability (h)
P20	20% Pongamia biodiesel + 80% diesel
P30	30% Pongamia biodiesel + 70% diesel
P30C100	100 ppm CeO_2 nanoparticles in P30
PUFA	polyunsaturated fatty acid
SCSF	straight chain saturation factors
SFA	saturated fatty acid
TAG	triacylglycerol
TDC	top dead center

Greek symbols

ν	kinematic viscosity (mm^2/s)
ρ	density (kg/L)
ω	accentric factor
η	dynamic viscosity (cP)

Subscript

b	property at boiling point
c	critical property
L	liquid property
m	property of a mixture (biodiesel)
r	reduced property
s	specific property

1 INTRODUCTION

1.1 Background

The global demand for fuel is increasing at an accelerated pace due to rapid economic growth and improved living standard expectancy worldwide. An increasing global population made the situation even more adverse. More than 80 percent of global primary energy consumption is still supplied through fossil fuels [1]. The global oil demand will rise to 103.5 million barrels per day (MB/day) in 2040 from 90.6 MB/day in 2014, out of which around 55% was used for the transport sector alone [1]. As of 2020, oil consumption in India was up to 5 mb/day [1]. On the other hand, the crude oil production in India is only 0.9 MB/day, which indicates the country's dependence on oil imports. Crude oil is a readily available fuel. There are well-established facilities for its extraction and processing. However, there is a rising concern about its non-renewable nature, environmental and health problems due to the harmful emissions and ultimate impact on global climate change. Therefore, limiting the consumption of fossil fuels (coal, natural gas, and oil) has been an obligatory aim of the 21st century. The alternative sources to fossil fuels should be sustainable, renewable, readily available, environment friendly, and affordable.

Electric vehicles are currently projected as the future of the urban transport sector. However, Apart from several daunting technological issues, the persistent question about electric vehicle reality as green transport as advertised remains. Anyhow, it may take a long time to assess the impact of electric vehicles on the environment. Biodiesel is another potential alternative fuel that has the ability to replace conventional fossil diesel [2,3]. It is chemically a monoalkyl ester of long-chain fatty acids obtained from edible and non-edible oils as well

as animal fats. It is an alternative fuel to diesel owing to similar thermo-physical properties. It is a clean, renewable fuel with less carbon monoxide, unburned hydrocarbon, net carbon dioxide, and sulfur emissions. It is not entirely new technology, as Rudolf Diesel himself tested his engine with vegetable oil. However, cheap and readily available petroleum products became favorable, and the use of vegetable oil as a fuel remained just an idea. As the oil from plant or animal sources has a high viscosity compared to diesel fuel, a reaction called transesterification is used to convert oil into biodiesel. It is a reaction of triglyceride (oil) with methanol in the presence of a catalyst (acid or base), which gives biodiesel with glycerol as a byproduct. The use of acid (H_2SO_4) or base (NaOH) catalysts mostly depends on the content of free fatty acids (FFAs) in the oil or animal fat. The reaction is carried out at around 60°C with continuous stirring. The conversion efficiency of oil to biodiesel is fairly high when the reaction is properly optimized for various parameters, namely the ratio of alcohol to oil, the catalyst used, time, temperature, and mixing intensity [4]. Even though the production of biodiesel is a fairly simple process, the source of oil for biodiesel is key in making the fuel viable as an alternative to diesel.

Table 1.1 presents the potential yield of different sources of biodiesel. The biodiesel source should not only provide biodiesel in abundance so that the growing need for energy is satisfied but also, the quality of the produced biodiesel should be in accordance with established fuel standards like ASTM D675 or EN14214. Initial biodiesel sources are called first-generation sources of biodiesel. They are mainly edible oil plants like soybean, sunflower, etc. Since they pose a problem of food vs. fuel security, it was later decided to switch to second-generation biodiesel sources like Jatropha, *Pongamia pinnata*, etc. They have the advantage that they are non-edible oil sources and can grow on wasteland; therefore, they do not compete with food crops. They also produce biodiesel with a good mix of saturated and unsaturated fatty acids, making them favorable for most of the properties. However, researchers have reported that second-generation biodiesel sources do

not have the potential to satisfy the demand–supply equation of diesel vehicles.

Table 1.1 Estimated oil yield from different feedstocks

Feedstocks	Oil content (%)	Oil yield ((L/ha/year)
1st generation [5]		
Sunflower	25-35	952
Soybean	15-20	446
Palm	30-60	5950
2nd generation [6]		
Jatropha	35-40	1892
Pongamia	30-40	1818
Rubber seed	40-50	4648
3rd generation [7]		
Microalgae	30 (on the lower side)	58700

Microalgae biodiesel has been identified as the third-generation source that can cater to the ever-increasing demand for transportation fuel [8]. Their photosynthetic efficiency is very high [9], and they can absorb atmospheric CO_2, thus have the added advantage of CO_2 fixation. They have also been explored for their growth in domestic wastewater by absorbing nutrients, thus possibly facilitating even wastewater treatment [10]. Also, they have been tested for their ability to remove heavy metals from various sources [11–13]. Microalgae can produce 19000 to 57000 liters of oil/acre in one year, better than any previous biodiesel source [9]. It is converted into biodiesel through a standard transesterification process. The remaining biomass also contains valuable components, such as residual lipids, proteins, and soluble polysaccharides, that can be used for the production of other biofuels like bio-oil [14,15] bioethanol [16], biohydrogen [17,18], and biogas [19,20] through various thermochemical and biochemical processes; thus improving the overall energy balance [21]. Microalgae also contain important pigments useful for the health and cosmetic industries [22].

In view of this, exploring microalgae as a source of biodiesel and evaluating it in a diesel engine becomes extremely important considering future transportation energy needs.

1.2 Motivation

In light of the persistent environmental challenges posed by fossil fuels, there is a growing imperative to identify sustainable and environmental friendly alternative fuels. Biodiesel, with properties closely resembling conventional diesel, holds promise in this regard. Microalgae, due to their rapid growth, ability to thrive without arable land, CO_2 sequestration potential, co-extraction of valuable compounds and waste water remediation, present an attractive source of biodiesel.

However, the literature predominantly concentrates on microalgae biotechnology at a laboratory scale, with limited attention given to the practical aspects of outdoor cultivation, large-scale biodiesel production, and their application in internal combustion (IC) engines. Moreover, microalgae biodiesel properties crucially depend on the fatty acid methyl ester (FAME) composition, which varies among species and cultivation conditions. This necessitates a deeper understanding of locally available microalgae species and their FAME profiles for optimal large-scale biodiesel production.

Furthermore, there is a notable absence of comprehensive studies on the performance and emissions of diesel engines fueled by microalgae biodiesel, compared to both conventional diesel and second-generation biodiesel. The potential of fuel additives to enhance the performance and emission characteristics of microalgae biodiesel in IC engines remains an unexplored territory. Addressing these gaps is essential for advancing the practical viability and sustainability of microalgae biodiesel as an alternative to fossil fuels.

1.3 Organization of the thesis

In the current chapter, the general introduction and motivation behind the research work are presented. In chapter two, the review of literature

on microalgae oil extraction, biodiesel composition, and properties and a summary of previous works related to engine performance evaluation using microalgae are reported. The screening study for microalgae species selection is presented in chapter three. The screening study compares six locally isolated microalgae species based on their lipid composition and estimated thermophysical properties. The large-scale cultivation of microalgae *Scenedesmus* sp. in raceway ponds is presented in chapter four. The chapter also discusses the oil extraction and biodiesel production from *Scenedesmus* sp. biomass. Chapter five discusses the performance and emission characteristics of the diesel engine using *Scenedesmus* sp. biodiesel. The further improvement in engine output characteristics by adding nanoparticles to biodiesel and mixing two different biodiesels is presented in chapters six and chapter seven. Finally, the future scope of the work which can be carried out is discussed.

2 LITERATURE REVIEW

Microalgae have various advantages over the first and second-generation sources of biodiesel. However, the intricate and costly biodiesel production processes are a concerning issue when it comes to the commercialization of microalgae biodiesel. Figure 2.1 shows the main stages of biodiesel production through microalgae. Microalgae can be cultivated in open raceway ponds or in photobioreactors, both having their respective advantages and disadvantages. Open pond, as the name suggests, is open to natural light, and it is simple in design, low cost, and the most widely used method. Contamination by other species, microorganisms, and dust is the main concern that makes cultivation difficult. Other disadvantages include variations in light availability and temperature [23]. Pure culture cultivation can be achieved by the use of photobioreactors in a controlled environment of light and temperature. However, the high cost involved in system design and operation currently limits their use for large-scale production. After the cultivation stage, microalgae biomass is harvested. The selection of a proper harvesting method is of great importance in biodiesel production as it accounts for 20-30% of the total cost involved [24]. Methods used for harvesting are centrifugation, gravity sedimentation, filtration, flocculation, etc. Gravity sedimentation is the most suitable method for the economical harvesting of biomass. After harvesting, biomass is dried and made ready for oil extraction. Sun-drying can be a preferred method for large-scale purposes. The next stage is oil extraction, which needs special attention due to its complex and energy-intensive nature. Each microalgae cell contains different components; specific extraction techniques are employed to extract components of interest. The use of an appropriate extraction method has significance in the overall

scalability of microalgal biodiesel production [25]. Finally, a conventional transesterification process carries out the conversion of extracted lipid/oil into biodiesel. The next two sections describe the composition and productivity of lipids from different microalgae species.

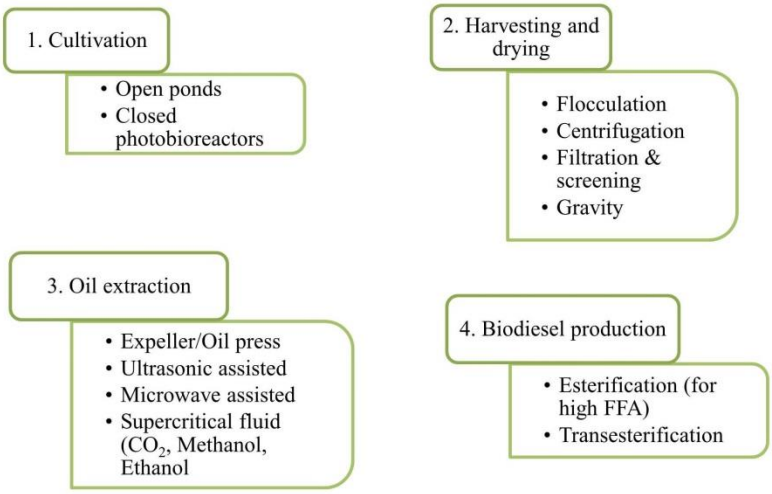

Figure 2.1 Microalgae Biodiesel production process

2.1 Lipids in microalgae cells

Each microalgae cell contains a complex mixture of different constituents like lipids, carbohydrates, proteins, pigments, and other cell components. Out of the above, lipid or oil content is the significant prerequisite in determining the aptness of microalgae for commercial biofuel production. Microalgae cells generally contain 30-80 % lipids [8]. Lipids are, in general, soluble in nonpolar (organic) solvents but insoluble in polar solvents due to the presence of a hydrophobic chain. Therefore, they are easily extractable using the organic solvent extraction method. They are further categorized as neutral (mono-, di-, triacylglycerols, and sterols) and polar types (phospholipids and glycolipids) [26]. The main function of the neutral lipid is energy storage, whereas polar lipids form structural components of the cell membrane [25]. Triacylglycerols (TAGs) are the most common neutral lipids found in cell cytoplasm as tiny droplets. They are formed when three same or different fatty acid molecules get attached to the

glycerol. In contrast, polar lipids are formed when fatty acid molecules get attached to the charged head group [25]. It is the neutral lipids that can be converted to biodiesel. Fatty acids of the lipids are represented as C, followed by two numeric numbers: the first is for the total number of carbon atoms, and the second is for the total number of double bonds. The absence and presence of double bonds categorize them as saturated fatty acids (SFA) and unsaturated fatty acids (UFA). UFAs are further classified as monounsaturated fatty acids (MUFA) and polyunsaturated fatty acids (PUFA).

Microalgae undergo biochemical changes during the different stages of growth, i.e., from the lag phase to the late stationary phase. The accumulation of neutral lipids during the growth is desirable for the production of biodiesel as compared to glycol - or phospholipids. The effect of the growth phase on lipid content and composition has been explored by researchers (presented in Table 2.1). Usually, lipid content in the cell is more in the late stationary phase than in the logarithmic phase (except for a few species, such as *Tetraselmis* sp., where lipid content in the logarithmic phase was higher). The increased lipid content in the stationary phase is at the expense of cell division. Additionally, the fatty acid composition also changes considerably during various growth phases. The higher amount of SFAs (C16:0) and MUFAs (C16:1 and C18:1) were obtained in the late stationary growth phase with simultaneous lowering down of PUFA (C18:3, C18:4, and C20:5).

2.2 Lipid productivity

The biodiesel production capacity of the microalgae species is anticipated by measuring lipid/oil productivity, a term inclusive of lipid content and biomass production rate. This is because species with high lipid content can have lower growth rates, resulting in lower biodiesel yield. Therefore, lipid productivity is considered the actual measure of the biodiesel production capacity of the species. The methods that are used to increase the lipid content in the species may not increase the overall lipid productivity because of the decrease in

biomass production rate at the same time. For example, Nitrogen limitation is used to increase the lipid content. The US aquatic species program, however, demonstrated that nitrogen limitation also decreases growth rates in the species [27]. At nitrogen starvation conditions, the cell growth stops after complete consumption of nitrogen, but it also leads to photosynthesis energy being utilized for lipid synthesis pathways. So, the lipid content increases at the starvation condition. Pruvost et al. [28] found that the neutral lipids compositions were higher for nutrient deficit conditions because of TAG accumulation, even though the cell division rate ceased. However, Griffiths et al. [29] claimed that nitrogen deficit condition has a positive influence on lipid productivity. Only for one species, Spirulina, they observed the opposite trend. The enhancement in lipid content in their study under nitrogen-limited conditions was comparatively higher than the decrease in biomass production rate. Similar trends in lipid productivity had been observed in the context of temperature by Converti et al. [30]. The decrease in temperature resulted in higher lipid productivity in the case of *C. vulgaris,* but *N. oculata* showed a decrease in lipid productivity. In both cases, lipid content increased with a decrease in temperature. At very low temperatures, the decrease in biomass concentration can be accredited to the poor metabolic activities of the cell. Similarly, lipid content in the microalgae cell has been found to increase with the increase in light intensity and salinity of growth media, but overall lipid productivity reduces due to a decrease in biomass production rate [31,32]. The increase in salinity leads to oxidative stress, causing an increment in the TAG content. Overall, unfavorable conditions for cell division stimulate neutral lipid accumulation. A balance of growth conditions is necessary such that the increase in lipid content by stress conditions should not be rendered ineffective by the decrease in biomass.

Table 2.2 summarizes the studies carried out in the past that compare different microalgae classes based on their lipid productivities. Chlorophytes (Chlorophyceae, Trebouxiophyceae, and

Chlorodendrophyceae) showed higher lipid productivity. *Nannochloropsis* sp. (class Eustigmatophyceae) was also found to have good lipid productivity. The table also shows that outdoor cultivation with tap water and NPK fertilizers has lower lipid productivity values. Lipid productivity, although an important characteristic, is not the single factor determining the suitability of microalgae for large-scale biodiesel production. Other factors such as minimum nutrient requirements, ability to withstand varying temperature and light conditions, easy and less energy-consuming downstream processes, etc., are also vital.

Table 2.1 Effect of growth phase on lipid content and fatty acid composition

Species	***Isochrysis galbana*** [33]			***Pavlova lutheri*** [34]			***Gymnodinium* sp.** [35]			***Nannochloropsis* sp.** [36]			***Tetraselmis* sp.** [36]			***Rhodomonas* sp.** [36]		
Cultivation condition	Seawater+nitrate, in incubator at 18 ± 1 °C, 115 μmol m^{-2} s^{-1}, 12:12 h light–dark cycle, bubbled with air 10 l/min			f/2 media with sea water, 22 ± 2 °C, 100 μmol m^{-2} s^{-1}, 12:12 h light–dark cycle aerated with 20 mL/min,			GSe medium, 18.5 °C, 80 μmol m^{-2} s^{-1}, 12:12 h light–dark cycle, initial cell density was 345 cell/ml			L1 medium, 24 °C, 43 μmol m^{-2} s^{-1}, 12:12 h light–dark cycle,								
Phase/days	L	ES	LS	9	23	40	8	22	43	L	ES	LS	L	ES	LS	L	ES	LS
Lipids (% of dry weight)	21.8	34.0	38.4				18.3	29.6	22.6	21.3	31.3	32.7	10.6	8.7	10.1	9.5	13.0	12.5
Neutral lipids (% of total lipids)	27-30		54-61		28	35												
Phospholipids (% of total lipids)	31-39		10-12	88	57	50												
C14:0	19.2	14.4	10.2	8.8	8.1	7.9	0.9	1.0	1.4	4.5	5.1	5.0	0.6	0.6	0.6	4.7	9.5	7.8
C15:0	0.26	0.27	0.32				0.5	0.5	0.6	0.3	0.4	0.5						
C16:0	14.9	12.5	18.6	17.3	22.8	23.4	20.5	23.4	26.7	25.3	30.8	37.5	27.8	31.7	32.8	11.2	21.3	19.7
C16:1	20.5	19.4	24.5	14.5	21.1	23.2				23.4	21.3	23.3				3.6	1.9	1.5
C18:0	0.52	0.42	0.67	0.3	0.3	0.3				0.9	0.8	0.9	0.9	1.0	1.1	0.7	2.4	3
C18:1	3.54	3.09	6.25	3	4.2	4.6	1.7	3.4	3.6	5.2	7.8	11.9	28.2	41.3	44	7	8	8.4
C18:2	2	0.68	1.23	0.6	0.5	0.8	4.5	5.1	6	2.2	2.2	1.5	9.3	7.5	6.8	0.7	2.5	3.3
C18:3	1.91	1.56	1.09	2.6	0.7	0.8							23.9	12.3	8.4	20.3	29.8	29.8
C18:4	12.5	15.1	8.68	10.9	6.2	4.9	3.1	3.8	1.8				3.7	1.8	1.3	33.1	12.8	11.7
C18:5							20.5	15.5	12.4									
C20:5	14.6	19.0	16.1	27.6	17.7	17	11.4	9.9	8	30.8	26.1	15.3	3.4	2	1.5	11.1	6.8	8.6
C22:6	5,64	7.85	8.26	7.9	11.2	9.2	28.4	27.8	31.3							4.1	2.1	3
SFA	35.2	28.8	30.7	26.7	31.5	31.9	23.7	26.7	30	31.9	37.7	44.8	29.3	33.3	34.8	17	34.1	31.5
MUFA	24.0	22.5	30.8	17.5	25.3	27.8	1.7	3.4	3.6	28.6	29.1	35.2	29.4	42.5	46.6	10.6	9.8	9.9
PUFA	40.7	48.6	38.4	54	40.4	36.8	69.8	63.8	62.1	39.4	33.4	20.1	41.2	24.3	18.6	72.4	56.1	58.6

Table 2.2 Comparison of lipid productivities of different microalgae species

Growth conditions	Species	Class	Lipid productivity * (mg/L/day)	Reference
Airlift photo bioreactors 3.2 L, freshwater species -3 N BBM medium, marine species f/2 or Walne's, halophilic species Zarrouk's medium, 25±1°C, 250 µmol photons /m^2/s, aerated 0.29 % CO_2 at 2 L min−1.	*Scenedesmus* (L)	Chlorophyceae	106	[29]
	Chlorella vulgaris (L)	Chlorophyceae**	67	
	Nannochloropsis (L)	Eustigmatophyceae	63	
	Cylindrotheca fusiformis (H)	Bacillariophyceae	55	
10 L, L1 medium. 24 °C, L/D photoperiod of 12:12 h 250 µmol photons/m^2/s.	*Tetraselmis* sp.	Chlorodendrophyceae	22.7	[36]
	Isochrysis sp.	Prymnesiophyceae	21.1	
	Nannochloropsis sp.	Eustigmatophyceae	20	
16 L tap water, soluble NPK (19:19:19) fertilizer, 31-33 °C, 130-464 µmol /m^2/s, aerated with 1 HP compressed air pump.	*C. variabilis* BTA4121	Trebouxiophyceae	1.98	[37]
	Chlorella variabilis BTA4036	Trebouxiophyceae	1.89	
	Chlorella sp. BTA4032	Trebouxiophyceae	1.34	
5 L of culture medium Conway (C), Zarrouk and WC , 25 °C, L/D photoperiod of 12:12 h, 4.5 ± 0.3 kLux, agitation provided by the continuous bubbling of air (2.0 mL/min).	*Chlorella* sp. (D101Z)	Chlorophyceae	190.1	[38]
	S. nidulans (D109WC)	Cyanophyceae	93.8	
	Chlamydomonas sp. (D132WC)	Chlorophyceae	83.4	
250 mL flasks, bubbled with a sterile air/CO_2 mixture (95/5, v/v), 25 °C, 100 µmol PAR photons/m^2/s.	*Nannochloropsis* sp. F&M-M26	Eustigmatophyceae	61	[39]
	Nannochloropsis sp. F&M-M28	Eustigmatophyceae	60.9	
	Chlorococcum sp. UMACC 112	Chlorophyceae	53.9	
	Scenedesmus sp. DM	Chlorophyceae	53.7	

* Top 3 or 4 species have been presented from each study; ** some studies consider *Chlorella vulgaris* in class Trebouxiophycea

2.3 Oil extraction

Lipids or oils from microalgae cells are extracted following harvesting and drying of biomass. The conventional mechanical press method, which is used extensively for oil extraction from edible and nonedible crop seeds, is not suitable for microalgae. As microalgae cells are very small and their cell walls are very strong, cells do not disrupt through simple squeezing operations inside the conventional mechanical press. Therefore, organic solvents extract lipids from microalgae cells based on the simple chemistry principle “like dissolves like” [40]. Organic solvent extraction is basically a mass transfer process in which lipid molecules diffuse across cell walls into organic solvent [41]. Lipid extraction through the soxhlet extraction method has been used extensively in the past from different types of biomass. Generally, non-polar solvents such as hexane and ethyl ether are used for such purposes. However, as the membrane-associated polar lipids form strong hydrogen bonds with protein molecules to make the cell membrane rigid, non-polar solvents cannot enter the cell easily, which is responsible for the poor efficiency of that method. Hence, an organic co-solvents system (a blend of polar-nonpolar solvents) can be applied for the extraction of lipids from microalgae cells. Bligh and Dyer [42] (chloroform/methanol, 1:2) and Folch et al. [43] (chloroform/methanol, 2:1) are popular methods of co-solvent combination.

Along with the co-solvent, if the lipid extraction process is preceded by a suitable cell disruption method, then extraction efficiency improves further. Cell disruption helps to easily extract lipids from the rigid cell wall surrounding the cellular material. Recently, modern techniques such as ultrasound, microwave, and supercritical fluids have been explored to expedite the lipid extraction process with high extraction efficiency. In the ultrasonic-assisted method, ultrasonic waves are used to disrupt the cell wall and assist the oil extraction. It is a mechanical acoustic wave with very high energy. The high power of ultrasound helps break the strong, attractive force between the molecules and generates cavitation bubbles. These bubbles grow as time passes and

experience huge expansion before collapsing violently. The pressure and temperatures developed during the bubble collapse (at the micro-level) are very high (T ~ 5000 K and P ~ 1000 atm) [44]. These high-energy shock waves cause a dispersive effect on cell walls. It causes intracellular materials to come out in the solvent medium, which can easily get dissolved [45,46]. In the case of microwave-assisted extraction, polar solvents like water, methanol, etc., get heated when exposed to electromagnetic waves. The electric and magnetic fields induced because of these waves change their direction very rapidly. In trying to align with the field because of the dipole moment, the polar molecules cause friction with other oscillating molecules and thus cause localized heating. This high temperature developed at the molecular level increases dissolution efficiency, leading to an increased extraction rate [41,47]. It is a non-contact heat source, which has the benefit of heating the sample uniformly. Supercritical fluids had been used previously in the transesterification process for the production of biodiesel from oil [48]. The use of CO_2 as supercritical fluid for lipid extraction through microalgae is gaining widespread interest [49,50]. The polarity of the solvent reduces at supercritical conditions so that they can also act as a solvent for non-polar lipids [51]. Another advantage of this method is that separation of solvents is very easy and the final product obtained will be purer compared to traditional methods of oil extraction.

Lately, Ionic liquids have also become popular for oil extraction purposes. They are salt with a very low melting point (below 100 ^{0}C). In a liquid state, they contain only ions: cations and anions. They have extremely low vapor pressure and are non-volatile, highly polar, thermally stable, and chemically inert [52]. The ionic liquids, when used in the extraction process,–dissolve microalgal biomass, keeping lipid bodies suspended in the solution. The lower-density lipids floating on the ionic liquid solution can easily be separated. This method can be combined with the ultrasonic or microwave-assisted method of oil extraction. However, the high cost of the ionic liquid is a

big concern currently. Other recent methods of oil extraction include the use of bio-based solvents [53], switchable hydrophilicity solvents (SHS) [54] and the use of surfactant for lipid extraction [55]. These methods mainly cover certain aspects like sustainable extraction, easy solvent recovery, etc. When compared with one another, all these methods have their respective advantages and limitations depending on the process parameters, solvent and species used, and quantity of biomass.

2.4 Biodiesel conversion: conventional and direct transesterification

The extracted oil from microalgae has a decent energy value and can be used as fuel in boilers and other power-generating devices. However, it cannot be used as a transport fuel in diesel engines due to mediocre thermo-physical properties and high viscosity. The high viscosity creates difficulty in the atomization of the fuel and causes other serious issues such as engine deposits, piston rings sticking, etc. Therefore, the extracted oil is further converted into biodiesel through a chemical process called transesterification. In a transesterification reaction, one mole of triacylglycerol (TAG) molecule reacts with three moles of alcohol (generally methanol) in the presence of a catalyst to give three fatty acid alkyl esters molecule and glycerol as a by-product of the reaction (Figure 2.2). As the reaction is reversible, a minimum molar ratio of 1:6 (oil: alcohol) is maintained to have a forward reaction. The process has successfully converted oil from first and second-generation sources into biodiesel. The same can be used for extracted microalgae oil.

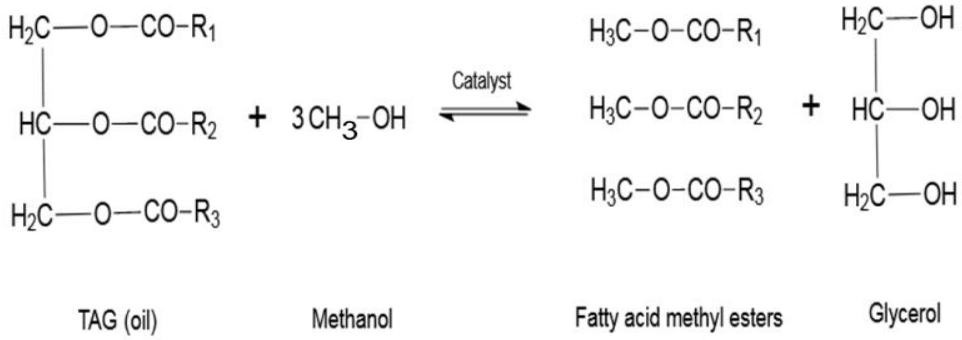

Figure 2.2 Transesterification reaction

The direct biodiesel conversion of microalgal biomass into biodiesel called as direct transesterification method has also been studied [56]. In this method; instead of extracting the oil first and then converting it into biodiesel, the microalgal biomass is subjected to solvent (alcohol) and suitable catalyst (acid or base) under the specific conditions to get it directly converted into biodiesel in a single step. The raw biomass used in this method can also be in a wet state. The drying step, in an algal biodiesel production process, consumes high energy and the net energy output of the process becomes negative [57]. The use of wet microalgae biomass for the transesterification process can help to conserve the energy spent during the drying step. This fact was well demonstrated by the life cycle analysis study [58] in which a colossal difference in overall energy balance was seen when dry and wet biomass was used as a raw material. However, wet biomass to biodiesel is not an easy step as the presence of water molecules around the cells hinders the interaction of catalyst and reactant with the lipid molecules as it does not allow them to easily penetrate through microalgae cell walls [57,59]. Water content more than a particular level can even inhibit the transesterification process completely [60]. Finding an optimum solvent to biomass ratio is also important for high biodiesel yield from wet/dry biomass transesterification. The solvent to biomass ratio can be minimized by the use of cell disruption methods like ultrasound and the use of co-solvent along with methanol [61]. The energy required for the recycling of solvents like hexane and methanol during the direct transesterification process is less than the

energy required for drying biomass [62]. Hence, the recovery and reuse of organic solvent is recommended for the direct transesterification process. No matter how attractive the direct transesterification method is, it is still a lab-scale method, and further research is necessary to develop the equipment and process for large-scale viability.

The commercial success of microalgae biodiesel is possible only when the harvesting, drying, and oil extraction processes are improved in terms of time and energy consumption. It was observed that a lot of research has been carried out on various aspects associated with microalgae biodiesel production. However, many aspects, like property estimation of biodiesel from various species, the fatty acid composition, and diesel engine testing, need to be studied in more detail.

2.5 Microalgae biodiesel: FA composition, properties and engine evaluation

Conversion of microalgal biomass into biodiesel is not the sole responsibility, as the suitability of biodiesel as an alternative to conventional diesel needs to be ensured. This is confirmed by measuring the important thermo-physical properties of biodiesel and comparing those with international standards such as ASTM D675 or EN14214. These standards aim to ensure the economic and environment-friendly use of biodiesel as an alternative transport fuel. Table 2.3 summarizes the limiting minimum/maximum values of important thermo-physical properties permitted under these standards taken from references [63,64].

Table 2.3 Biodiesel properties as per ASTM D675 and EN14214

	ASTM D6751		EN 14214	
	Limit	**Method**	**Limit**	**Method**
Flash point (°C, min)	130	D93	101	ISO CD 3679e
Cloud point (°C, min)	Report	D2500	-	-
Kinematic viscosity @ 40 °C (mm^2/s)	1.9–6.0	D445	3.5-5.0	EN ISO 3104
Cetane no. (min)	47	D613	51	EN ISO 5165
Density (kg/m^3) @ 15 °C	-	-	860–900	EN ISO 3675
Iodine Value (g I_2/100 g, max.)	-	-	120	prEN 14111
Acid no. (mg KOH/g, max.)	0.8	D664	0.5	prEN 14104
Oxidation Stability (h @ 110 °C, min)	-	-	6	prEN 14112k
Sulphated ash content (% mass, max.)	0.02	D874	0.02	EN3987
Total Sulphur (ppm, max.)	0.05% mass	D5453	10 ppm	--
Water and sediment (vol. %, max.)	0.05	D2709	500 mg/Kg	EN ISO 12937
Free glycerine (% mass, max.)	0.02	D6584	0.02	prEN 14105m
Total glycerine (% mass, max.)	0.24	D6584	0.25	prEN 14105m
Monoglycerides (% mass, max.)	-	-	0.8	pr EN 14105m
Diglycerides (% mass, max.)	-	-	0.2	pr EN 14105m
Triglycerides (% mass, max.)	-	-	0.2	pr EN 14105m
Methanol (wt. %, max.)	-	-	0.2	prEN 141101
Ester Content (wt. %, min)	-	-	96.5	prEN 14103d
Linolenic acid methyl ester (% mass, max)	-	-	12	prEN 14103d

2.5.1 Relationship between FA composition and biodiesel properties

As shown earlier, biodiesel is a mixture of fatty acid esters consisting of mostly 16 to 18 carbon atoms. The number of carbon atoms present in fatty acid and their type (SFAs, MUFAs, and PUFAs) are prime factors controlling the biodiesel properties. When considering individual fatty acid ester molecules, properties like cetane number, melting point, boiling point, calorific value, and viscosity show an increasing trend with chain length, whereas an increase in the number of double bonds shows a decrease in all these properties [65]. As a result, long-chain SFAs could have better combustion properties due to high cetane numbers, but at the same time, their high viscosity can pose a problem in fuel atomization. The unsaturated FAs will have lower viscosity, but their cetane number and calorific values are also lower. Also, the unsaturated molecules have allylic and bis-allylic sites. These phenomena make them susceptible to degradation by reacting with atmospheric oxygen and producing unwanted products [66]. Hence, the presence of higher PUFAs in biodiesel indicates lower oxidative stability. Cold flow properties determine the temperature conditions above which fuel can be used in the engine without any trouble. It is generally expressed by the cold filter plugging point (CFPP) of the fuel. Although its limit has not been recommended in both the standards, it should be decided based on local conditions. SFAs have higher cloud points and pour points compared to MUFAs and PUFAs, indicating a high CFPP value. Therefore, biodiesel containing more saturated fatty acids content exhibits poor cold flow properties. It is clear from the above discussion that a higher percentage of just one type of fatty acid (i.e., SFA, MUFA, and PUFA) is not desirable from the prospect of virtuous biodiesel. Ideally, biodiesel can be a good mixture of long-chain SFA and short-chain MUFA or PUFA. The presence of only saturated or polyunsaturated fatty acids in biodiesel will lead to extreme properties, which is not desirable considering the adverse effect of a few of these properties on engine performance and emission characteristics.

Many previous studies have shown that the composition of fatty acids in biodiesel is important from the prospect of biodiesel properties as a transport fuel[67,68]. The primary aim of these studies was to explore the effect of chain length as well as the number of double bonds present in the fatty acids of biodiesel on engine performance and emission behavior. As the chain length of fatty acid increases, the maximum pressure developed during the combustion decreases as well as the maximum heat release rate [67]. They accredited the observed behavior in favor of higher cetane number and high bulk modulus of long-chain fatty acid esters. The above two factors lower the ignition delay period and the amount of fuel participating in premixed combustion. Zhu et al. [69] also observed similar behavior in their experimental study. They attributed it to increased viscosity and surface tension of the fuel, which causes poor atomization and reduced air/fuel mixture quality. Hence, very little fuel burns in the premixed combustion phase. However, the peak pressure developed, and heat release rates remained invariant when the ignition delay was kept the same, irrespective of the increase in the carbon chain of fatty [70]. Overall, an increase in the carbon chain of fatty acid results in a higher amount of CO, unburnt hydrocarbon, and smoke emissions. But, NOx emissions are reduced. The particulate emissions contain a large number of nucleation mode (5 to 40 nm dia.) particles for higher chain fatty acid ester molecules. The authors did not provide a specific reason for the above phenomenon. Compared to fatty acid ester fuel, diesel fuel emitted a higher total mass of particle emissions due to many accumulation mode particles [67].

Coming to the number of double bonds, higher unsaturated fatty acid ester presence induces longer ignition delays, resulting in higher peak pressure and high heat release rates. Improved combustion inside the engine even facilitates reducing pollutants, i.e., CO and HC emissions. The above behavior can also be because of the low viscosity of unsaturated fatty acid, which assists in better atomization [71] and, hence, improved combustion in the premixed phase. But, the adiabatic

flame temperature of the fuel increases with an increase in the number of double bonds present in fatty acid. This is a possible reason for an increase in the NOx emissions for unsaturated fatty acids [69]. Saturated fatty acid ester molecules were observed to emit more nucleation mode particles (5-40 nm), whereas unsaturated esters showed high smoke opacity because of a higher number of accumulation mode particles (50-487 nm) [70]. The unsaturated fatty acids with three or more double bonds are not desirable as they will lead to extreme values of properties.

2.5.2 Fatty acid composition of microalgae biodiesel

Table 2.4 presents the fatty acid composition of important microalgae species biodiesel belonging to different classes and the biodiesel prepared from a few other main sources from the first and second generations. The lipid productivities of two classes (Chlorophyceae and Trebouxiophyceae) of microalgae are higher compared to other classes; therefore, more species belonging to these classes have been presented in the table. Species of microalgae belonging to these two classes have been widely explored in past research works. Apart from these, species of the Eustigmatophyceae class also have high lipid productivity, but the SFA content is very low in this species. It is evident that the composition of saturated and unsaturated fatty acids varies largely, even among one particular class of microalgae. C16 series fatty acid is mainly present in the form of saturated fatty acid (Palmitic acid, C16:0), and in one species, the percentage of Palmitic acid is present up to 50%. Whereas the C18 series is mainly present in an unsaturated form (C18:1, C18:2, and C18:3). In a few species, the oleic acid composition of up to 60% is even found. Most of the species contain linolenic acid above the limit imposed by EN14214 standard (12%).

FA profiles of some of the vegetable oil biodiesel are also shown in the table. Vegetable biodiesel also contains high PUFA (19 to 42%), except palm biodiesel. Their high PUFA content is mostly because of

high linoleic acid. Palm biodiesel contains the highest SFA and MUFA among all the vegetable oil sources presented in the table.

The higher content of linolenic acid is the main limiting parameter of the microalgal biodiesel. Some of the properties may not satisfy the limits imposed by given standards due to a very high amount of PUFAs. Therefore, even though microalgae have a high potential to produce biodiesel fuel, the lower quality can act as a barricade in its use as a diesel engine fuel. The selection of proper species having high oil-yielding capacity with better fuel properties becomes an obligatory step for the sustainability of microalgal biodiesel as a transport fuel. Measurement of fuel properties of individual species physically is a cumbersome task and, indeed, a very costly process. As these properties are dependent on fatty acid composition, empirical equations proposed in the past to relate properties with FA composition can facilitate a handy tool to speculate these properties related to engine performance[72–74]. Based on these correlations and experimental lipid productivity, studies have been performed to determine the suitability of microalgae species as a source of biodiesel [75–78].

There are few studies in the literature that have produced enough quantity of microalgae biodiesel to measure properties physically. Table 2.5 shows the measured properties of pure biodiesel fuels obtained from different microalgae species as well as vegetable biodiesel.

Table 2.4 Fatty acid percentage in various biodiesel feedstocks

FA composition	C14	C16:0	C16:1	C18:0	C18:1	C18:2	C18:3	Other	SFA	MUFA	PUFA
Trebouxiophyceae											
Botryococcus braunii [75]	0.73	7.17	-	1.59	77.22	5.16	5.34	-	9.49	77.22	10.5
Chlorella protothecoides [79]	0.27	13.42	-	3.4	58.94	19.86	-	-	19.79	58.94	19.86
Chlorella vulgaris [80]	2.3	6	16.4	10.3	26.5	-	20.8	-	18.6	42.9	20.8
BTA4036 C. variabilis [37]	1.2	22.3	5.8	5.2	3.4	7.6	9.2	10.1[a]	34.3	24.2	25.4
Chlorella emersonii [76]	-	14.75		9.8	17.01	9.04	29.32	-	24.55	17.01	38.37
Chlorella salina [76]	-	21.5	2.62	7.83	14.39	10.88	29.75	-	29.34	18.52	40.63
Chlorophyceae											
Ankistrodesmus sp. [76]		16.24	3.06	7.18	17.66	8.8	28.68	-	23.43	23.27	37.16
Chlamydomonas sp. [75]	1.61	50.77	0.28	11.54	13.77	3.93	2.76	-	63.92	14.05	6.69
Dunaliella salina [81]	0.51	18.2	0.98	0	4.56	13.24	30.26	11.24[b]	18.71	5.54	58.9
Dunaliella sp. [76]	-	9.19	0.8	4.27	22.51	3.84	44.31		13.47	24.74	48.15
Monoraphidium contortum [38]	0.9	20.9	0.8	0.3	17.3	10.5	23.9	14.7[c]	24.4	18.1	56.3
Scenedesmus sp. [76]	-	15.62	4.06	2.97	15.23	7.00	22.99	-	18.59	26.86	30.00
Eustigmatophyceae											
Nannochloropsis oculata [82]	3.9	20.5	25.2	1.8	4.1	2.2	0.9	29.7[d]	10.4	39.5	36.9
Bacillariophyceae											
P. tricornutum [82]	7.4	11.3	22.4	0.4	2.8	1.5	1.4	16.7[a], 28.4[d]	20.2	25.3	49.8
Prymnesiophyceae											
Pavlova salina [82]	0.4	15.1	30.4	1.0	3.8	1.5	2.2	19.1[d]	30.7	34.2	29.4
Rhodophyceae [82]											
Porphyridium cruentum [82]	0.5	28.6	2.9	0.8	2.0	8.2	0.7	21.1[d]	31.1	5.0	40.8
Cryptophyceae											
Chroomonas salina [82]	5.0	13.5	2.0	3.0	5.2	1.2	10.8	12.9[d]	10.7	7.5	65.5
2nd gen. oil sources											
Jatropha [83]	0.2	13.4	0.8	6.4	36.5	42.1	0.3	-	20	37.3	42.4
Karanja [84]	-	7.4	-	3.8	65.6	15.4	4.4	-	11.2	65.6	19.8
Palm [85]	1.22	47.9	0.04	4.23	37	9.07	0.26	-	54.12	37.04	9.33
Mahua [86]	0.08	21.53	-	18.96	39.14	19.55	0.16	-	40.57	39.14	19.71
Rapeseed [87]	-	3.49	-	0.85	64.4	22.3	8.23	-	4.34	64.4	30.53

a= C16:2 and C16:3; b= C16:4; c= C16:3; d=EPA

It is clear that the measured property database of microalgae biodiesel has not matured yet, and a lot of research scope remains in this field. The cetane number of studied microalgae biodiesel was slightly lower, whereas sulfur content was higher than vegetable biodiesel. It can also be noticed that few of the species have a density (*Crypthecodinium cohnii and Chlorella protothecoides*) and viscosity (*Crypthecodinium cohnii* and *Spirulina platensis)* slightly higher than EN14114 limits. Biodiesel obtained from *Chlorella protothecoides* species seemed to have better fuel properties than other species; also, it had better oxidation stability (~12 h). Poor oxidation stability of other species can be accredited to the high PUFA content present in them. But overall, microalgae biodiesel properties were found to be comparable with other vegetable oil sources. In the next section, the effect of properties of microalgae biodiesel on diesel engine performance and emissions are discussed. As the large-scale production of pure microalgae strain is very difficult, very few works associated with engine performance as well as exhaust characteristic evaluation, have been carried out.

2.5.3 Performance and emissions characteristics of microalgae biodiesel

The past two decades have seen tremendous interest in biodiesel to study its potential as diesel engine fuel [88,89]. Lots of engine performance evaluation studies using a variety of first and second-generation biodiesel have been carried out in the past under various operating conditions. Mostly, satisfactory performance and emission results were observed. However, very limited engine performance evaluation studies were reported related to microalgae biodiesel. These studies are summarized in Table 2.7. The table presents the type of microalgae species, engine description, testing conditions, engine performance parameters, and results of exhaust analysis.

Table 2.5 Properties of biodiesel obtained from various sources

Source	***Crypthecod-inium cohnii* sp.** [90]	***Chlorella* sp.** [91]	***Nannochlor-opsis* sp.** [92]	***Chlorella protothecoi-des*** [93]	***Spirulina Platensis*** [94]	***Chlorella* sp.** [59] *	***Nannochloropsis* sp.** [95] *	**Jatropha carcus** [83]	**Karanja** [84,96]	**Palm** [96,97]	**Mahua** [86]	**Rapeseed** [98]
Flash point (^oC)	95	179	144	124	130	164.21	-	172	160	135	130	>150
CFPP (°C)	-	-	-	-	-	0	-	-	-16	12	-	-16
Pour point (^oC)	-	-	-6	-	-18	3.56	-	-	-15	-	-	-10
Cloud point (^oC)	16	-	7	-	-	6.68	0.97	-	-15	16	-	-4
Cetane number	46.5	-	-	52	-	55.82	63.27	58.5	55.1	54.6	62	51
Density (kg/m3) @ 15° C	912	883.6	869	900	860[a]	890	870	884.2		864.42[b]	873.8	884
Calorific value (MJ/kg)	39.86	37.06	40.72	40.04	41.36	40.77	39.82	41.3	-	39.83	36.9	37.23
Iodine number (g I_2/100 g)	-	97.12	-	-	-	-	48.46	93	-	-	-	112
Viscosity at 40 ^oC (mm^2/s)	5.06	4.73	4.19	4.22	5.66	4.22	4.69	4.4	4.5	4.71	4.39	4.7
Acid number (mg KOH/g)	0.14	0.37	-	-	0.45	0.56	-	0.11	0.3	0.24	0.47	0.03
Oxidation stability (h)	-	6.76	-	12	-	-	11.85	6.7	1.5	13.37	-	-
Sulphated ash content (%)	-	-	-	-	-	0.07	-	<0.01	0.002	0.002		0.007
Sulphur (ppm)	7.5	8.1	-	2	-	-	-	-	-	-	-	< 3
Water and sediment (vol %)	0	-	-	-	-	-	-	-	0.03	0.01	-	-
Monoglycerides (%mass)	-	0.792	-	-	-	-	-	0.01	-	-	-	-
Diglycerides (%mass)	-	0.122	-	-	-	-	-	0.02	-	-	-	-
Triglycerides (% mass)	-	0.197	-	-	-	-	-	>0.02	-	-	-	-
Total glycerin (%mass)	-	-	-	-	-	-	-	0.03	0.01	0.01	0.02	-
Sulphur mass (%)	-	-	-	-	-	-	-	0.004	0.003	0.003	-	-
Ester content (wt. %)	-	97.42	-	-	-	-	-	98.9	97.6	-	-	-

a: @ 40° C, b: @25° C, *: properties are predicted based on fatty acid profile

Makareviciene et al. [91] carried out a comparative study of B30 blends of biodiesel from microalgae *Chlorella vulgaris* (AME) and rapeseed oil (RME). The properties of both biodiesel blends were observed to be almost similar. An improvement in BTE (brake thermal efficiency) by 2.5 to 3%, a decrease in CO emissions by around 10% and HC emissions by 5 to 25% when the engine was fueled with AME and RME biodiesel blends was observed. No substantial change in NOx emissions was reported for fuels used in the study. Haik et al. [92] tested microalgae biodiesel (blends ratio B50, B100) obtained from *Ankistrodesmus braunii* and *Nannochloropsis* sp. for combustion characteristics. The biomass cultivation was done in 15000 liter open ponds with nutrients from the sewage water supply. The oil yield from dried biomass by standard soxhlet method was 12-15% from *A. braunii* and 10% from *Nannochloropsis* sp. It was concluded that the amplified combustion noise and lower torque output for microalgae biodiesel can be countered by retarded injection timing and lower compression ratio. Islam et al. [90] investigated biodiesel from *C. cohnii* (blends B10, B20, B50) and waste cooking oil (B20) in a CRDI engine. The authors used purchased dry biomass to obtain microalgae biodiesel. It was observed that the B20 blend of microalgae biodiesel displayed satisfactory emission characteristics as compared to diesel. However, the proposed blend was still inferior to diesel when BTE and BSFC (brake specific fuel consumption) were compared. Jaypabhakar and Karthikeyan [99] produced biodiesel from algae biomass collected from the local seashore and compared 20% blends (B20) of algae biodiesel and rice bran biodiesel with diesel. Rice bran biodiesel showed slightly superior BTE than algae biodiesel but it was lower than that of diesel. Advanced injection timing resulted in improved BTE for biodiesel blends. Algae biodiesel blends had the highest NOx emissions but lowest HC and smoke emissions than that of rice bran biodiesel and diesel. Al-lwayzy and Yusaf [93] experimented biodiesel from *Chlorella protothecoides* species (blends B20, B50 and B100). The *C. protothecoides* oil was purchased and transesterified to produce biodiesel. It was found that only the B20 blend was comparable to

diesel in terms of the average torque and power output. However, all biodiesel blends showed lower average exhaust emission values compared to diesel. In another study [100], a comparison of first, second and third-generation biodiesel (blends B10 and B20) was performed. *Chlorella vulgaris was* used as a third-generation source that was cultivated in the photobioreactor. The oil extraction was done in soxhlet extractor followed by standard transesterification. Highest BSFC and lowest power output were obtained for *C. vulgaris* biodiesel blend. Of the three types of biodiesel used, microalgae biodiesel caused very low CO and HC emissions but increased NOx emissions. Jayaraman et al. [101] studied single-cylinder diesel engine with biodiesel (B20) from algae biomass collected from a freshwater lake. The biomass was subjected to mortar-pestle and hexane-isopropanol solvent for oil extraction. Transesterification was carried out with methyl, ethyl and butyl alcohol. Biodiesel with methyl ester produced the most satisfactory results with higher BTE and lower emissions of HC, CO, and smoke. Though, NOx emissions were higher. Nautiyal et al. [102] produced biodiesel from *Spirulina platensis* microalgae biomass and evaluated it in a diesel engine. Biodiesel decreased peak pressure and HRR owing to short ignition delay (a decrease of 2.7 degrees of crank angle compared to diesel). This study also observed a decline in HC, CO and smoke emissions as well as augmented NOx emissions when the engine is fueled with biodiesel blends. Venu et al. [103] tested biodiesel from *Chlorella emersonii* microalgae in a diesel engine. Cultivation was done in a raceway pond and oil extraction was carried out in a soxhlet apparatus. The tested blends were B10 to B40 by an increment of 10% and B100. At full load, the BTE of B10 and B100 was lower than diesel by 9.01% and 24.03% respectively. The ignition delay was shortened for biodiesel because of the increased cetane number. CO and HC emissions declined whereas NOx and CO_2 emission increased for all biodiesel blends. Other emissions such as acetone and formaldehyde increased and emission of toluene decreased with an increasing biodiesel percentage in the blend. Rajak et al. [104] analyzed *spirulina* microalgae biodiesel blends from B20 to B100 by

an increment of 20%. BTE for B20 reduced up to 3.03% and for B100 up to 7.7%. Contrary to many studies, the NOx emission reduced with blend percentage (4.9% and 26.6% for B20 and B100 respectively). Similarly, smoke emissions also decreased considerably by using *spirulina* microalgae biodiesel. In another study [105], B20 and B100 blends of *spirulina* microalgae biodiesel were investigated at variable compression ratio (CR). At all the compression ratios, the cylinder pressure and the exhaust temperature were slightly more for biodiesel. The combustion duration also decreased when fueled with biodiesel and it was lo west for B100. The NOx emissions were highest for B100 except at CR 17.5 where pure diesel emitted the highest NOx emissions.

The above studies showed that microalgae biodiesel can produce comparable performance and emission characteristics. Blends up to 20 % show similar results to diesel fuel with the added advantage of complete combustion due to extra oxygen in the fuel itself. As the studies regarding engine evaluation are very few, more research is necessary to study large-scale microalgae biodiesel obtained from different species.

2.5.4 Metal oxide nanoparticles as additives

Microalgae biodiesel also has a similar disadvantage of somewhat inferior fuel properties just like initial biodiesel sources, which results in reduced engine efficiency as the blending percentage increases. However, the emission characteristics of the engine improve with the use of microalgae biodiesel. The poor performance at a high blending percentage can be normalized by using fuel additives in biodiesel blends. These fuel additives improve the fuel properties, spray atomization process, and combustion phenomenon in the engine, ultimately leading to superior engine performance. Metal oxide nanoparticles are frequently investigated as a fuel additive to improve performance and reduce emissions. Some of the previous studies are mentioned below.

Al_2O_3 nanoparticles were added to the jojoba biodiesel blend and studied in a diesel engine by El-seesy et al. [106]. The largest emission reduction was for 20 ppm concentration and the highest increase in BTE was for 40 ppm concentration of nanoparticles. Appavu et al. [107] demonstrated similar gains for the Pongamia biodiesel by the addition of 50 and 100 ppm CeO_2 nanoparticles. The combination of CeO_2 and water emulsified diesel-biodiesel blend was found to be very effective in increasing the performance and reducing the emissions as compared to diesel by [108]. The effect of TiO_2 nanoparticles addition to waste cooking oil biodiesel blend was investigated by Örs et al. [109]. The nanoparticles were used in a mass percentage of 0.01%. There was an improvement of 9.74% in the average power of the engine by the addition of TiO_2 nanoparticles. All the emissions, except NOx, were reduced quite significantly. CuO nanoparticles reduced NOx and smoke emissions and improved the BTE; when added in 100 ppm concentration to Pongamia biodiesel [110]. Ge et al. [111] attempted to improve the engine output characteristics by adding 75 ppm Al_2O_3 nanoparticles to 15% and 30% blends of *Spirulina* microalgae biodiesel. 15% biodiesel with nanoparticles was found to be better among all the biodiesel blends in terms of performance. The emissions of nanoparticle-biodiesel blends were also lower than that of diesel. Thus, the effect of nanoparticles addition on the performance and exhaust characteristics of an engine using first and second generation biofuels had been explored quite well by researchers. Some more studies are tabulated in Table 2.6. While there are other studies on the effect of nanoparticle addition on microalgae biodiesel [112–117]; most of these come from the same research group. Different nanoparticles such as CuO_2, ZnO, TiO_2, SiO_2, ZrO_2, RuO_2 and CeO_2 were tested on microalgae (*Neochloris oleoabundan*s, *Botryococcus braunii*) and macroalgae (*Azolla* sp.) biodiesel in these studies. In essence, it was established that a 100 ppm concentration of nanoparticles improved the efficiency of an engine and reduced emissions of CO and HC considerably. The NOx emissions increased in most of these studies.

Table 2.6 nanoparticle added first and second generation biodiesel studies

Author (Reference)	Biodiesel Source	Nanoparticle	Blends*	Concentration of nanoparticle
Rastogi et al. [118]	Simmondsia Chinensis (Jojoba)	CuO	D, B20, B20+N	25, 50 and 75 ppm
Kumar et al. [119]	Rubber seed	Al_2O_3	D, B25, B25+N	125 and 150 ppm
Arunprasad et al. [120]	Jojoba	La_2O_3	B20, B20+N	50 and 100 ppm
Sridhar et al. [121]	Grape seed	CeO_2	D, B10+N, B20+N, B30+N	20 ppm
Mujtaba et al. [122]	Palm+ Sesame mix	Carbon Nanotubes (CNTs), TiO_2	D, B30, B30+N	100 ppm
Ağbulut et al. [123]	Waste cooking oil	Al_2O_3, TiO_2, SiO_2	D, B10, B10+N	100 ppm
Devarajan et al. [124]	Mahua	CuO	D, B100, B100+N	100 ppm
Soudagar et al. [125]	dairy scum oil	Graphene oxide	D, B20, B20+N	20, 40 and 60 ppm
Ranjan et al. [126]	Waste cooking oil	MgO	D, B100 B20, B10, B100+N, B20+N, B10+N	30 ppm
Mendonca et al. [127]	Simarouba	Al_2O_3	D, D+N, B20, B20+N	50 ppm
Jiaqiang et al. [128]	Rapeseed	CeO_2	D,B5, B5W6, B5W4, B5W2, B5W6+N, B5W4+N, B5W2+N	90 ppm
El-Seesy et al. [129]	Jatropha	Graphene nanoplatelets (GNPs).	D, B20, B20+N	25, 50, 75 and 100 ppm
Sivakumar et al. [130]	Pongamia	Al_2O_3	D, B25, B25+N	50 and 100 ppm
Devarajan et al. [131]	Neem	Ag_2O	D, B100, B100+N	5 and 10 ppm
Keskin et al. [132]	Canola	Palladium, ferrocene based	D, B20, B50, B20+N, B50+N	25 ppm

Mehregan et al. [133]	Waste cooking oil	Mn_2O_3, Co_3O_4	B20	25 and 50 ppm
Praveen et al. [134]	Calophyllum Inophyllum	Al_2O_3	D,B20, B20+N, B20 + 20% EGR, and B20 +N + 20% EGR	40 ppm
Hosseini et al. [135]	Soybean	Carbon Nanotubes (CNTs)	D, B5, B10, B20, B5+N, B10+N	30, 60 and 90 ppm
Ashok et al. [136]	Calophyllum Inophyllum	TiO_2 + butylated hydroxytoluene (BHT)	D, B100, B100+N, B100+BHT	50 and 100 ppm, 200 and 500 ppm BHT

* D: Diesel; B10: 10% biodiesel in diesel and so on; B+N: biodiesel+nanoparticle blend

2.5.5 Mix-fuel blend

Mixing two or more biodiesels can be another method of optimizing the fuel properties and improving the engine output characteristics. Some previous studies of mix-fuel blends are presented in this section. Raheman et al. [137] mixed Madhuca Indica oil and Simarouba oil in equal proportion to optimize biodiesel production because of very high FFA content of Madhuca Indica. The produced biodiesel blend (B10 and B20) was successfully tested in a diesel engine with satisfactory engine output characteristics. Habibullah et al. [138] investigated 30% biodiesel blend of palm (P30) and coconut (C30) in a diesel engine and compared it with mix-fuel blend having 15% palm and 15% coconut (PB15CB15). The coconut biodiesel had very high SFA content whereas palm biodiesel was composed of palmitic (SFA) and oleic acid (MUFA) mainly. Performance of the engine with mix-fuel was better than P30 but was inferior to C30 blend. However, average NOx emission trend was opposite as C30 showed highest NOx emissions. The mix-fuel blend exhibited lower NOx emissions than C30 by average 1.2%. Sanjid et al. [139] prepared mix-fuel blend from palm and jatropha biodiesel by mixing 5% biodiesel (PBJB5) and 10% biodiesel (PBJB10) of each. Of the two biodiesels, palm was having high SFA content than jatropha biodiesel. Also, Jatropha biodiesel had high linolenic acid (PUFA) content. The observed trend for engine output parameters for PBJB5 was in between PB10 and JB10; with

PB10 superior amongst the three except NOx emissions. Same results were obtained for PBJB10 when compared with PB20 and JB20. In another study [140], kapok biodiesel and moringa oilifera biodiesel was mixed similar to previous study and compared with 10% and 20% individual biodiesel blends. The mix-fuel showed second best performance and lowest CO and HC emissions for most of the operating speeds. The authors have not reported the fatty acid content of the biodiesels. Ruhul et al. [141] prepared mix-fuel consisting of Croton megalocarpus and Ceiba pentandra biodiesel in different proportions. 10% mix (CM10CP10) of both biodiesels produced better performance and emissions except NOx when compared to that of 20% blend of each biodiesel. Both the biodiesels had high PUFA content consisting of linoleic acid mostly. Srithar et al. [142] prepared mix-fuel blends from pongamia and mustard biodiesel and tested them in a diesel engine. However, individual biodiesel blends of pongamia and mustard were not compared in the study. Authors found out satisfactory performance and emissions for the mix-fuel. Hosamani and Katti [143] mixed two biodiesel simarouba and jatropha in the ratio of 3:1 and prepared B20 to B100 blends from the mix-fuel to study the combustion behavior in an the diesel engine. Simarouba biodiesel had slightly inferior properties out of these two. The maximum cylinder pressure and combustion duration were amplified by the use of biodiesel blends and NOx emissions were higher as compared to diesel. Khan et al. [144] prepared mix-fuel blends from castor and karanja biodiesel in their experimental study. C5K10 with 5% castor biodiesel and 10% karanja biodiesel was reported as most suitable among the studied blends. Sharma and Duraisamy [145] produced biodiesel by mixing oil from three sources viz. jatropha, karanja and cottonseed in optimized proportion (30-30-40%). The mix-fuel improved most of the thermophysical properties as well as the output characteristics of an engine when compared with individual biodiesels. Kumar et al. [146] optimized biodiesel production from mixed jatropha-algae oil. The produced biodiesel was tested in an engine in the blend ratio of B5, B10 and B20. It was observed that B20

was better in performance and emissions, except NOx emissions, as compared to other blends. Sudalaiyandi et al. [147] added the biodiesel of linseed and rubberseed in the proportion of 5 to 25% each in diesel to prepare different blends and study them in a diesel engine. Optimum performance and emission output of an engine was obtained with mix-fuel blends containing 5% and 10% each of the two biodiesels. Similarly, Swarna et al. [148] prepared biodiesel from mixed oil of pongamia and Mahua and tested it along with the addition of alcohols as additives. Authors observed that 20% mix-biodiesel with 20% heptanol in diesel to be a superior blend among the studied blends.

In this way, mixing of two or more biodiesels can be an option to enhance engine performance and emissions.

2.6 Research gaps

1. Significant variation exists in the lipid content and lipid productivity of different microalgae species. Lipid productivity further varies with the growth phase and growth conditions. Optimization and screening studies are needed to select microalgae with high lipid productivity under local conditions.
2. Advanced lipid extraction methods such as ultrasonic, microwave, supercritical fluids, and ionic liquids increase the yield, but they are yet to be made cost-effective for scalable oil extraction.
3. Direct conversion of microalgae biomass to biodiesel eliminates the drying and lipid extraction steps, but more research is necessary to make the process commercially viable.
4. The fatty acid composition analysis of different microalgae biodiesel showed significant variation among different species. However, the high PUFA content seems to be a common characteristic of microalgae biodiesel. Mixing of different biodiesels with FA composition can have a mix-fuel with suitable properties.
5. Microalgal biodiesel properties were comparable to that of initial biodiesel sources. The properties depend on the fatty acid

composition; thus, it can be optimized by properly regulating the growth conditions and harvesting time. Research at the molecular level can also help to achieve this.

6. The performance and emission characteristics of lean blended microalgae biodiesel are satisfactory. More research is necessary to find out ways to use microalgal biodiesel at higher blend ratios and in pure form in an engine.

2.7 Major objectives of the current study

The following objectives are identified for the current research work based on the extensive literature review,

1. Microalgae growth and adaption are very sensitive to the local environmental conditions. Hence, screening and identification of suitable microalgae for semi-outdoor biomass cultivation for biodiesel production has been identified as the first objective of the current research work. For this purpose, six locally isolated strains are compared based on their lipid content and FAME composition. Also, the estimated thermophysical properties of resulting biodiesel from these strains are compared at an enlarged temperature scale pertaining to engine operation.
2. Based on the above analysis, the second objective is to cultivate the selected microalgae species for large-scale biomass in the in-house polyhouse raceway pond structure and to extract oil from dried microalgae biomass for conversion into biodiesel. Initially, the isolated strain is grown inside the lab for large-scale inoculation purposes, and the growth media for the large-scale production of microalgae biomass is also optimized through preliminary experimentation.
3. The next objective is to study the FAME composition and properties of produced microalgae biodiesel and evaluate its use as a blend in the diesel engine. Detailed experiments are carried out on 20% and 30% biodiesel blends. Their

performance and emission characteristics are experimentally compared with diesel.

4. To overcome the poor performance level of the microalgae biodiesel blend, the final objective is to study the effect of fuel additives, i.e., nanoparticles, on diesel engine performance and emissions. Cerium oxide nanoparticles are selected for that purpose. In addition, the mixing of two biodiesels as a remedial approach to improve the performance and emissions characteristics is also explored.

Table 2.7 Studies on performance and emission characteristics of microalgae biodiesel

Sr no	Microalgae species	Engine	Condition	Blends	Performance analysis compared to diesel fuel				Exhaust emissions compared to diesel fuel			
					BSFC (g/kWh)	BTE (%)/ brake power(kW)	Peak pressure (bar)	Torque (Nm)	CO	HC	NOx	Smoke
1	*Nannochloropsis* sp. [92]	Single cylinder, Ricardo E6 IDI, Max power=14.0 kW, CR= 22, Injection timing- 20-45° BTDC	Varying speed	Diesel fuel, B100, B50, Raw algae oil	-	-	Maximum: B100 - 29.1 D – 25.9 @ 1440 rpm	Maximum @1800 rpm: B100 – 8.4 D – 10	-	-	-	-
2	NA [149]	Four-cylinder, Mitsubishi canter, DI, 3907 CC, Max power = 89 kW at 3200 rpm, Torque = 295 Nm at 1800 rpm	Varying speed	Diesel fuel, B5, B10, B25, B50, B100	-	Max @2400 rpm: B100 – 56.9 kW D – 60.08 kW	-	Max @ 1600 rpm: B100 – 248.3 D – 262.9	Max @ 2800 rpm: B100 – 332 ppm D – 368 ppm	-	Max @ 1200 rpm: B100 – 1089 ppm D – 848 ppm	-
3	*Chlorella* sp. [91]	Three-cylinder, DI, 3300 CC, Max power=30 kW @ 1500 rpm	Varying power	Diesel fuel, B30	@low load: B30 – 695 D – 661 @high load: B30-270 D - 242	Maximum: B30 – 36.2 % D – 34.8 %	-	-	Maximum: B30 – 194.7 ppm D – 209.6 ppm	Maximum: B30 – 290.8 ppm D – 328.4 ppm	Not much change	Maximum: K value, B30 – 0.15 D – 0.31
4	*Chlorella vulgaris* [150]	Kirloskar single cylinder, DI, 661 CC, Max power= 3.5 kW, CR= 14:1 to 18:1	Varying power	Diesel fuel, B10, B15, B20	-	Maximum: B20 – 21.5 % D – 20.1 %	-	-	Maximum: B20 – 2,4 % D – 2.7 %	Maximum: B20 – 61.3 ppm D – 88.1 ppm	Maximum: B20 – 1094.2 ppm D – 1029.7 ppm	Maximum: B20 – 81.3 % D – 97.6 %
5	*Crypthecodinium cohnii* [90]	Four-cylinder, 2000 CC, Max power=100 kW at 4000 rpm, CR= 18, Turbocharged.	Varying power	Diesel fuel, B10, B20, B50	Maximum: B50 – 305.4 D – 290.6 at lower loads, Decreases at high load	Maximum: B50 – 37.5 % D – 38.2 %	Maximum: B50 – 90.3 D – 96.7 at lower loads, at high loads no difference	-	-	Maximum: B50 – 4.7 g/kWh D – 9.65 g/kWh	Maximum: B50 – 4.8 g/kWh D – 3.92 g/kWh	-
6	*Chlorella protothecoides* [93]	Single cylinder, 2190 CC, rated power 3.09 kW @3600 rpm, fuel injection 16.5° BTDC.	Varying speed	Diesel fuel, B20, B50, B100	@ low rpm: B100 – 393.5 D - 363.2 @ high rpm: B100 – 292.5 D - 260	@ low rpm: B100 – 24.2% D - 23 % @ high rpm: B100 – 34.2% D - 34.9 %	@ low rpm: B100 – 64.5 D – 69.5 @ high rpm: B100 – 56.8 D - 60	@ low rpm: B100 – 11 D – 11.46 @ high rpm: B100 –9.2 D - 10.7	@ low rpm: B100 – 3.92% D - 4.49 % @ high rpm: B100 -0.13% D - 0.58 %	-	@ low rpm: B100 – 393 ppm D - 426 ppm @ high rpm: B100 – 480 ppm D - 559 ppm	-

3 SCREENING AND SELECTION OF MICROALGAE SPECIES BASED ON THEIR LIPID CONTENT, FATTY ACID PROFILE, AND APPARENT FUEL PROPERTIES

3.1 Introduction

As explored in the literature review, microalgae have been classified into different classes and consist of thousands of species. These different classes of microalgae species show variation in their biomass and lipid (oil) production ability [29]. Therefore, the selection of microalgal species with high quantity and quality of biodiesel is necessary to maximize the net energy output of the microalgae biodiesel production process. Quantity is determined by the oil or lipid yield in a unit mass of dried biomass. Different methods used in the literature for lipid content analysis are gravimetric, spectrophotometric using a fluorescent dye, and use of instruments like GC or HPLC. The biodiesel should qualify for international property standards such as EN 14214 or ASTM D6715 to determine the quality. Direct assessment of the properties of biodiesel, in the case of the microalgae selection process, is not an easy and recommended approach. Instead, FAME composition-based correlations are available in the research work carried out by Ramírez-Verduzco et al. [74] (viscosity, density, and higher heating value), Mishra et al. [151] (cetane number); Ramos et al. [152] (CFPP) and Park et al. [153] (Oxidation stability). These equations mainly consider molecular weight, number of carbon atoms, and number of double bonds of individual FAMEs as a base to calculate the properties. Many past researchers have followed the properties prediction approach (based on FAME composition) along with lipid content analysis to compare the suitability of microalgae for large-scale production. Nascimento et al. [75] compared 12 microalgae

species based on their lipid productivity and FAME composition. The studied species belong to Trebouxiophyceae and Chlorophyceae class. The highest lipid productivity was found in species of Trebouxiophyceae class. However, as none of the biodiesel from either class justified all property requirements, they suggested mixing biodiesel from both classes to get rid of the situation. Talebi et al. [76] also used a similar approach to screen microalgae species. Eleven species were used in their study belonging to Chlorophyceae, Trebouxiophyceae, and Bacillariophyceae class. They suggested that in addition to lipid productivity and biodiesel quality, other factors such as ease of cultivation and harvesting and environmental conditions are also vital in microalgae species selection for biodiesel production. Islam et al. [77] compared locally isolated nine species belonging to seven different classes based on their FAME composition. They reported *N. Oculata* (Eustigmatophyceae) as the best among the studied species. They further concluded that the effect of the growth phase was found to be more on biodiesel quality than the effect of the nutrients provided. Eight strains of *Scenedesmus* species (class Chlorophyceae) were experimentally investigated by authors El-Sheekh et al. [78]. Based on higher lipid productivity and estimated properties (adheres to intentional standard EN14214), the *S. obliquus* was suggested as the best species. All these studies established that knowing the FAME composition becomes the foremost important criteria to estimate the properties of biodiesel. Apart from these studies, some studies have made effort to analyze other important thermo-physical properties of biodiesel, which are more relevant for the spray and combustion modeling purpose of biodiesel [154–156]. These properties are calculated at a wide temperature range, from room temperature to critical temperature of the fuel. A similar calculation in the case of microalgae will be further helpful in their comparison.

Therefore, the present study investigated six microalgal species isolated locally based on their lipid production and FAME composition. The species used are of three classes: Trebouxiophyceae,

Chlorophyceae, and Cyanophyceae. The species are grown in a similar environment. The calorimetric SPV method determines the lipid content, and FAME composition is determined by GC analysis after direct transesterification of biomass to biodiesel. After the initial screening of species based on their lipid content and a few important predicted thermo-physical properties (cetane number, viscosity, density, Iodine value, CFPP, heating value, and oxidation stability), the species selection process is further refined by the calculation of other important properties (vapor pressure, density, viscosity, latent heat of vaporization and vapor diffusivity) in wide temperature range considering spray and combustion modeling requirement. These properties are also compared with that of diesel surrogate fuel to predict their effect on combustion and emissions as compared to diesel fuel.

3.2 Experimental procedure

3.2.1 Cultivation of microalgae species

The current study used six microalgal species isolated previously in the laboratory from wastewater samples collected from the Indore region (Madhya Pradesh). Two of them are unicellular green algae species; *Chlorella* sp. (class Trebouxiophyceae) and *Chlorococcum/Scenedesmus* sp. (class Chlorophyceae), and four belong to filamentous cyanobacterial species (class Cyanophyceae) i.e. *Chroococcus* sp., *Calothrix* sp., *Nostoc* sp., and *Lyngbya putealis*. These were cultured in 250 mL Erlenmeyer flasks with 150 mL standard BG-11 media. The light intensity of 2800 lux with 12:12 h light: dark cycle at 30 ± 3 °C temperature was maintained during the cultivation period. The purity of cultures was checked under a microscope initially as well as on the last day of the cultivation period. The experiment is set up in triplicates for all the cultures. All the cultures were harvested on the 31st day of the growth cycle, i.e., the late stationary phase, to ensure the maximum formation of neutral lipids inside the cells [76]. The harvesting was done by centrifugation,

and the lower biomass pellet was collected, washed, and lyophilized to get dry biomass.

3.2.2 Lipid content measurement

The lipid content of all six species was determined by sulpho-phospho-vanillin assay[157]. This phospho-vanillin reagent was prepared fresh every time, just before the start of the lipid estimation reaction. The standard curves were prepared using glyceryl trioleate and Sunflower oil as standards. A known quantity of biomass was taken for lipid content analysis of microalgae species. 100 µl water was added to both these samples (lipid standard and microalgae biomass), followed by the addition of 2 mL concentrated H_2SO_4. The sample was then heated at 100 °C in the water bath for 10 min. and cooled in ice for 5 min. 5 mL of phospho-vanillin reagent was added to the sample and incubated in a rotary shaker incubator at 37 °C for 15 min. A visible pink color develops at the end of the reaction. The absorbance of the final sample obtained was measured at 530 nm using a spectrophotometer. The SPV reaction method is simple and less time-consuming as compared to the gravimetric method. The quantity of biomass required in this method is much less.

3.2.3 FAME composition analysis

FAME profiling was done using the method given by Ríos et al. [46]. 10 mg biomass was suspended in 4.5 mL of reagent $CH_3OH/CHCl_3$/HCL (4:1:1; v/v/v) and heated under magnetic stirring at 90 °C hot plate temperature for 2 h. After completion of the reaction, samples were cooled at room temperature and vortexed after the addition of 1.5 mL distilled water. 3 mL of hexane/chloroform (4:1, v/v) was added finally and again vortexed for one minute. The whole mixture was collected in a clean test tube and allowed to settle for 30 min (Figure 3.1). After settling, the upper layer containing solvent and FAMEs was collected for GC analysis. All the experiments were performed in triplicates.

To analyze the FAME composition, 1 mL of the FAME-solvent solution was taken in 1.5 mL clean GC glass vial. The samples were analyzed using an Agilent 7890 GC system equipped with a flame ionization detector (FID) and Select^{TM} Biodiesel CP9080 column (30 m×0.32 mm×0.25 µm). Helium (purity 99.99 %) was used as a carrier gas with a 1.5 mL/min flow rate. The 2 µl volume was injected with a split ratio of 10:1. The temperature program was kept as given by Shirazi et al. [158]. The peaks were identified by comparing the peaks of an external standard (FAME mix C4:C24; Sigma Aldrich #18919-1AMP) under similar conditions.

The reagents methanol, chloroform, and hexane were all of chromatography grade and purchased from Merck. Concentrated Hydrochloric acid was purchased from Rankem. C4:C24 FAME mix standard was obtained from Sigma Aldrich.

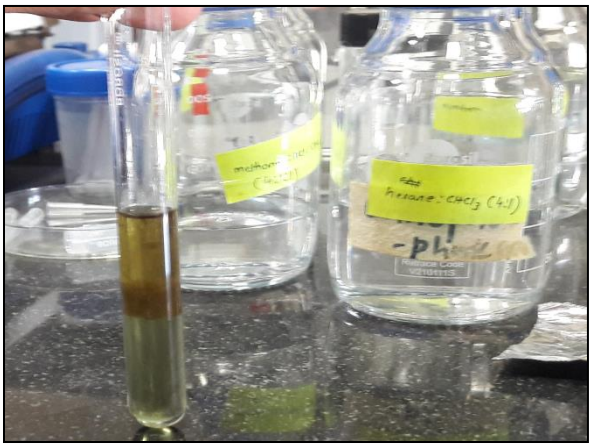

Figure 3.1 Direct transesterification of biomass (upper layer containing FAMEs and hexane)

3.2.4 Property prediction

Property prediction of biodiesel obtained from six microalgae species was carried out, and the comparative analysis was done based on the predicted properties. The empirical equations used for the same are given below.

The cetane number of the biodiesel was predicted using Eq. (3.1) [151]

$$CN = 63.41 - (0.0728 \times DU_m) + 0.03495 \times SCSF - 3.26 \times 10^{-4} \times DU_m \times SCSF \quad (3.1)$$

and,

$$DU_m = (1 \times MUFA, Cn: 1, wt\ \%) + (2 \times PUFA, Cn: 2, wt\%) + (3 \times PUFA, Cn: 3, wt\%)$$

$$SCSF = \left(\frac{1}{100}\right) \sum M \times wt\ \%\ of\ saturated\ methyl\ esters$$

where,

DU_m: degree of unsaturation, SCSF: straight chain saturation factor, M: molecular weight of FAME.

The iodine value (IV) of the biodiesel was calculated by Eq. (3.3) [159]

$$IV = \sum \frac{(254 \times D \times N)}{M} \quad (3.2)$$

where,

D: number of double bonds, N: percentage of FAME.

The cold filter plugging point (CFPP) of the biodiesel was calculated by Eq. (3.3) [152],

$$CFPP = 3.1417 \times LCSF - 16.477 \quad (3.3)$$

where LCSF: long-chain saturation factor is given by,

$LCSF = (0.1 \times C16: 0) + (0.5 \times C18: 0) + (1 \times C20: 0) + (1.5 \times C22: 0) + (2 \times C24: 0)$.

The viscosity (mm^2/s @ 40 °C), density (g/cm^3 @ 20 °C), and higher heating value (MJ/kg) of the individual methyl esters were calculated by Eq. (3.4), (3.5), and (3.6) and then the summation of properties of

individual methyl esters multiplied by their weight percentage in the biodiesel gives biodiesel property [74].

$$\ln(\nu) = -12.503 + 2.496 \times \ln(M) - 0.178 \times D \tag{3.4}$$

$$\rho = 0.8463 + \frac{4.9}{M} + 0.0118 \times D \tag{3.5}$$

$$HHV = 46.19 - 1794/M - 0.21 \times D \tag{3.6}$$

The oxidation stability of biodiesel is obtained as per Eq. (3.7) [153],

$$OS = \frac{117.9295}{X} + 2.5905 \tag{3.7}$$

where, X is the combined percentage of Linoleic (C18:2) and Linolenic (C18:3) acid.

Table 3.1 Checking validity of equation (3.1) to (3.7) with experimental observation

Property	Microalgae					
	Islam et al. [90]			Al-lwayzy and Yusaf [93]		
	Exp.	Pred.	% Error	Exp.	Pred.	% Error
Cetane number	46.6	45.71	1.9	52.0	56.6	8.8
Viscosity	5.06	3.26	35.5	4.22	4.31	2.1
Density	0.912	0.907	0.4	0.900	0.850	5.9
Heating value	39.86	39.62	0.6	40.04	38.55	3.7
Oxidation stability	N.A.	4.31	-	12.0	9.36	21.9
CFPP	N.A.	-8.6	-	N.A.	-8.1	-
Iodine value	N.A.	289.4	-	N.A.	82.4	-

As these equations are used to compare different microalgae strains, it is essential to check the validity of these equations. The validity of the above equations (Eq. (3.1) to Eq. (3.7)) has been checked by comparing their prediction against the experimental properties of

Crypthecodinium cohnii reported by Islam et al. [90] and *Chlorella protothecoides* reported by Al-lwayzy and Yusaf [93].

Table 3.1 presents the results of the above comparison. It is clear from the above table that the estimated properties match fairly well with the experimental observations except in the case of viscosity (35%) for *Crypthecodinium cohnii* and oxidation stability (22%) for *Chlorella protothecoide.* High error in the viscosity of *Crypthecodinium cohnii* is less likely to occur as the viscosity of each profiled fatty acid reported in that species is much lower than the experimentally measured value - except stearic acid (mass composition 0.56%). Similarly, the large error in the oxidation stability of *Chlorella protothecoides* may be accredited to undetected components of fatty acids in their analysis.

This study compared properties and lipid content with the help of a multi-criteria decision aid (MCDA) method called PROMETHEE-GAIA [160] using the Visual PROMETHEE software tool.

3.2.5 Detailed property estimation

The properties calculated above are valid only at a certain temperature. To know the spray, atomization, and combustion events occurring in the combustion chamber for a particular fuel, properties at a wide temperature range need to be found. Therefore, properties are calculated using suitable empirical equations, which are valid from room temperature (20 °C) up to critical temperature. The properties estimated are vapor pressure, latent heat of vaporization, liquid density, liquid viscosity, and vapor diffusivity, as these are some of the most important properties for spray and combustion of fuel [156]. Similar to the previous section, these properties are also dependent on the structure of individual FAMEs.

The first step of this analysis is the calculation of the critical properties (critical temperature, critical pressure, and critical volume) of individual FAMEs. The critical temperature and pressure are calculated using the Ambrose method, and the critical volume by the

Joback method as given in Reid et al. [161]. Table 3.2 presents the critical temperature (T_c), critical pressure (P_c), and critical volume (V_c) of common FAMEs, along with their normal boiling point temperature (T_b), which is taken from Graboski and McCormick [162]. Then, the critical properties of microalgal biodiesel, critical temperature (T_{cm}), critical pressure (P_{cm}), and critical volume (V_{cm}), are calculated by applying the Lee-Kesler mixing rule [154]. Afterward, the physical properties of biodiesel were calculated as per the following subsection. The acentric factor required for these calculations was calculated by Yuan et al. [154].

Table 3.2 Critical properties and normal boiling point of methyl esters

Methyl ester	T_b (K)	T_C (K)	P_C (bar)	V_C (cm^3/mol)
C12:0	535.15	694.13	15.26	789.50
C14:0	568.15	724.14	13.74	901.50
C16:0	611.15	767.13	12.50	1013.50
C16:1	612.15	770.34	12.76	993.50
C18:0	625.15	774.20	11.46	1125.50
C18:1	622.15	772.30	11.68	1105.50
C18:2	639.15	795.26	11.91	1085.50
C18:3	639.15	797.20	12.14	1065.50

Note: T_b *is taken from Graboski and McCormick (1998). Tc, Pc, and Vc are calculated from Reid et al. (1987).*

Vapor pressure of biodiesel

The vapor pressure of different biodiesels was calculated by using the Pitzer equation (3.8) [161], which correlates reduced vapor pressure with reduced temperature and biodiesel acentric factor value.

$$\ln\left(P_{vp_r}\right) = f^{(0)}(T_r) + \omega_m f^{(1)}(T_r) \tag{3.8}$$

where P_{vpr}: reduced vapor pressure (P/P_{cm}), T_r: reduced temperature (T/T_{cm})

$f^{(0)}$ and $f^{(1)}$ are,

$$f^{(0)} = 5.92714 - 6.096480/T_r - 1.28862 \times \ln T_r + 1.069347 \times T_r^6$$

$f^{(1)} = 15.2518 - 15.6875/T_r \ - 13.4721 \times \ln T_r + 0.43577 \times T_r^6$

Liquid density of biodiesel

The liquid density of different biodiesels was calculated by modified Racket equation Eq. (3.9) [161], which gives specific volume (V_s) at a particular temperature,

$$V_s = V_s^R (Z_{RA})^{\phi} \tag{3.9}$$

And,

$\phi = (1 - T_r)^{2\backslash 7} - (1 - T_r^R)^{2\backslash 7}$

where V_S^R : specific volume at reference temperature $T_{R,}$ T_r^R: reduced temperature (T_R/T_c) at reference temperature $T_{R,}$ Z_{RA}: unique constant for each compound

The above equation in density (kg/L) term is given as,

$$\rho = \frac{\rho^R}{Z_{RA}^{\phi}} \tag{3.10}$$

To know the constant. Z_{RA}, two reference densities at two temperatures are required; this was achieved by equations proposed by [163,164] to calculate the densities of individual methyl esters. In this case, this was done at 20 °C and 90 °C. The summation of these as per weight percentages of individual methyl esters in biodiesel gives biodiesel density at those two temperatures, from which the value of Z_{RA} can be found. The final equation for biodiesel density will be,

$$\rho = \rho_{@20\,^{\circ}C} \times {Z_{RA}}^{-\phi} \tag{3.11}$$

where,

$\phi = (1 - T_r)^{2\backslash 7} - (1 - 293.15/T_{cm}\ )^{2\backslash 7}$

Liquid Viscosity of biodiesel

The liquid viscosity at low temperature (Tr <0.7) of biodiesel was estimated by Orrick and Erbar method Eq. (3.12) [161], which gives the dynamic viscosity of pure methyl ester components.

$$\ln \frac{\eta_L}{\rho_L M} = A + \frac{B}{T} \tag{3.12}$$

where,

η_L: liquid dynamic viscosity (cP),ρ_L: liquid density (kg/L @ 20 °C), which was assumed to be the same as mixture density calculated previously, A and B were obtained by group contribution method [161].

Final biodiesel viscosity was obtained by Grunberg-Nissan method (Eq. (3.13))

$$\ln \eta_m = \sum y_i \ln(\eta_i) + \sum\sum y_i y_j G_{ij} \tag{3.13}$$

where,

η_m: biodiesel dynamic viscosity (cP), y_i: mole fractions of methyl esters present, G_{ij}: interaction parameter between components i and j. In the case of biodiesel, G_{ij} is neglected [120].

High temperature (0.7<Tr<1) liquid dynamic viscosity of biodiesel was estimated by Letsou and Stiel method (Eq. (3.14)) [161].

$$\eta_{SL}\xi = (\eta_L\xi)^{(0)} + \omega_m(\eta_L\xi)^{(1)} \tag{3.14}$$

where,

$(\eta_L\xi)^{(0)} = 10^{-3}(2.648 - 3.725T_r + 1.309T_r^2)$

$(\eta_L\xi)^{(1)} = 10^{-3}(7.425 - 13.39T_r + 5.933T_r^2)$

$\xi = 0.176\left(\frac{T_{cm}}{M^3 P_{cm}^4}\right)^{1/6}$, M = average molecular weight of biodiesel.

Latent heat of vaporization

The Pitzer correlation (Eq. (3.15)) [161] was used to determine the latent heat of vaporization at a temperature range $0.6 < T_r \leq 1$.

$$\Delta H_v = RT_{cm} \times 7.08\,[(1 - T_r)^{0.354} + 10.95\omega_m(1 - T_r)^{0.456}] \quad (3.15)$$

where,

ΔH_v: latent heat of vaporization (J/mol).

ΔH_v at the low-temperature range was estimated through Fish and Lielmez's method (Eq. (3.16)) [161],

$$\Delta H_v = \Delta H_{vb} \frac{T_r}{T_{br}} \frac{\chi + \chi^q}{1 + \chi^p} \quad (3.16)$$

And, $\chi = \frac{T_{br}}{T_r} \frac{1-T_r}{1-T_{br}}$

where,

ΔH_{vb}: latent heat of vaporization at normal boiling point (calculated as per Pitzer correlation), T_{br}: the reduced temperature at T_b (T_{bm}/T_{cm}), p = 0.13856 and q = 0.35298 [161].

Vapor diffusivity

Vapor diffusivity of individual methyl esters was estimated by the method of Fuller et al. (Eq. (3.17)) [161], where the diffusion coefficient of FAMEs into the air ($D_{AB;}$ cm^2/s) is given by:

$$D_{AB} = \frac{0.00143T^{1.75}}{PM_{AB}^{\frac{1}{2}}\left[(\sum v)^{\frac{1}{3}}_A + (\sum v)^{\frac{1}{3}}_B\right]^2} \quad (3.17)$$

where,

$M_{AB} = 2\left[\left(\frac{1}{M_A}\right) + \left(\frac{1}{M_B}\right)\right]^{-1}$

P: operating pressure (bar), M_A and M_B: molecular weights of FAMEs and air (g/mol), $\sum v$: summation of atomic diffusion volume as per Reid et al. [161].

The vapor diffusivity of biodiesel is then calculated by the summation of the diffusion coefficient of individual methyl esters multiplied by their weight percentage in the biodiesel.

Similar calculations of all the above properties were made for diesel fuel, taking $C_{14}H_{30}$ as a surrogate for diesel fuel [156]. The comparison of diesel fuel properties with that of microalgae fuel properties was made to predict their spray and combustion behavior.

3.3 Results and discussion

3.3.1 Comparison of fatty acid profile

Table 3.3 shows the percentages of different FAMEs present in biodiesel obtained from different species, and Figure 3.2 shows the total percentage of saturated fatty acid (SFA), monounsaturated fatty acid (MUFA) and polyunsaturated fatty acids (PUFA) present in them. It can be observed that FAMEs with 16 and 18 carbon atoms are mainly found in biodiesel of all microalgae species. SFA content of unicellular green microalgae is lower than cyanobacteria species *Nostoc*, *L. putealis*, and *Calothrix*. Palmitic acid (C16:0) is the main fatty acid of the SFA series. The percentage of Palmitic acid is higher in filamentous cyanobacteria, especially in *Nostoc* sp., *L. putealis*, and *Calothrix* sp. C18:0 is found only in two cyanobacterial species, *L. putealis* and *Calothrix*. The high percentage of SFA is desirous of the prospect of a higher cetane number, but the high viscosity of the resulting biodiesel leads to poor atomization of the biodiesel. PUFA content of unicellular green species is higher in general than filamentous cyanobacterial species. In fact, only two species (*Calothrix* sp. and *L. putealis*) satisfy the constraint of the EN14214 standard for Linolenic acid (C18:3 ≤ 12%). The highest percentage of Palmitoleic acid (C16:1) and Oleic acid (C18:1) was found in *L. putealis* and *Nostoc* sp., respectively. The cyanobacterium *Chroococcus* contains

PUFA comparable to unicellular green microalgae species. It is clear from the above discussion that FAME content varies largely for studied microalgae species. The high PUFA content of *Chlorella Scenedesmus* and *Chroococcus* species, high MUFA content of *L. putealis*, and high SFA content of *Calothrix* species can be limiting factors in their properties. Therefore, it would be interesting to observe differences in their predicted biodiesel properties.

Table 3.3 FAME profile (%) of biodiesel obtained from different microalgal species

Fatty acids	**Microalgae species**					
	Chlorella	*Scenedesmus*	*Chroococcus*	*Nostoc*	*L. Putealis*	*Calothrix*
C12:0	1.70 ± 0.5	3.10 ± 2.23	ND	ND	ND	ND
C14:0	3.81 ± 0.66	ND	ND	ND	3.63 ± 0.98	4.1 ± 0.06
C16:0	24.22 ±0.63	24.56 ± 0.42	25.59 ± 0.2	33.47 ± 1.36	38.06 ± 0.60	46.25 ± 4.53
C16:1	ND	ND	2.28 ± 1.16	ND	23.94 ± 0.20	17.74 ± 2.56
C18:0	0.50 ± 0.3	ND	ND	ND	3.45 ± 0.29	3.54 ± 0.62
C18:1	8.54 ± 0.79	18.37 ± 2.82	19.27 ±1.52	23.06 ± 2.12	11.21 ± 0.18	9.95 ± 0.57
C18:2	29.05 ± 1.16	33.17 ± 1.16	30.30 ± 0.39	27.14 ± 1.60	19.72 ± 0.32	18.41 ± 2.07
C18:3	32.18 ± 1.6	20.80 ± 1.49	22.56 ± 1.46	16.33 ± 1.92	ND	ND

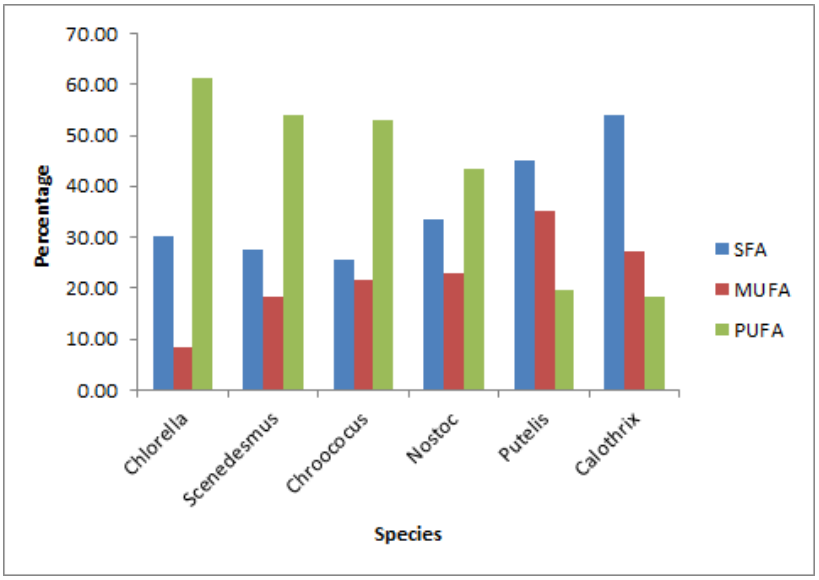

Figure 3.2 Variation in the percentage of SFA, MUFA, and PUFA in different microalgae species

3.3.2 Comparison of estimated properties

Table 3.4 presents the summary of the properties of different microalgae species. The cetane number of *Chlorella* sp. biodiesel is the lowest among all. It is found to be even lower than the limiting value of 51, as suggested by the EN14214 standard. Despite the high SFA content of *Chlorella* sp., its poor cetane number is due to the high percentage of linolenic acid. The high proportionate of oleic and linolenic acid in *Nostoc* sp. offset the advantage of high Palmitic acid. It leads to only a moderate increase in its cetane number. The low cetane number of the fuel is characterized by a high ignition delay period [106]. High ignition delay results in more fuel participation in the premixed combustion phase, which leads to higher peak pressure and peak heat release rates.

The higher peak pressure and peak heat release rates result in reduced CO and unburnt HC emissions but at the cost of increased NO_x emissions because of the high temperature developed during combustion [70]. The remaining two species have a very high cetane number, owing to the high percentage of SFA compared to PUFA. The iodine value of the biodiesel fuel represents the unsaturation level present in fatty acids. It can be seen that species with high PUFA

content have Iodine values even exceeding the limits imposed by EN14214 (< 120). *Nostoc* sp. has a moderate Iodine value, whereas *L. putealis* and *Calothrix* sp. have very low Iodine values. A higher Iodine value is an indicator of lower oxidation stability but better cold flow properties of the fuel. The reason for lower oxidation stability is the susceptibility of the double bond site to oxidation reaction, which forms unwanted compounds responsible for the deterioration of fuel quality [66]. The cloud points and pour points of unsaturated FAs are lower than saturated FAs; therefore, a higher Iodine number implies better cold flow properties of the fuel. Owing to this, CFPP values of *Chlorella* sp., *Scenedesmus* sp., and *Chroococcus* sp. are better compared to other species. The two cyanobacterial species, *L. putealis* and *Calothrix* sp., have positive CFPP values among the studied species, but only these two species have oxidation stability satisfying EN14214 norm (> 6 h).

Table 3.4 Estimated properties of different species and total lipid content

Properties	**Microalgae species**						
	Chlorella	*Scenedesmus*	*Chroococcus*	*Nostoc*	*L. Putealis*	*Calothrix*	Diesel (for comparison)
Cetane number	50.07	51.74	51.54	53.64	59.27	60.74	40-46
IV (g/100g)	141.27	127.14	129.69	109.99	66.26	57.06	--
CFPP (°C)	-8.07	-8.76	-8.43	-5.96	0.894	3.61	--
Viscosity (mm^2/s)	3.75	3.89	3.93	4.06	4.09	4.14	1.9-4.1
Density (g/cm^3)	0.882	0.88	0.881	0.878	0.873	0.871	0.740-0.840
Higher heating value (MJ/kg)	39.52	39.58	39.63	39.65	39.55	39.55	45.62–46.48
Oxidation stability (h)	4.51	4.77	4.82	5.3	8.57	8.99	--
Lipid content (%)	32.3	28.8	21.19	24.94	10.54	19.14	--

All the studied species produced biodiesel with viscosity and density values satisfying EN14214 norms. The difference in higher heating value (HHV) of studied biodiesel fuels is also not significant. In this section, the density and viscosity are calculated just to compare them against the norms. The temperature-dependent calculations of viscosity and density are discussed in the next section.

Table 3.4 also shows the result of lipid content analysis. Lipid content is a very important criterion in the selection of species for commercial biodiesel production. As expected, green unicellular species have an edge over cyanobacterial species. The highest lipid content is found for *Chlorella* sp. (32.3%), and the lowest is found for *Calothrix* sp. and *L. putealis* (19.14 and 10.54%), respectively. The low lipid content of these two species can make them undesirable for large-scale biodiesel production even though they are better in some of the properties discussed in the previous paragraph.

3.3.3 MCDA analysis

The properties and lipid content of the different species presented in Table 3.4 are compared using the MCDA (multi-criteria decision aid) software PROMETHEE-GAIA. Important aspects like lipid content, cetane number, and viscosity have been provided with an increased weighing factor (two). Rests of the properties are given a weighing factor of 1 as either they do not influence the combustion characteristics, or negligible difference is observed for these properties among different species. Figure 3.3 shows GAIA (graphical analysis for interactive aid) plot obtained from software for the studied species with the described criteria. The quality of the result reported by the software is 95.8%, showing that the variation is explained quite well by GAIA analysis.

The species are represented by points (green), and the criteria are represented by blue axes originating from the center in the GAIA plot. The position of the species and orientation of criteria axes are important in the analysis of the GAIA plane. The position of species

along the direction of the criteria vector indicates their suitable values for that criterion. For example, *Calothrix* sp. and *L. putealis* are better in terms of cetane number, density, oxidation stability, and Iodine value; therefore, they are orientated along those particular vectors. The decision axis (the thick red line) represents the importance of different criteria. Table 3.5 presents the ranking of the species as obtained from the software. The PROMETHEE ranking is done with the help of Phi (ϕ) value, which is calculated by considering how much the species is preferred based on its strengths and weaknesses compared to others. The best ranking of *Calothrix* sp. is due to its higher cetane number, high oxidation stability, low density, and low iodine value regardless of moderate lipid content. Similarly, a good ranking for *Scenedesmus* is due to its high lipid content, lower viscosity, and low CFPP. The comparison of detailed properties of these two species will be interesting as one of them is a cyanobacterial species, and the other is a green unicellular species.

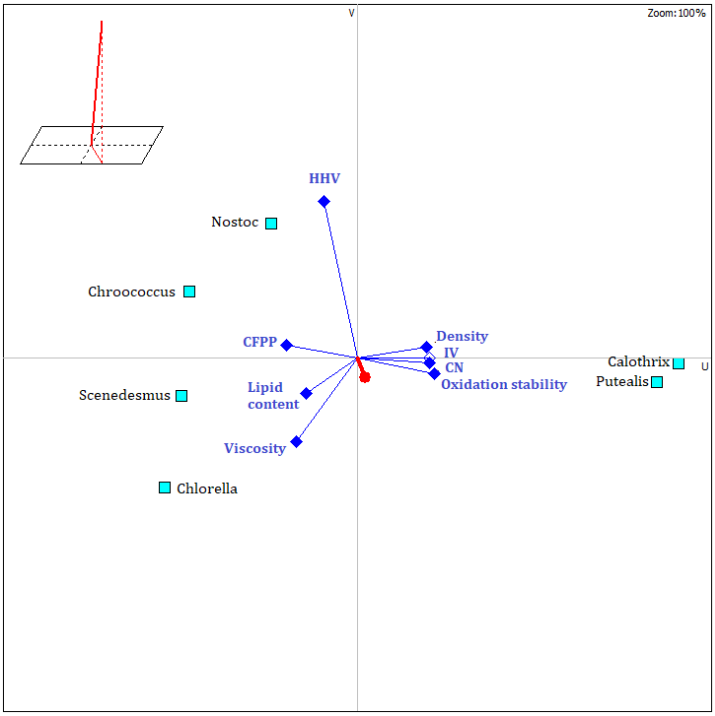

Figure 3.3 GAIA plot for species selection based on properties

It is evident from the above discussion that the biodiesel of both species has certain desirable and certain undesirable characteristics.

Also, the above analysis does not include variations of important fuel characteristics (vapor pressure, viscosity, density, etc.) with respect to fuel spray generation and combustion phenomena occurring inside the combustion chamber. Therefore, to have an exhaustive comparison of the properties of these two species, property estimation has been carried out for the extended temperature scale, considering the significance of fuel injection and combustion process inside the diesel engine.

Table 3.5 PROMETHEE table showing the ranking of species

Rank	Species	Phi
1	*Calothrix* sp.	0.1006
2	*Scenedesmus* sp.	0.0231
3	*Chlorella* sp.	0.0004
4	*Chroococcus* sp.	-0.0331
5	*Lyngbya Putealis*	-0.0424
6	*Nostoc* sp.	-0.0487

3.3.4 Comparison of detailed properties of two microalgal biodiesel

This section presents a comparison of the detailed temperature-dependent biodiesel properties of two species (*Calothrix* species and *Scenedesmus* species) and also with diesel surrogate fuel ($C_{14}H_{30}$). The critical properties of the surrogate fuel are taken from Reid et al. [161]. Figure 3.4 presents the vapor pressure of biodiesel from two microalgae species. It is observed that the vapor pressure of fuel increases with an increase in temperature. The high vapor pressure of fuel promotes a higher evaporation rate at the droplet surface, which is helpful for the initiation of combustion inside the diesel engine [156,165]. Figure 3.4 clearly indicates that the vapor pressure of *Calothrix* sp. species biodiesel is found to be around 15% higher than that of *Scenedesmus* species for the studied temperature range. As a consequence, *Calothrix* sp. is slightly better in terms of vapor pressure.

The vapor pressure of both microalgal biodiesel is significantly lower ($1/12^{th}$ at room temperature and 1/3rd at critical temperature) than that of diesel surrogate fuel.

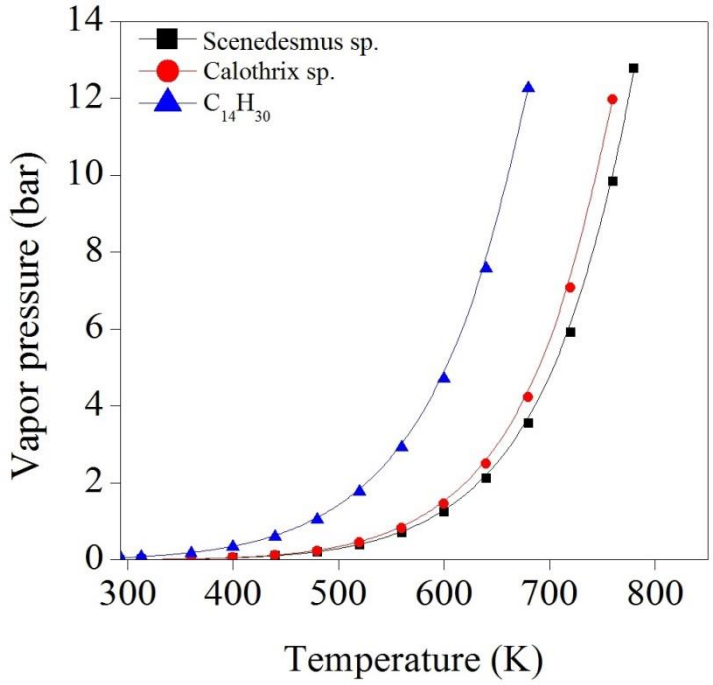

Figure 3.4 Comparison of the vapor pressure of two species and diesel surrogate fuel

Figure 3.5 presents the density of microalgae biodiesel and diesel surrogate fuel. The density of the fuel affects the flow of fuel droplets in the combustion chamber. Too high density will produce sprays with large sauter mean diameters (SMD) and high axial penetration lengths, which can impinge on the piston walls [165]. Too low density can reduce the possibility of air-fuel mixing because of the very low momentum of the traveling droplets inside the combustion chamber [156]. The average density of *Scenedesmus* sp. biodiesel is 1.9% higher than *Calothrix* sp. biodiesel. Also, as expected, the density of diesel surrogate fuel is very low compared to microalgae biodiesel. The densities of the two microalgae biodiesel are 13% higher than that of diesel surrogate fuel at room temperature. This difference increases to 38% at the critical temperature of the surrogate fuel.

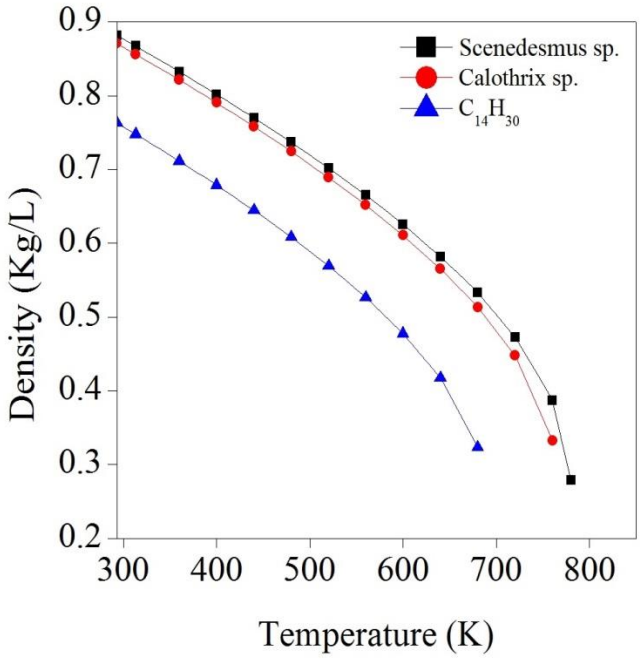

Figure 3.5 Comparison of density of two species and diesel surrogate fuel

Figure 3.6 presents the viscosity of two microalgal species, biodiesel, and diesel surrogate fuel. Viscosity is one of the most important properties affecting the spray and combustion characteristics of the diesel engine. The low viscosity of the fuel promotes better atomization and spray characteristics that result in the formation of very fine liquid fuel droplets. This enhances the fuel vaporization rate to facilitate the formation of a combustible air-fuel mixture [156]. The viscosity of *Calothrix* species biodiesel is 16.41% higher than that of *Scenedesmus* species biodiesel at 293 K. After around 400 K, this trend reverses. This can be accredited to a higher rate of decrease in the viscosity of saturated fatty acids in comparison to unsaturated fatty acids with an increase in temperature. Because fuel is injected at a lower temperature range, the spray breakup process is affected most by viscosity at that temperature range [165]. Therefore, lower-viscosity biodiesel is expected to have better spray and atomization characteristics. The *Scenedesmus* sp. is better in terms of this property. Also, the average viscosity of the two microalgae species' biodiesel is around 2.5 times higher than that of diesel surrogate fuel.

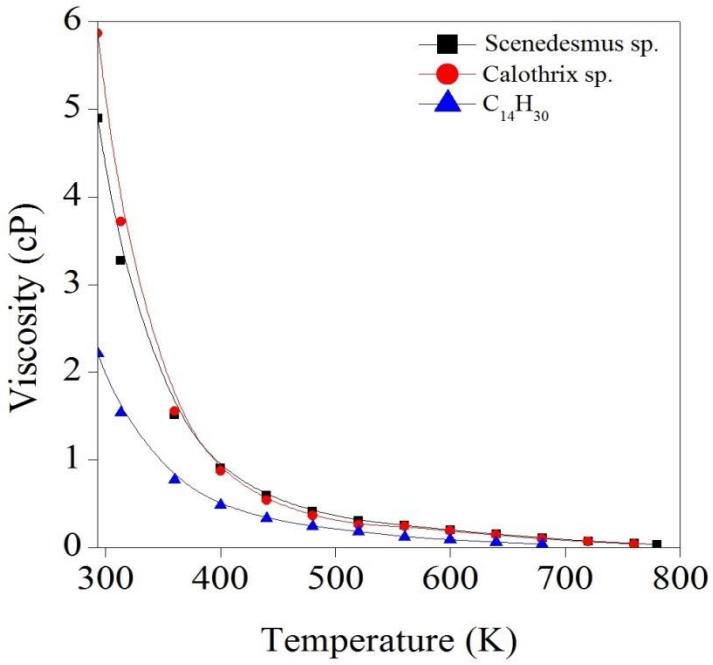

Figure 3.6 Comparison of the viscosity of two species and diesel surrogate fuel

Figure 3.7 presents the latent heat of vaporization of microalgae species and diesel surrogate fuel. Fuel with high latent heat of vaporization will require more heat for vaporization, which is undesirable. The ultimate influence of this property is expected to be the same on engine performance, as explained earlier in the vapor pressure part. The difference in latent heat of vaporization between *Calothrix* sp. and *Scenedesmus* sp. is negligible (average difference of 2.6%). It is found that the latent heat of vaporization of microalgae biodiesel is around 35% higher at room temperature than diesel surrogate fuel, which increases up to around 65% at the critical temperature of diesel surrogate fuel.

Figure 3.8 presents the vapor diffusivity of microalgae species and diesel surrogate fuel. Vapor diffusivity governs how fast fuel vapors can diffuse into the air inside the combustion chamber [156]. The difference in vapor diffusivity of the two microalgal species' biodiesel is very low (1.6%) throughout the temperature range. Diesel surrogate

fuel has higher vapor diffusivity (15.7% high) compared to microalgae biodiesels.

Based on this section of the current study, it is found that for *Calothrix* sp., higher vapor pressure is favorable, whereas for *Scenedesmus* sp., lower viscosity is desirable from the prospect of ideal fuel. Since viscosity is the dominant factor in the spray and combustion process, it has the ability to compensate for the vapor pressure. The difference in the rest of the properties (density, latent heat of vaporization, and vapor diffusivity) of both species is almost negligible (*Calothrix* sp. is slightly superior). However, the higher lipid content of *Scenedesmus* species (50.4% higher than *Calothrix* sp.) cannot be overlooked, considering the large-scale commercial biodiesel requirement. Hence, considering better commercial viability, the *Scenedesmus* sp. seems a superior alternative to *Calothrix* sp. The method used in the study is useful in an initial assessment of different microalgae species for checking their suitability as a source of biodiesel. This method is simple and less laborious and compares microalgae species based on their fatty acid composition without requiring cultivation at a large scale. Even though the individual effect of properties on different in-cylinder processes has been mentioned, the spray and combustion behavior is an intricate process governed by the combined effect of properties as well as external factors like the geometry of the engine, load, speed condition, etc. But still, some level of understanding regarding the quality of the biodiesel can be achieved by comparison of described properties. The exact effect of particular biodiesel on in-cylinder processes can be better understood by experiment only. Therefore, the next part of the study focuses on cultivation in raceway ponds to obtain biomass and carry out performance and emission tests on diesel engines.

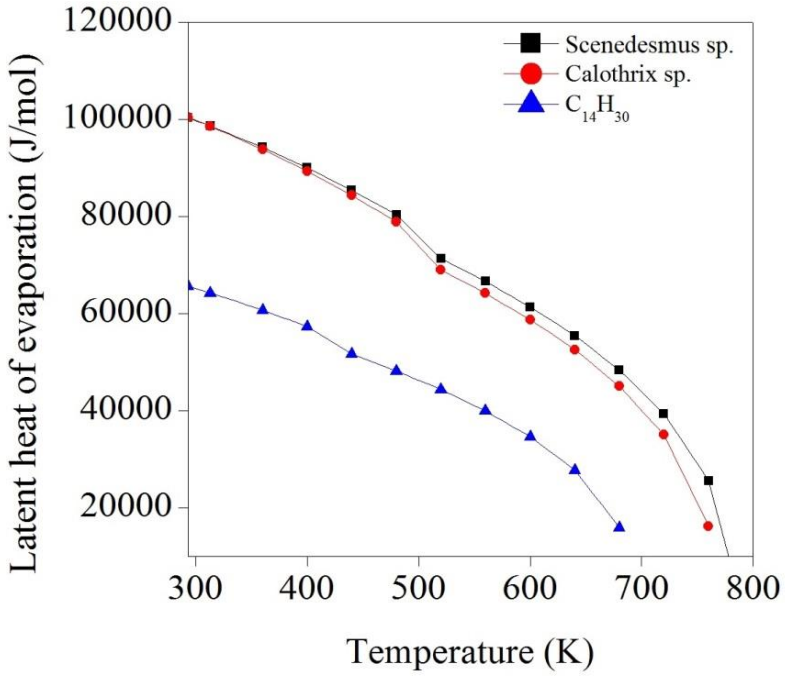

Figure 3.7 Comparison of LHV of two species and diesel surrogate fuel

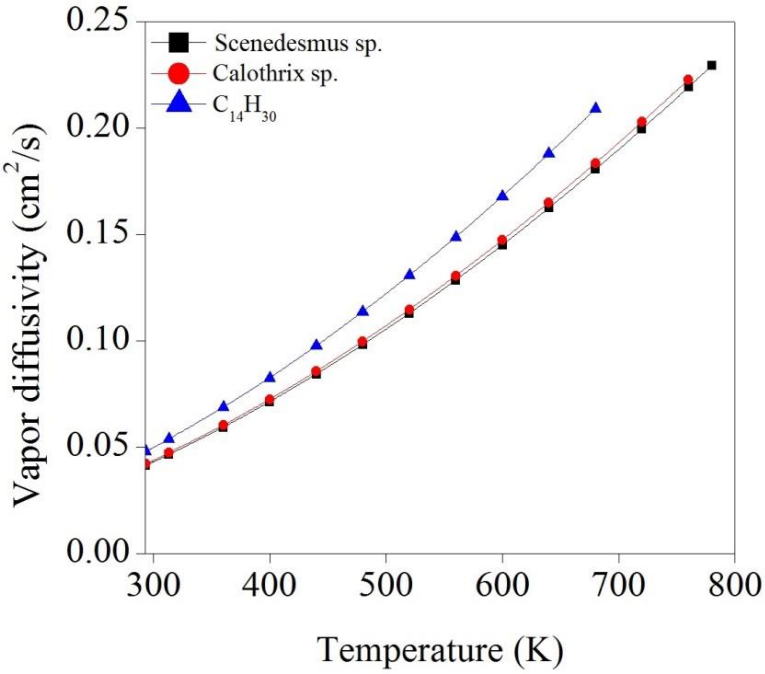

Figure 3.8 Comparison of vapor diffusivity of two species and diesel surrogate fuel

3.4 Conclusions

The fatty acid composition of biodiesel strongly indicates its properties and, hence, spray and combustion behavior. The fatty acid profile of the studied species showed a higher PUFA percentage for green algae species compared to cyanobacterial species. Fatty acids with sixteen and eighteen carbon atoms are found abundant in all the species. Because of the high PUFA content in *Chlorella* sp. and *Scenedesmus* sp., they were found to have low cetane number and high density compared to other species, except *Chroococcus* sp., which showed high PUFA despite being from cyanobacterial class. However, the viscosity of *Chlorella* sp. and *Scenedesmus* sp. was observed to be better as compared to others. Cetane number, viscosity, and density values were as per EN14214 standard for all the species. The iodine values of biodiesel from only three species were as per standard, whereas only two species followed the standard for oxidation stability. There was not much variation in the case of HHV amongst species. As expected, the lipid content of two green algae species was higher than that of cyanobacterial species. This shows their high potential for large-scale biodiesel production.

Based on this analysis, the MCDA tool has ranked *Calothrix* sp. and *Scenedesmus* sp. as first and second, respectively. Extended property analysis of these two species shows that the higher vapor pressure of the former and the low viscosity of the latter is their decisive fuel characteristic. Density, latent heat of vaporization, and vapor diffusivity are not too different for the two species. However, the lipid content of *Scenedesmus* species is much higher, which makes it more suitable for large-scale biodiesel production.

The next chapter discusses the outdoor cultivation of the selected species in raceway ponds to obtain microalgae biomass for biodiesel production.

4 LARGE-SCALE CULTIVATION TO OBTAIN MICROALGAE BIOMASS

After selecting species (chapter 3), the next step is cultivating microalgae biomass for biodiesel production. The selected microalgae species is grown under semi-outdoor conditions in raceway ponds for that purpose. The current chapter describes the outdoor cultivation of microalgae *Scenedesmus* species and subsequent biodiesel production from biomass.

4.1 Construction of raceway ponds and polyhouse

This part of the study focuses on the large-scale cultivation of microalgae species to produce biodiesel and evaluate its use in CI engines for performance and emission characteristics. The raceway ponds were constructed, as shown in Figure 4.1. The cement concrete oval-shaped raceway ponds have a paddlewheel mechanism to enable water circulation around the partition constructed at the center. The paddlewheels are made of polypropylene and are operated by motors equipped with variable frequency drives to control the speed. A total of 6 ponds were constructed: four with a total capacity of 1000 liters and two with a total capacity of 5000 liters. The ponds were tested for water leakages by storing water for 10-day period. The sprinkler system, as well as the fan and pad system, was installed for cooling and humidifying the inside environment. Thermometers were placed at different locations to take temperature readings. The small buffer room was also constructed at the entrance to prevent outside dust contamination and also for material storage.

4.2 Preparation of inoculum for raceway ponds

For large-scale biomass production, *Scenedesmus* sp. species have been selected based on the study from the previous section. The

process was initialized by first growing the species in two-liter flasks in the laboratory (Figure 4.2). The culture for this was taken from the mother culture. Instead of using the DI water in this case, autoclaved tap water has been used, keeping laboratory conditions of light (2800 lux with 12:12 hour light/dark cycle) and temperature (at 30 ± 3 °C). The standard BG11 media was replaced by more economical urea (1g/liter) and DAP (0.134g/liter). The calculation for the same has been done in view of the level of nitrate and phosphate in BG11 media. After the successful adaptation of species in new media and autoclaved tap water, the biomass was transferred to 20-liter bottles provided with bobbling by an aquarium air pump (Figure 4.2). In this step, normal tap water was used without an autoclave, keeping other conditions the same as in the previous step. It was observed that species showed sufficient growth in these conditions in most of the bottles. After the 12^{th} day, when the culture was in an exponential growth phase, it was transferred to a 200-liter polypropylene tank in the polyhouse. After initial difficulties, such as contamination of fungi or other microalgae species, the species was successfully acclimatized to new conditions. The culture was then used as an inoculum for raceway ponds. Throughout the process, the purity of the culture was checked regularly under the microscope, as shown in the figure.

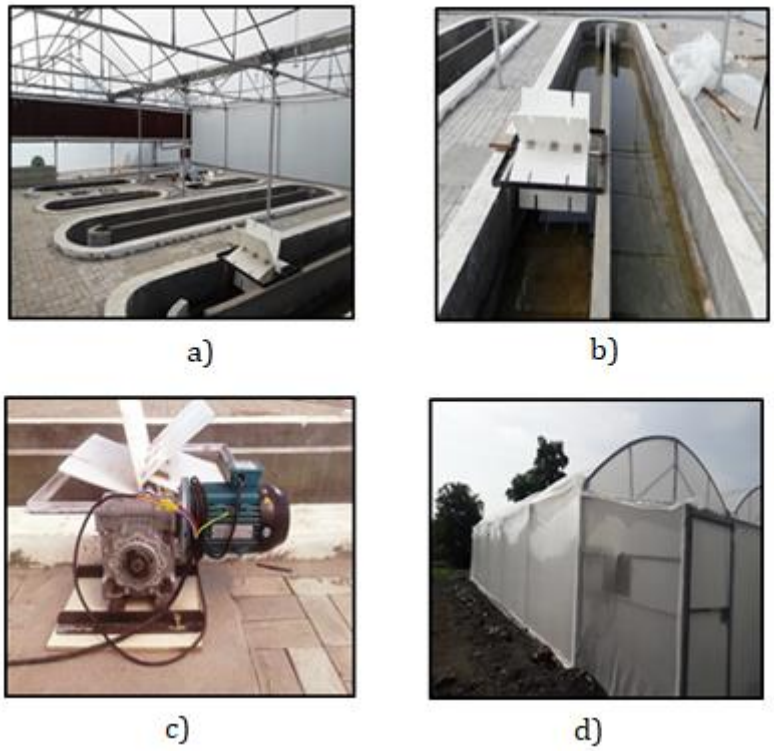

Figure 4.1 Polyhouse and open raceway ponds facility

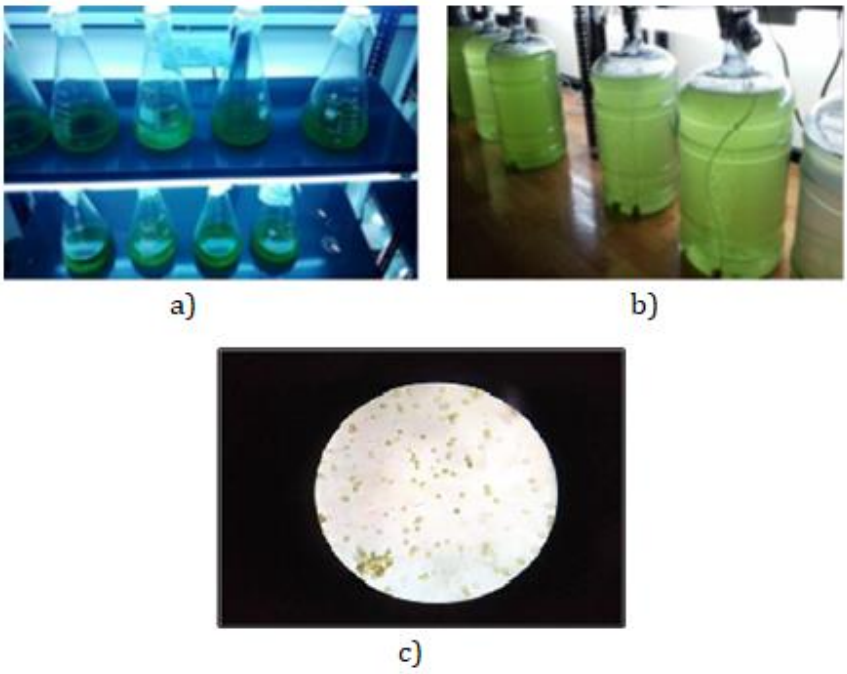

Figure 4.2 Inoculum preparation for raceway ponds

4.3 Growth, harvesting, and drying

Figure 4.3 shows the cultivation of microalgae in raceway ponds. The growth was found to be quite satisfactory, as can be seen in the figure. It was observed that once *Scenedesmus* species started to grow at sufficient speed, it became dominant over other contaminants and utilized the nutrients effectively to make the culture sufficiently pure. After 15 days of growth in the ponds, the whole culture was allowed to settle at the bottom, and step-by-step harvesting was performed to obtain wet biomass with minimum water content, as shown in Figure 4.4. The upper water layer was discarded or used for another pond based on the availability, and the lower wet biomass was collected in a 1000-liter pond left specifically for that purpose. The culture was again allowed to settle there for 24 hours, after which the upper layer was again discarded. The lower wet biomass paste was then collected manually in plastic tubs kept for the sun-drying process. During harvesting, the cultivation for the next batch of biomass was started simultaneously in raceway ponds using around 10% of the lower layer of wet biomass as inoculum.

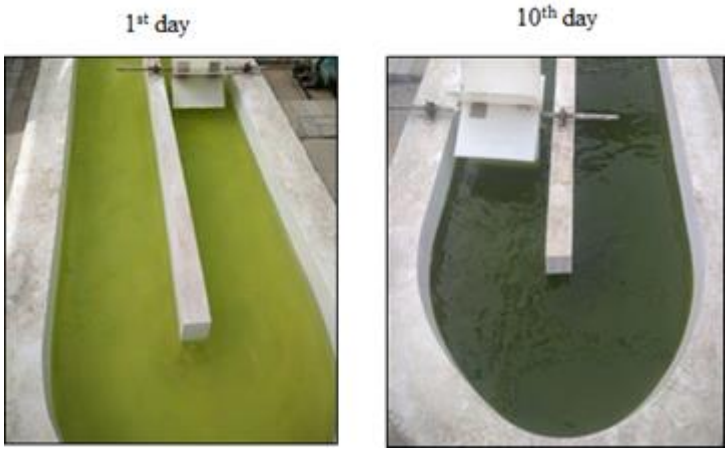

a)

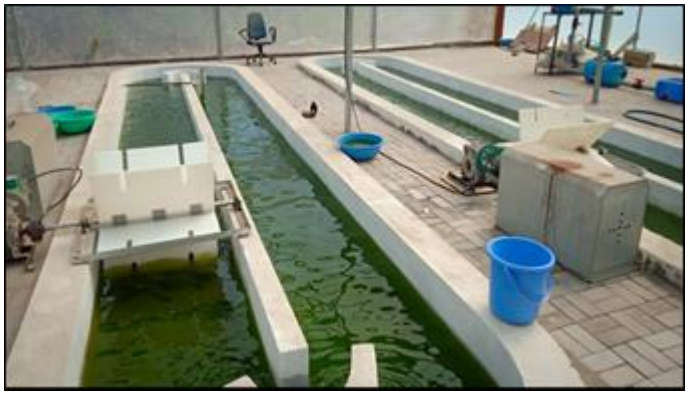

b)

Figure 4.3 Growth in raceway ponds a) small tank b) large tank

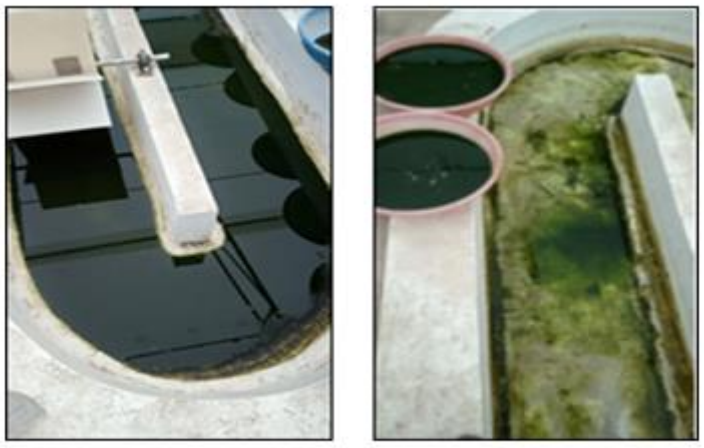

a) b)

Figure 4.4 Step by step harvesting of the biomass

a) b)

Figure 4.5 Sun drying of biomass in tubs

Figure 4.6 Dried microalgae biomass

4.4 Oil extraction and conversion to biodiesel

The dried biomass was collected and processed to make fine powder, as shown in Figure 4.6. The total dry microalgae biomass obtained was 12.3 kg in the cultivation period of four months. The oil extraction was carried out using the soxhlet extraction method with n-hexane as a solvent with a 2-liter capacity apparatus, as shown in Figure 4.7. For 1 kg biomass, around 24-hour extraction time was found to be sufficient for optimum yield. In this way, the oil yield of 14.2% was obtained using the soxhlet extraction method. The extracted oil was then separated by hexane using a rotary evaporator. Additionally, Pongamia oil was purchased from a local supplier for its conversion to biodiesel as a second-generation biodiesel source.

The oil-to-biodiesel conversion of Pongamia oil is carried out by a two-stage transesterification method, as its FFA content was around 10%. In the first stage, the reaction of the oil with methanol (methanol to oil molar ratio 1:6) is performed at 65° C for 1.5 h in the presence of catalyst 1% sulfuric acid (w/w of oil). In the second stage, the reaction is performed keeping the same operating parameters in the presence of NaOH (0.5%) catalyst. The microalgae oil is transesterified with a single-stage process with NaOH catalyst as described above, as the FFA content was very low. The prepared fuels are shown in Figure 4.8. The fatty acid content of the *Scenedesmus* sp. and Pongamia biodiesel was determined using GC analysis (Table 4.1). The FAME profile shows that Scenedesmus sp. biodiesel consists of almost two times

higher SFAs than pongamia biodiesel. The higher SFAs increase the cetane number of the fuel. On the other hand, they increase the viscosity and deteriorate fuel's usefulness in cold climatic conditions. It also has a higher proportion of PUFA (29.75%) than that of pongamia biodiesel (20.79%). Very high PUFA content is detrimental as it adversely impacts the fuel properties such as calorific value and density. The double bonds in PUFAs are prone to oxidation; therefore, higher PUFA content impacts the long-term stability of biodiesel. One desired effect of higher PUFA content is the low viscosity of fuel. As can be seen in Table 4.1 that, pongamia biodiesel contains very high (54.99%) MUFAs and lesser linolenic acid (C18:3) than *Scenedesmus* sp. biodiesel. This seems to compensate for the low SFA percentage in pongamia biodiesel. Interestingly, outdoor cultivation affected the fatty acid composition as it was slightly different for the same species under laboratory conditions and different media [166]. The outdoor conditions and seasonal changes affect the FA growth in cells as also evident from literature studies [167,168]. Based on the fatty acid analysis, the thermo-physical properties of the biodiesel were estimated as per section 3.2.4 (Table 4.2). The biodiesel properties are found to justify the EN14214 biofuel property standard [64]. The viscosity of pongamia biodiesel was slightly higher than *Scenedesmus* sp. biodiesel due to very high mono-unsaturated fatty acid content. Its latent heat of vaporization was also higher as compared to *Scenedesmus* sp. biodiesel. However, pongamia biodiesel was better than *Scenedesmus* sp. biodiesel when density, cetane number, and calorific value were compared. In these experiments, the blends of microalgae biodiesel with diesel will be tested in diesel engines for combustion and emission evaluation. Additionally, to improve the performance of biodiesel, the application of fuel additives will also be carried out.

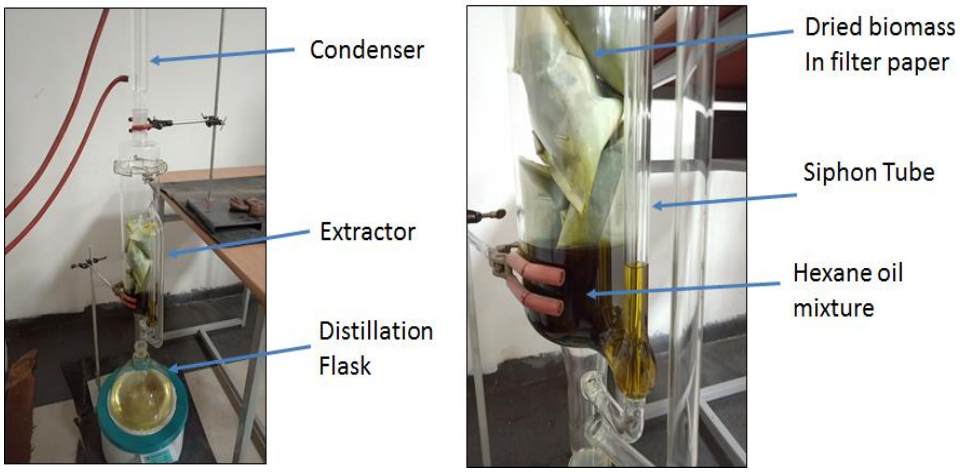

a)

b)

Figure 4.7 Soxhlet oil extraction and hexane evaporation to separate oil

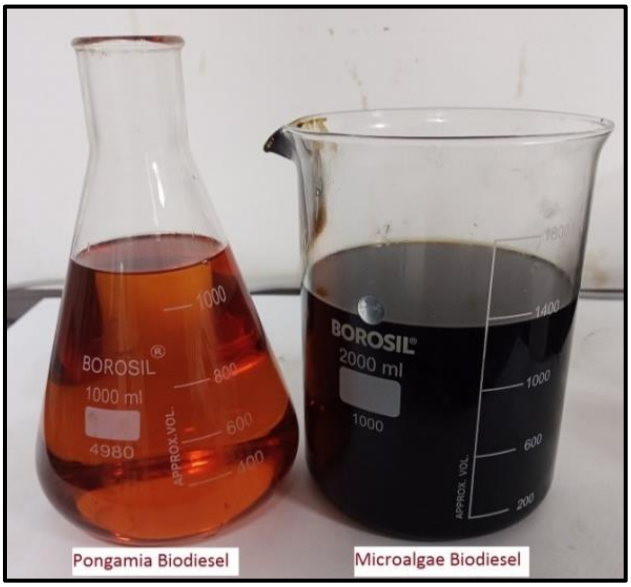

Figure 4.8 *Scenedesmus* sp. and Pongamia biodiesel

Table 4.1 FAME composition of *Scenedesmus* sp. and pongamia biodiesel

Sr. no	FAME	Percentage (%)	
		Scenedesmus sp.	Pongamia
1	C14:0	1.78	
2	C16:0	32.79	9.94
3	C16:1	1.81	
4	C18:0	3.86	7.06
5	C18:1	15.68	53.73
6	C18:2	15.99	17.61
7	C18:3	13.76	3.18
8	C20:0		1.54
9	C20:1		1.26
	SFA	38.43%	18.54
	MUFA	17.49%	54.99
	PUFA	29.75%	20.79

Table 4.2 Estimated properties of *Scenedesmus* sp. and pongamia biodiesel based on FAME profile

Properties	***Scenedesmus* sp.**	**Pongamia**	**Diesel** [64]
Cetane number	55.75	56.32	40-46
Viscosity (mm^2/s)	4.17	4.75	1.9–4.1
Density (g/cm^3)	0.880	0.875	0.750-0.840
IV (g/100g)	91.7	86.67	-
CFPP (°C)	1.97	-2.26	-
Calorific value (MJ/kg)	39.6	39.8	45.62–46.48
Latent heat of vaporization [a] (KJ/mol)	58.83	59.41	-
Oxidation stability (h)	6.1	8.26	-

a : represented at boiling point of biodiesel

4.5 Conclusions

1. The growth of *Scenedesmus* sp. in outdoor cultivation was found to be quite adequate with low-cost urea-DAP as nutrient media. However, an overall biomass production rate of 3.07 kg per month could only be obtained because of a simple and economical method for harvesting (gravity sedimentation).
2. The oil yield of 14.2% was achieved through n-hexane as a solvent and soxhlet apparatus.
3. Advanced methods for harvesting, drying, and oil extraction can increase the biodiesel production rate through microalgae, but that will increase the cost of biodiesel production.
4. The biodiesel produced from *Scenedesmus* sp. had high PUFA content and acceptable SFA content. Nevertheless, it displayed thermophysical properties within the range specified by international standards.

5 EVALUATION OF FEASIBILITY OF USING MICROALGAE BIODIESEL IN DIESEL ENGINE

5.1 Introduction

The prepared *Scenedesmus* sp. biodiesel (discussed in the previous chapter) needs to be evaluated for its usefulness as a fuel for diesel engines. For this purpose, the engine performance and emission characteristics are examined experimentally. Because of the intricate biodiesel production process from microalgae, there are very few studies in the literature evaluating microalgae biodiesel blends in the diesel engine. These studies were presented in chapter 2 of the thesis (section 2.5.3). In this chapter, microalgae biodiesel blends, with 20% and 30% (A20 and A30) biodiesel in diesel, are tested and compared with conventional diesel fuel. The experimental procedure and results of the work are explained in the following sections.

5.2 Experimental setup

The evaluation of *Scenedesmus* sp. biodiesel was carried out in a water-cooled turbocharged four-cylinder indirect injection (IDI) diesel engine. The details of the engine and schematic drawing are presented in Table 5.1 and Figure 5.1, respectively. The experiments were conducted by varying the load from zero to full load, keeping the speed constant at 2500 rpm. The load variation was achieved by an eddy current dynamometer, and the load was measured by an S-type load cell. The piezoelectric pressure transducer measured the in-cylinder pressure, whereas a crank angle encoder was attached to measure the crank position with respect to TDC. Other parameters such as temperature, air flow rate, and fuel flow rate were determined with the help of thermocouples (Type K and pt100), an airflow transmitter, and a fuel flow transmitter. Exhaust gas was sampled through an AVL Di-

gas 444N gas analyzer and NETEL smoke meter to measure exhaust emissions. The data acquisition unit was used to record various experimental readings by averaging data received for 50 cycles. The engine was allowed to run for a few minutes during each test to attain steady conditions before taking the readings. For biodiesel blends, the remaining fuel after each reading completion was removed, and the engine was operated with diesel again for some time to prevent fuel deposits if any.

The uncertainty analysis of the experimental results was performed as given in [169]. The accuracy of instruments and percentage uncertainty values of various parameters is presented in Table 5.2. The uncertainty (w_R) of dependent parameters was calculated by using eq. (5.1).

$$w_R = \sqrt{\left[\left(\frac{\partial R}{\partial x_1} w_1\right)^2 + \left(\frac{\partial R}{\partial x_2} w_2\right)^2 + \cdots + \left(\frac{\partial R}{\partial x_n} w_n\right)^2\right]} \tag{5.1}$$

Here, R is a function of independent variables x_1, $x_2 \ldots x_n$; whose uncertainties are w_1, $w_2 \ldots w_n$.

Table 5.1 Details of the engine used in the experiment

Parameter	Specification
Make/Model	Tata Indica, Type 475 IDI Turbo Diesel
Engine type	4 stroke 4-cylinder diesel
Cooling	Water-cooled
Injection type	Indirect injection
Aspiration	Turbocharged
Rated power	52 kW @4500 rpm
Bore X stroke	75 mm x 79.5 mm
Compression ratio	18.5:1
Fuel injection	23° BTDC
Dynamometer	Eddy current, water-cooled

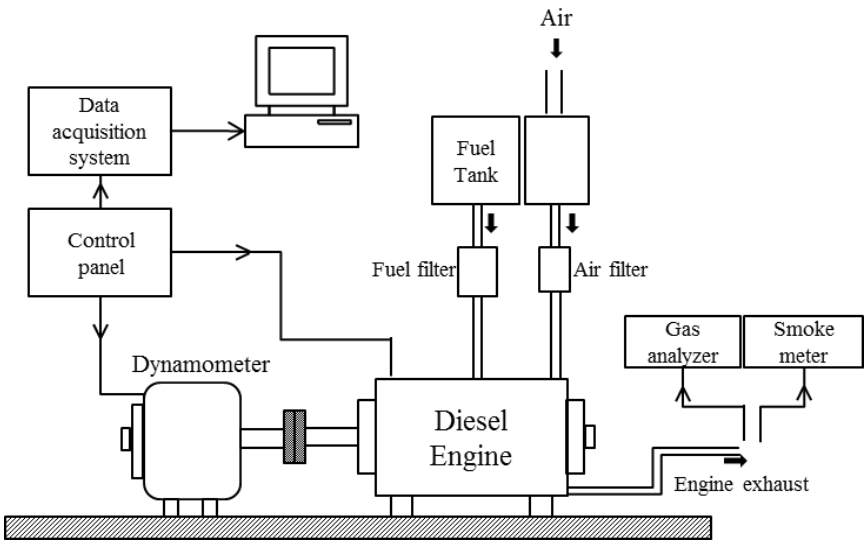

Figure 5.1 Schematic diagram of the engine test rig

Table 5.2 Uncertainty of experimental results for various parameters

Parameter	Accuracy	% Uncertainty
Engine speed (rpm)	±10	0.5
Load (kg)	±0.025%	0.3
Fuel flow (kg/h)	±0.065%	1.6
Pressure (bar)	± 0.1 bar	0.6
Crank angle (degree)	±1°	0.3
Brake power (kW)	-	0.7
BTE (%)	-	1.8
BSFC (kg/kWh)	-	1.8
NOx emission (ppm)	±5 ppm	2.1
CO_2 emission (%)	±0.3%	1.3
Smoke emission (HSU)	-	1.8

5.3 Results and discussion

5.3.1 Performance Characteristics

Figure 5.2 shows the comparison of brake thermal efficiency (BTE) of the engine for different fuels considered in this study. BTE represents the useful energy generated from chemical energy produced by fuel

combustion. The BTE increases with load due to higher temperature and reduced friction losses at higher loads. It was also observed from Figure 5.2 that when microalgae biodiesel blends were used, the BTE of an engine was lower compared to the same for diesel. This effect was consistent with other studies in the literature [102,103]. The lowered BTE for biodiesel blends can be attributed to the low calorific value, high viscosity, and density of microalgae biodiesel (see Table 4.2). It also has a high latent heat of vaporization (LHV) [156]. These properties affect the spray and atomization event, which ultimately induces larger droplet formation and inferior fuel evaporation rate [170]. At 25% load condition, the BTE for A20 and A30 blends were 6.8% and 10.1% lower than diesel. This difference reduces at the full load where BTE for A20 and A30 blends were 1.1% and 3.6% lower than diesel. Biodiesel also has inherent oxygen content and improved lubricity, which aids in a better combustion process. This effect can be seen at above 50% loads for the A20 blend, where its BTE was almost similar to that of diesel. The difference in BTE between A20 and A30 blends was observed to be an average of 3.4%, which meant the increase in blend percentage decreased the BTE. Overall, the inferior properties like viscosity, density, calorific value, and LHV adversely affected the BTE, but the oxygen content, lubricity, and early combustion start due to high cetane number had a positive effect on BTE. Therefore, biodiesel blends had comparable performance to diesel.

Figure 5.3 shows the comparison of brake-specific fuel consumption (BSFC) of the engine for different fuels. The BSFC trend is complementary to BTE values for different fuels. It is a measure of the fuel consumption rate of an engine per unit of brake power produced. It can be observed that blends of *Scenedesmus* species biodiesel had higher BSFC values than diesel at all loading conditions. The average BSFC of A20 and A30 blends were 5.2% and 9.7% higher than diesel. This can be credited to inferior viscosity and density, which causes slightly poorer air-fuel mixing. Furthermore, the lower calorific value

of microalgae biodiesel means more fuel for the same amount of energy to be produced. The difference in BSFC at lower loads is larger than the difference at full load because of improved combustion at full load conditions.

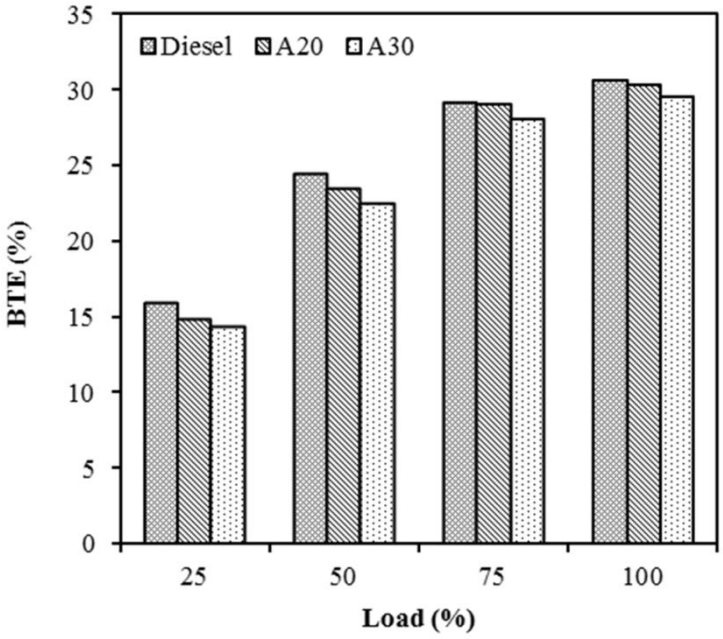

Figure 5.2 Variation of BTE with load

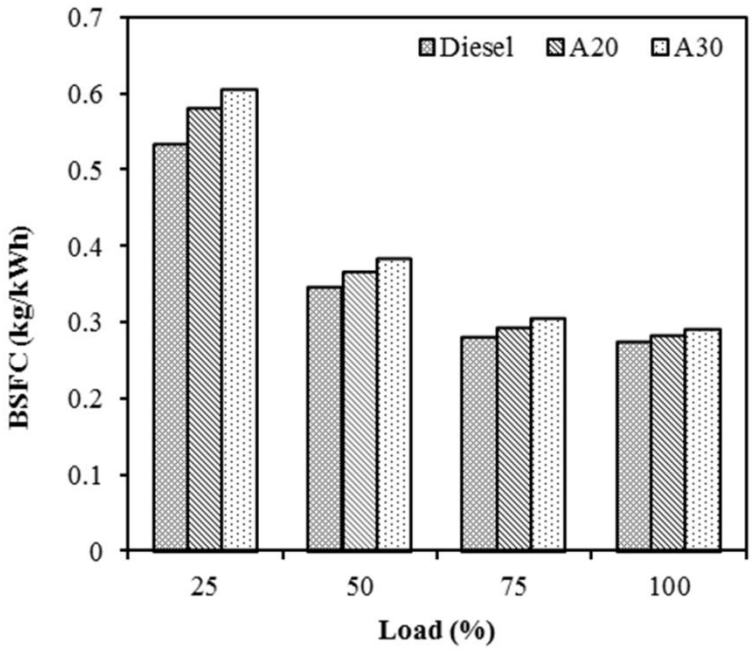

Figure 5.3 Variation of BSFC with load

5.3.2 Combustion characteristics

Figure 5.4 compares the in-cylinder pressure variation for diesel and microalgae biodiesel blends. The engine under consideration in the current experiment is of indirect injection (IDI) type. IDI engines have a swirl chamber or pre-combustion chamber along with the main chamber where the fuel is injected and air-fuel mixing occurs. Therefore, the air-fuel mixing is slightly more effective in this case as compared to direct injection engines. As can be seen from Figure 5.4, the difference in pressure values for fuels used in the study is not too high, with slightly higher peak pressure values for biodiesel blends. This is in agreement with previous studies where increased peak pressure for biodiesel blends was observed in the case of an IDI diesel engine [171–174]. Also, with an increase in blend percentage, higher peak pressure values were obtained except at full load, where the difference in peak pressure became very small. This is because, at full load conditions, additional factors such as very high temperature also play a crucial role in combustion.

Figure 5.5 compares the heat release rate (HRR) variation for diesel and microalgae biodiesel blends. In a typical diesel engine, the combustion of the fuel is divided into premixed combustion, diffusion or controlled combustion, and after-burning. The first two phases are important deciding factors regarding the engine operation. The high cetane number of biodiesel leads to short ignition delay. As the combustion started earlier, the premixed combustion phase was completed earlier for biodiesel blends, resulting in higher HRR values initially. This is evident from Figure 5.5, especially at 50% and higher load conditions. The oxygen content of the biodiesel blend also contributed to the difference in HRR trends of diesel and biodiesel blends [172]. For blends with a higher biodiesel percentage (A30), peak HRR was attained earlier than other fuels because of the aforementioned reasons. This was in agreement with previous studies [170,172]. However, the overall difference between HRR values of

biodiesel blends and diesel was found to be small, indicating the suitability of the biodiesel blend for diesel engine operation.

Figure 5.6 shows the exhaust gas temperature (EGT) for microalgae biodiesel blends and diesel. It was observed that the EGT was highest for the A20 blend, followed by diesel, except for the no-load condition. At no load, the EGT of different fuels was almost similar, which can also be seen from the HRR graph (Figure 5.5) at no load condition. The reason for the high EGT of A20 at other loads is the inherent oxygen content of the biodiesel that facilitates the combustion reaction. Therefore, the in-cylinder temperature developed tends to be higher for lower biodiesel blends. The higher cetane number and the early start of combustion are also the reasons behind high EGT [103]. For the A30 blend, worsening properties such as viscosity, density, and LHV adversely affected the spray and atomization process. Also, the high cetane number and short ignition delay of the A30 blend resulted in high HRR during the premixed combustion phase (Figure 5.5), but the EGT was somewhat lower considering the entire combustion range due to inferior properties. The longer ignition delay, absence of inherent oxygen, and more diffusion combustion resulted in a marginally lower EGT of diesel compared to A20. Nonetheless, the difference in EGT of the fuels used is in the range of 1.5% to 2.5% only.

5.3.3 Emission characteristics

The IDI diesel engines produce fewer emissions as compared to DI engines [172]. In this study, it was observed that the emissions of HC and CO were very low and within the error limit of the instrument used. Therefore, only NOx and smoke emissions are presented in the following paragraphs. Figure 5.7 compares the NOx emissions emitted under different loading conditions. Nitrogen is inert at normal temperature and pressure conditions. However, the temperature developed during the combustion is very high, in the range of 1500° C to 2500° C for the current study. At such high temperatures, nitrogen becomes reactive and forms oxides of nitrogen by reaction with oxygen. NOx formation is categorized based on the mechanism of

formation as thermal NOx, prompt NOx, and fuel NOx. In thermal NOx, Zeldovich mechanism consisting of a reaction of oxygen with nitrogen at a very high temperature is involved [102]. Prompt NOx reaction consists of hydrocarbon fragments reacting with nitrogen to form unstable compounds, which then react with oxygen to form NOx [102]. Prompt NOx mechanism forms around 30% of total NOx emissions [162]. Fuel NOx is formed from nitrogen present in the fuel itself.

NOx formation is typically governed by temperature, the residence time of fuel (combustion duration), and the oxygen content of the fuel. Figure 5.7 shows that NOx emissions were highest for diesel as compared to biodiesel blends. In the literature, some studies found an increase in NOx emissions, whereas some other studies reported reduced NOx emissions with the use of biodiesel. Some authors argued that the increase in cetane number and reduced ignition delay lead to increased NOx emissions. However, a counterargument was made in which it was claimed that high cetane number and short ignition delay, in fact, reduce NOx emission [88,93,175]. This could be the possible reason for the reduced NOx emission of biodiesel blends in the current study. Also, as seen in Figure 5.6, the difference in EGT of the fuels was not large. Therefore, oxygen content and residence time could have been more influencing factors than temperature. The oxygen content of A30 is slightly more than that of A20, which leads to its higher NOx emissions, especially at high loads, but it was still lower than diesel. This also shows that higher blends of biodiesel (>A30) may emit more NOx emissions than diesel. Overall, NOx emissions were lower by an average of 13.1% and 10.7% for A20 and A30 blends, respectively, than that of diesel.

Figure 5.8 compares the smoke emissions for diesel and biodiesel blends under different loads. The microalgae biodiesel blends produced significantly lower smoke emissions. In the current study, it was found that there was an average 36.7% and 58.9% reduction in smoke emissions for A20 and A30 blends, respectively, to diesel. This

can be credited to low Sulfur and aromatic content and also the lower C/H proportion of the biodiesel [102,103]. Also, A30 emitted fewer smoke emissions than A20 due to increased oxygen content. The smoke emission formation mainly occurs in the diffusion period of the combustion; therefore, diesel produced the highest smoke emissions among the three fuels. The values of smoke emissions were high at high loads due to the large quantity of fuel injected, which resulted in the formation of fuel-rich zones. The air deficiency in these zones creates more smoke. Smoke was also high at 25% load as compared to 50% and 75% loads. This may be because switching from free acceleration (no load) to loading condition initially created air deficiency and somewhat incomplete burning of the fuel.

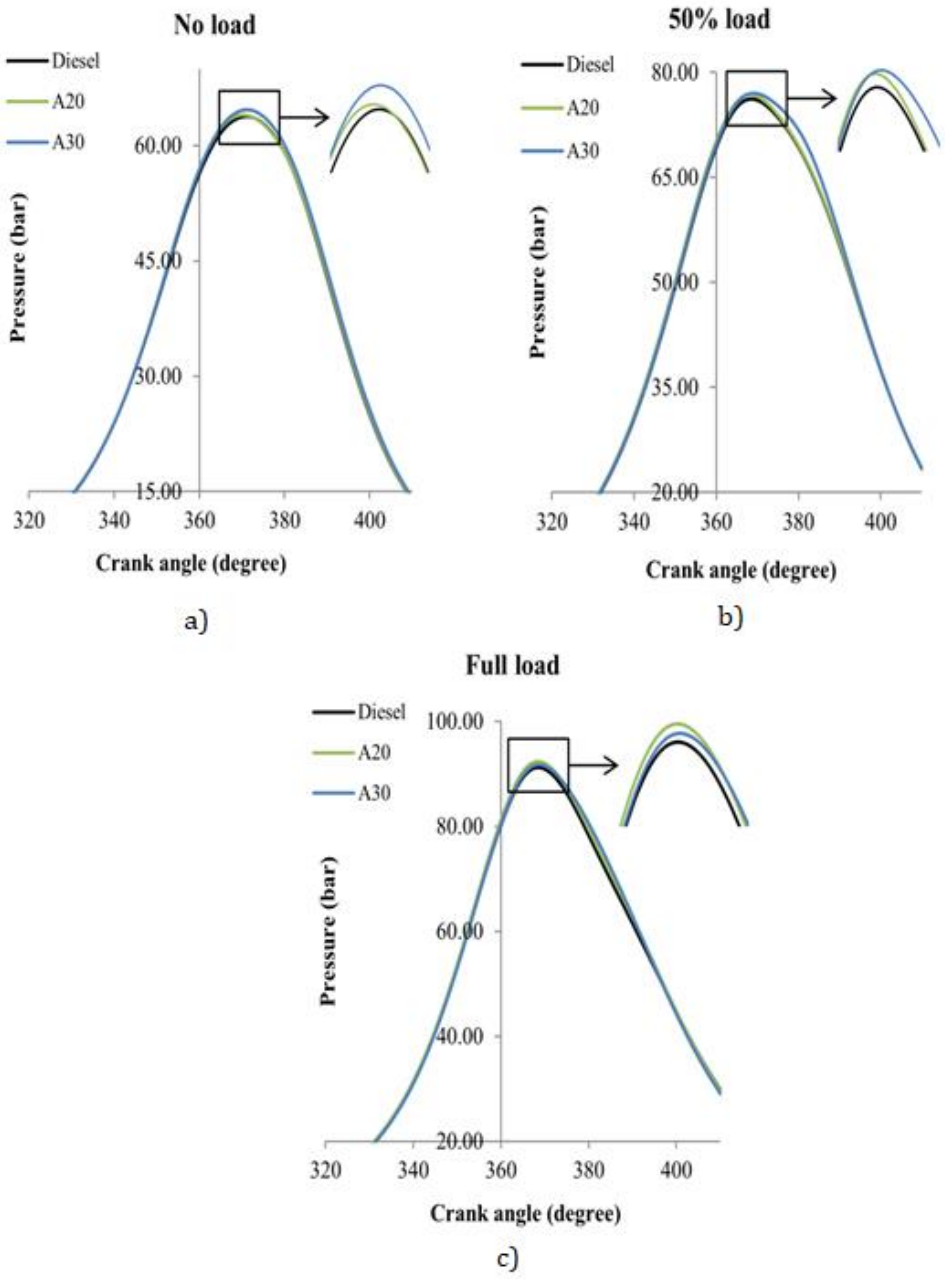

Figure 5.4 Variation of in-cylinder pressure with respect to crank angle during combustion

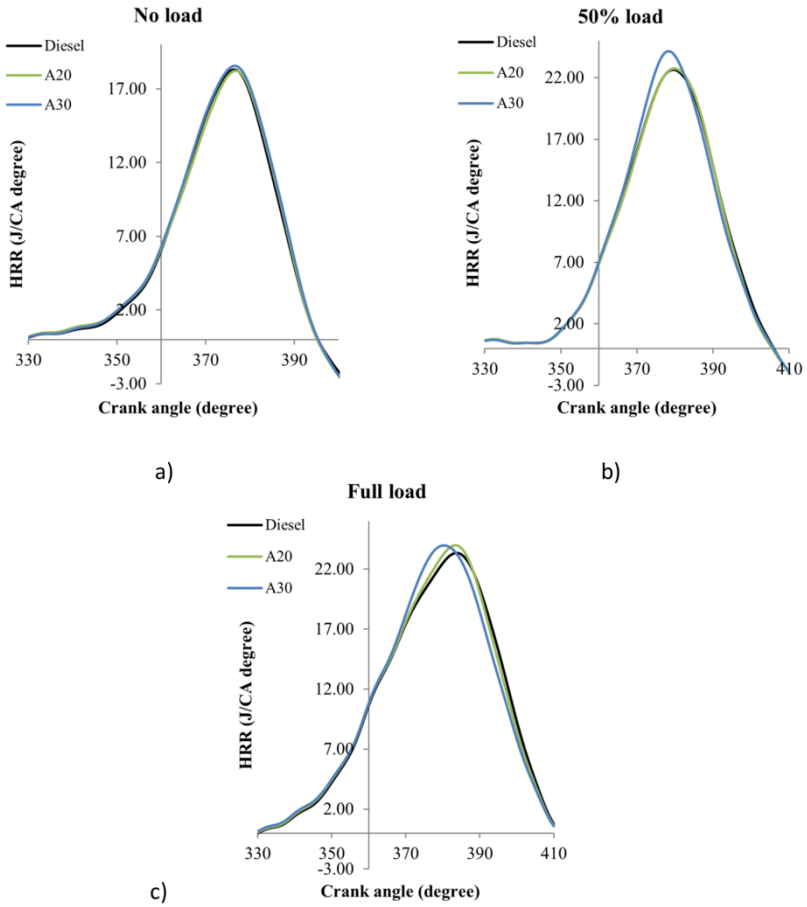

Figure 5.5 Variation of heat release rate with respect to crank angle during combustion

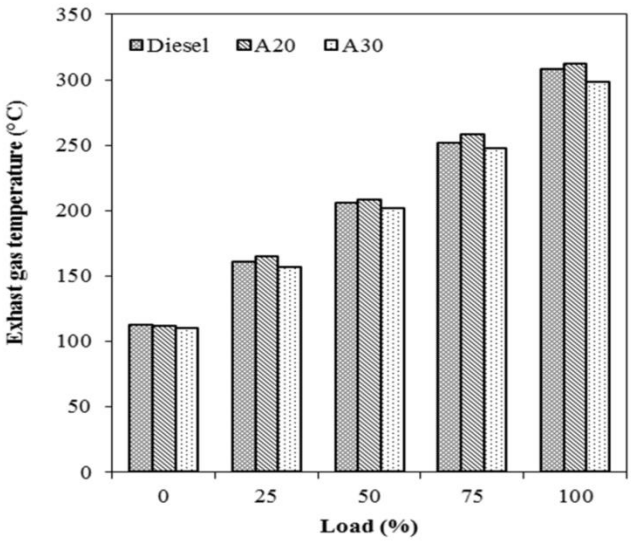

Figure 5.6 Variation of exhaust gas temperature with load

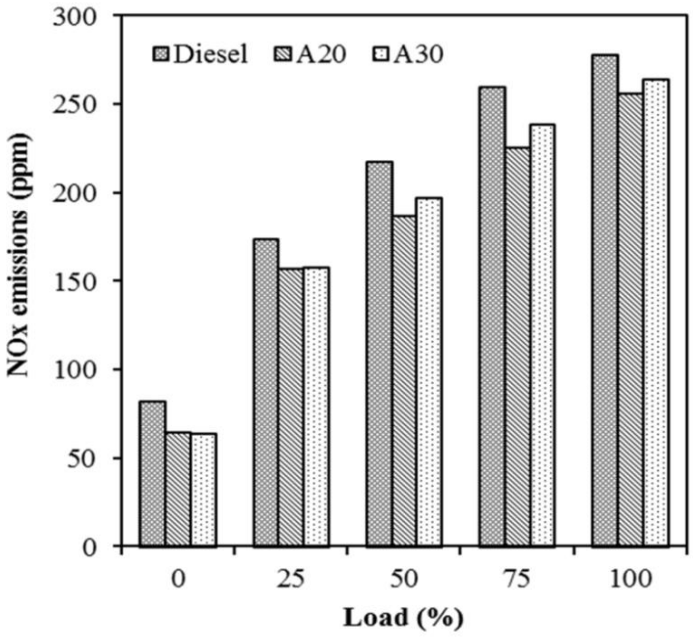

Figure 5.7 Variation of NOx emissions with load

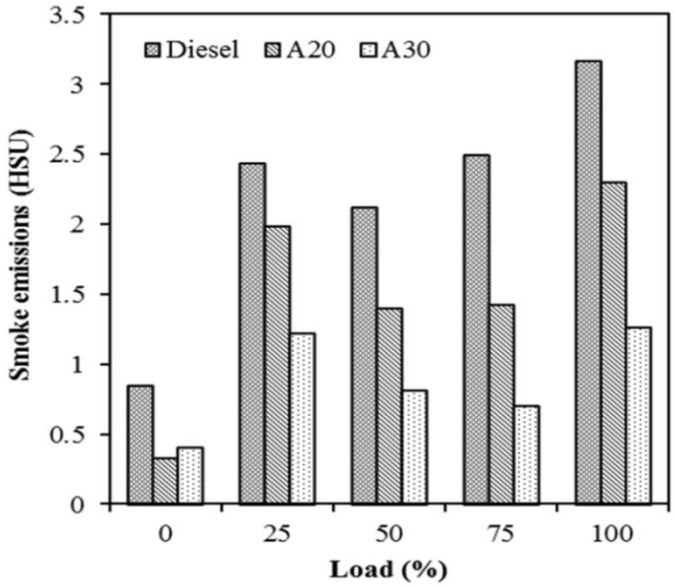

Figure 5.8 Variation of smoke emissions with load

5.4 Conclusions

The following conclusions were drawn from the study of Scenedesmus sp. biodiesel blends in a diesel engine.

- It was found from the study that a 20% microalgae biodiesel blend gave a satisfactory performance of an engine having brake thermal efficiency almost equal to diesel at loads greater than 50%. The

effect of a 30% microalgae biodiesel blend on the performance of an engine was also not too detrimental; with only 3.6% lower BTE at high loads.

- The effect of *Scenedesmus* sp. biodiesel on the emission characteristics of the engine was quite substantial. The NOx emission reduction by 20% biodiesel blend was in the range of 7.9% to 20.7% at different loads. Similarly, a 30% biodiesel blend reduced NOx emission in the range of 5.0% to 21.9% as compared to diesel.
- Smoke emissions were reduced drastically by microalgae biodiesel blends. 20% biodiesel lowered smoke emissions by 18.4% to 61.1% at different loads. Similarly, 30% biodiesel reduced smoke emissions by 50.0% to 61.3% at various loading conditions.

In conclusion, biodiesel blends from microalgae *Scenedesmus* sp. can be used satisfactorily in the diesel engine.

6 PERFORMANCE IMPROVEMENT BY FUEL ADDITIVE AND COMPARISON WITH SECOND-GENERATION BIODIESEL

6.1 Introduction

In this chapter, biodiesel from locally isolated microalgae species (*Scenedesmus* sp.) and second-generation (Pongamia) biodiesel were compared for their effect on diesel engine performance along with the study of the influence of cerium oxide nanoparticles on both biodiesels. The details of both these biodiesel are explained in section 4.4. The experimental set-up details are the same as explained in section 5.2. Cerium oxide (CeO_2) nanoparticles exhibit benefits like flexible capacity in valence transition, big oxygen storage, and high thermal properties; as a result, CeO_2 nanoparticles are thought to have a significant amount of potential to be an addition to the diesel engine. The cerium oxide (CeO_2) nanoparticle powder is purchased from Sigma Aldrich with an average particle size <50 nm. The CeO_2 nanoparticles were added to biodiesel and mixed with the help of a magnetic stirrer (30 minutes), then subsequently kept in the ultrasonicator (24 kHz frequency) for 30 minutes to avoid the agglomeration of added nanoparticles. The stability checking of nanoparticles is presented in Figure 6.1. It is found from visual inspection that the nanoparticles are well suspended in the biodiesel for up to 2 hours. Some percentage of nanoparticles start settling at the bottom after 6 hours of mixture preparation. After 24 hours, almost complete nanoparticles settled down at the bottom. Nonetheless, the nanoparticle-biodiesel blends are used immediately after preparation to avoid any effect of blend instability on the results. It is feasible to keep the fuel with nanoparticles added for up to a year by using techniques including homogenization, stirring, ultrasonication, controlling the pH

of the base fluid, and adding surfactant or dispersant. The prepared blends are – thirty percent biodiesel blends of *Scenedesmus* sp. (A30) and Pongamia (P30) in diesel, 100 ppm CeO_2 nanoparticles in A30 (A30C100), and 100 ppm CeO_2 nanoparticles in P30 (P30C100), and diesel.

6.2 Results and discussion

6.2.1 Performance characteristics

Figure 6.2 shows the comparison of BTE of the engine for different fuels used in this study. BTE denotes the actual energy utilized from the total energy produced by fuel combustion. The BTE of the engine increases with an increase in applied load. However, the percentage increase in BTE reduces at high loads as heat losses happening through exhaust air start overturning the benefits of the high-temperature combustion process. It is clear from Figure 6.2 that both microalgae and Pongamia biodiesel blends (A30 and P30) had a noticeably lower BTE (6.3% and 6.7%) than diesel. This can be attributed to low calorific values, higher viscosity, and density of the biodiesels. The high latent heat of vaporization is another important property responsible for the lower BTE of biodiesel blends, as it affects the evaporation rate of the fuel droplet, leading to poor air-fuel mixing [156,170]. Comparing the performance trend of A30 and P30 biodiesel blends, it is found that P30 had better performance at low loads, whereas the A30 blend had superior performance at high loads. Nanoparticle addition to the biodiesel blends improved the BTE of an engine. It is well evident that nanoparticles have an extremely high surface area to volume ratio, and nanoparticle-added fluid has superior heat transfer characteristics than base fluid. Nanoparticles help in improving the atomization of fuel through secondary atomization. Fuel droplets generated through aerodynamic forces and turbulence, which then encapsulate nanoparticles, tend to expand faster and break down further into fine-diameter droplets due to interaction with surrounding hot gas. Additionally, traveling nanoparticles also help in the breaking of larger-diameter droplets. Secondary atomization of fuel droplets not

only facilitates the evaporation rate but also boosts the air-fuel mixing process. Apart from the above, the catalytic effect of nanoparticles [106] also augments the combustion of fuel happening inside the engine. Average improvements of 4.2% and 3.8% in BTE, respectively, have been observed over A30 and P30 blends. At high loads, the BTE of A30C100 reaches almost equal to the diesel fuel.

Figure 6.3 shows the comparison of the BSFC of the engine for different fuels. It represents the amount of fuel consumed to produce unit brake power in unit time. The BSFC trend complements the BTE values. Therefore, biodiesel blends P30 and A30 had the highest BSFC among the tested fuels. The average BSFC of P30 and A30 blends are 9.9% and 9.7% higher than diesel. Biodiesels have lower calorific values compared to diesel; therefore, more fuel is consumed per unit break power. The higher bulk modulus of biodiesel blends advances the injection timing, forcing more volume of biodiesel blends inside the combustion chamber. At low loads, the BSFC of P30 is lower than A30; a vice-versa trend is observed at higher loads. CeO_2 nanoparticle addition helped in reducing BSFC by an average of 4.1% and 4.5% for P30C100 and A30C100 biodiesel blends as compared to P30 and A30. This is because nanoparticle addition helps in improving the atomization and combustion process, leading to less fuel requirement.

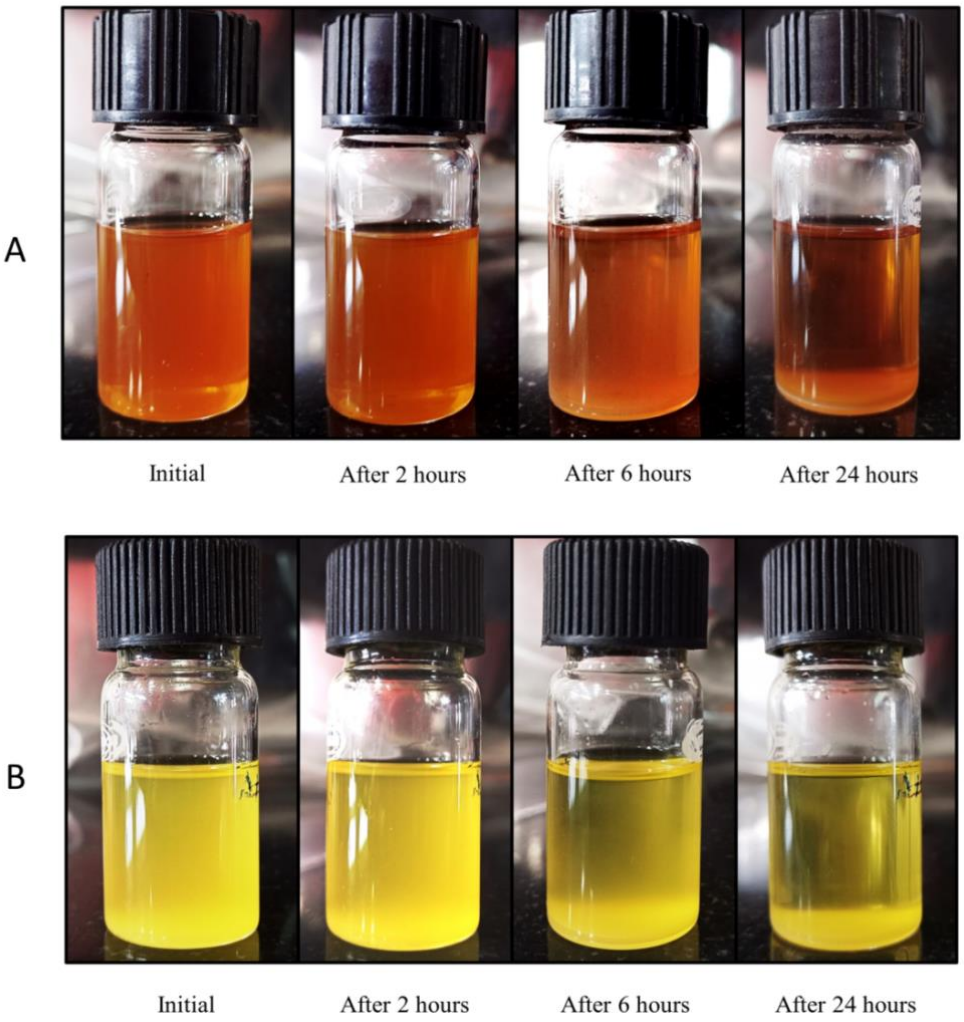

Figure 6.1 Nanoparticle stability inspection in biodiesel blends of A) A30C100 B) P30C100

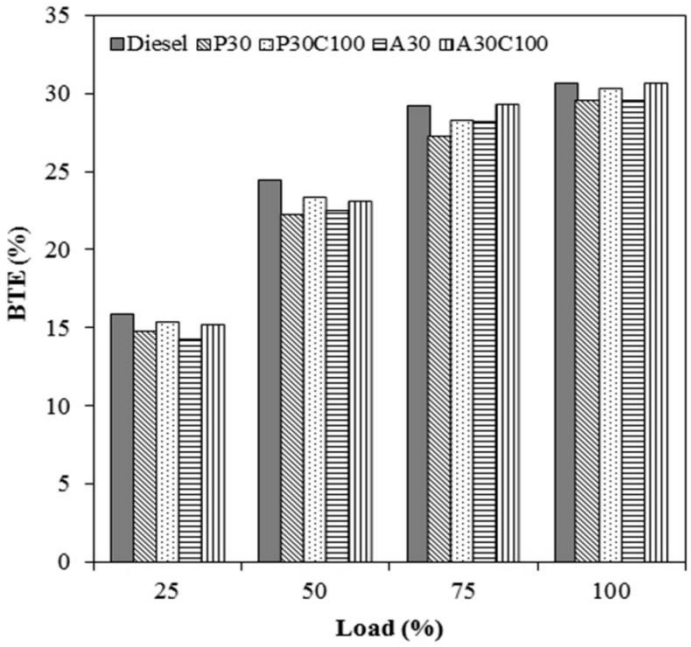

Figure 6.2 Variation of BTE with load

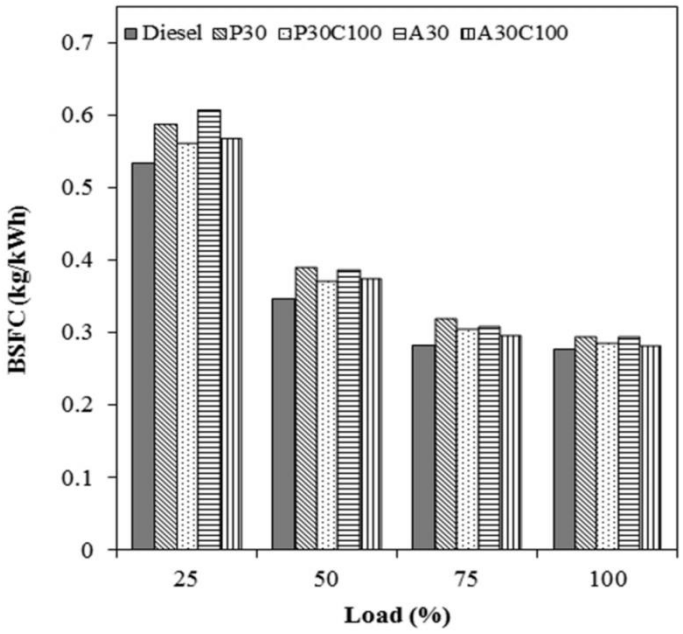

Figure 6.3 Variation of BSFC with load

6.2.2 Combustion characteristics

Figure 6.4 presents the in-cylinder pressure variation for diesel and biodiesel blends. A slightly higher peak pressure is observed for the biodiesel blends than for diesel. The observation is in agreement with previous studies of IDI diesel engines [171–174]. In general, higher

oxygen content is present in the biodiesel molecules that facilitate the combustion process, leading to higher peak pressure. As more oxygen content is present in microalgae biodiesel, the minutely high peak pressure is observed for the A30 blend than P30 despite a lower cetane number of the A30 blend. It may also be responsible for the longer peak pressure duration of the A30 blend. As biodiesel is associated with a poor atomization process, the peak pressure position is slightly shifted in the case of microalgae blends. However, at 100% load condition, the high temperature in a combustion chamber normalizes the ill influence of poor atomization, leading to the almost identical position of peak pressure. The nanoparticles blended fuel affected the combustion process considerably. It is evident from a considerable increase in peak pressure values of A30C100 and P30C100. Improved air-fuel mixing, secondary atomization and catalytic effect of nanoparticles during combustion seems to be possible reason behind it. Also, the addition of nanoparticles increases the oxygen content of the fuel, which improves the burning rate of the fuel. The peak pressure location becomes identical for A30C100 and P30C100 blends at 100% load.

Figure 6.5 presents the heat release rate (HRR) variation for the tested blends. The higher cetane number of microalgae and Pongamia biodiesel leads to a shorter ignition delay than diesel. As the combustion starts earlier, the premixed combustion stage is completed earlier for biodiesel blends (A30 and P30), resulting in higher initial HRR values. The effect is clearly visible at 100% load condition. The diffusion combustion HRR for the biodiesel blends is lower than that of diesel, specifically at higher loads. The excess oxygen content of the biodiesel blend also contributes to the dissimilarity in HRR trends of diesel and biodiesel blends [172]. Nanoparticle-added blends A30C100 and P30C100 blends have changed the HRR trend as compared to A30 and P30 blends. For example, there is a shift in the peak HRR slightly away from the top dead center, indicating better and more uniform air-fuel mixing for nanoparticle-added blends. This may be attributed to

the higher surface area-volume ratio of nanoparticles and the increased thermal conductivity of the blend. As observed from the figure, the HRR is higher for diesel and nanoparticle-added blends during the later part of the combustion. The above observation is in agreement with previous studies [170,172]. It may also be noted that the peak HRR trend also depends on the operating condition, as in the case of El-Seesy et al. [129], where nanoparticle addition decreased peak HRR at 1500 rpm but increased peak HHR at 2000 and 2500 rpm. The higher oxygen content of the microalgae biodiesel blend seems to normalize the combustion rate during the diffusion-burning process. The peak HRRs were 23.34, 23.97, 23.95, 23.47, and 23.87 J/CA degrees for diesel, A30, A30C100, P30, and P30C100 at full load, respectively.

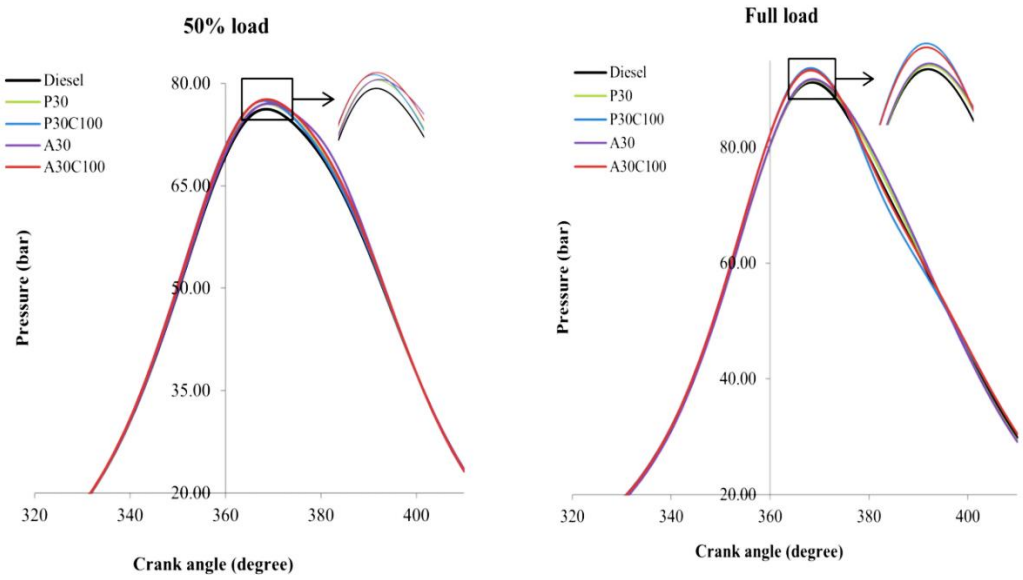

Figure 6.4 Variation of in-cylinder pressure with respect to crank angle during combustion

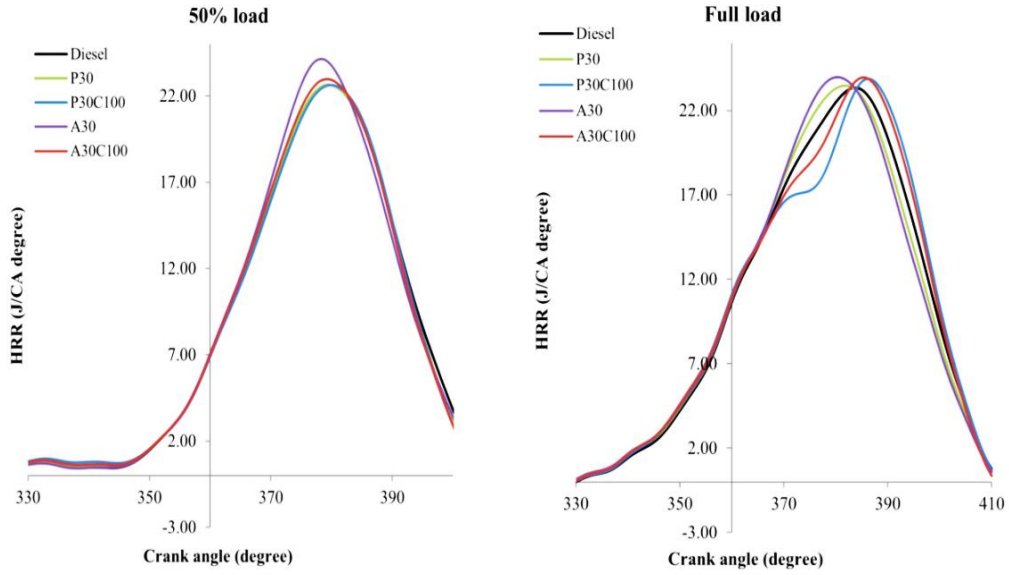

Figure 6.5 Variation of heat release rate with respect to crank angle during combustion

6.2.3 Emission characteristics

Figure 6.6 compares the NOx emissions emitted under different loading conditions. There are contradicting results about NOx emissions in the literature for biodiesel blends where biodiesel was reported to both increase as well as decrease the NOx emissions compared to diesel. The NOx emission is a crucial parameter in CI engine emissions as it has a severe ill impact on the environment. Apart from temperature, several other parameters such as cetane number, viscosity, density, bulk modulus, excess oxygen, residence time, engine geometry, and compression ratio also impact NOx emission. The situation becomes adverse because of the complex influence of a variety of additives in general recommended for performance enhancement or emission regulations. In general, oxygen-richness, higher viscosity and density, advancement in fuel injection, and enriched combustion increase NOx emissions, as reported for biodiesel and their blends [176–182]. However, the current study found that the NOx emissions of the blends A30 and P30 are lower than diesel by 7.26% and 5.67%. A similar kind of observation was

reported for Madhuca Indica [86], Jatropha and Chinese pistache [183], waste vegetable [184] and Cottonseed [185] biodiesel. In the case of a higher percentage of biodiesel (similar to the current study), the atomization process starts producing fuel droplets of large size; the heat of vaporization (for blended fuel) increases, and there is a decrease in the calorific value of the resulting fuel. It may have caused lesser NOx generation. It is also observed that P30 blends had higher NOx emissions than A30. The higher Cetane number of Pongamia biodiesel seems to be an expected reason behind the above observation. The average NOx emissions are found to be higher by 2.17% and 6.17% for A30C100 and P30C100 blends compared to their biodiesel blends without nanoparticles. The observed trend is due to better combustion characteristics of CeO_2 nanoparticles added to blended biodiesel. The oxygen content also increases due to the addition of CeO_2 nanoparticles, causing more NOx formation. Appealingly, the A30C100 blend NOx emissions are lower than the P30C100 despite higher thermal performance. Better heat transfer characteristics of the A30C100 blend may be responsible for the observed behavior, so it enjoys better combustion in the premixed stage.

Figure 6.7 compares the smoke emissions for diesel and biodiesel blends under different loads. The smoke emissions shoot up with an increase in load as the injection of more fuel at high loads generates fuel-rich zones. The air deficiency in these fuel-rich zones is responsible for the creation of more smoke [103,186]. The smoke emissions at 25% load are found to be higher than 50% and 75% loads. The above observation may be due to switching from free acceleration (no load) to loading conditions initially creating air deficiency and somewhat incomplete burning of fuel. As compared to diesel, all the blends of biodiesel produced significantly lower smoke emissions. The smoke emissions are found to be 54.0% and 58.9% less for P30 and A30 blends than diesel. The smoke formation mainly occurs during the diffusion period of the combustion for the diesel; therefore, it produces

the highest smoke emissions. The biodiesel's low carbon content and the presence of free oxygen facilitated in lowering the smoke emissions. The low Sulfur and aromatic content of biodiesel also helps in reducing smoke emissions [102,103]. The average smoke emission of the A30 blend is found to be 15.0% lower than the P30 blend. The presence of more free oxygen and lower chain fatty acid methyl esters (C16) in Scenedesmus sp. appears to be the possible reason behind the above observation [69,70,187]. An appreciable decrease in smoke emissions has been found due to the addition of CeO_2 nanoparticles in both biodiesel blends: the increased oxygen content and the enhanced ignition characteristics provided by CeO_2 help achieve complete combustion. Thus, average smoke emissions for A30C100 and P30C100 blends are found to be 28.3% and 16.9% lower than A30 and P30 blends. As P30 is already associated with more smoke emissions, comparing smoke reduction on a percentage basis by the addition of nanoparticles gives fewer values for P30 as compared to that for A30. However, in absolute terms, nanoparticles decreased smoke emissions sufficiently for both A30 and P30 blends.

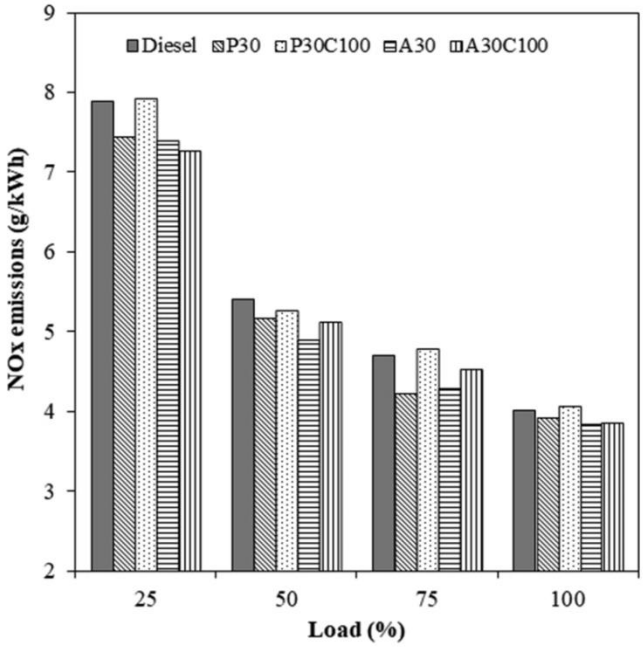

Figure 6.6 Variation of NOx emissions with load

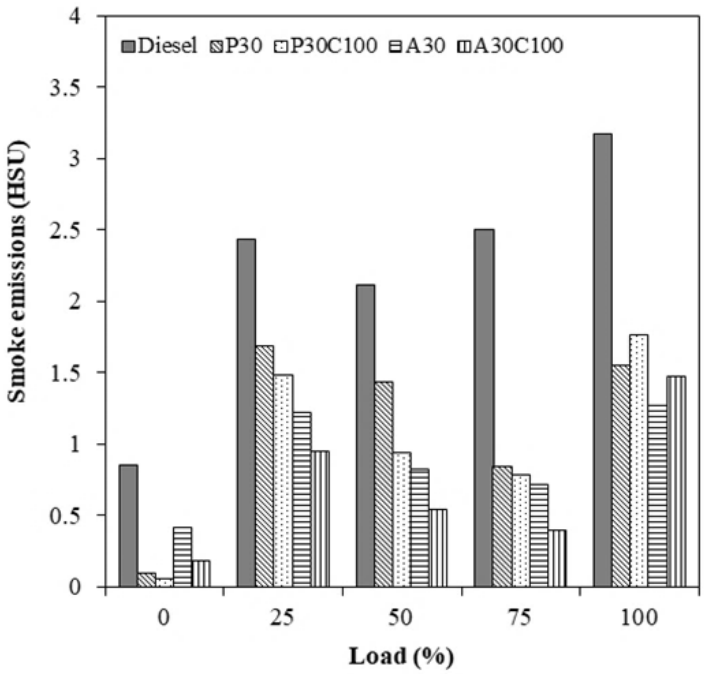

Figure 6.7 Variation of smoke emissions with load

6.3 Conclusions

Scenedesmus sp. biodiesel and Pongamia biodiesel had lower calorific values and higher viscosity and density than diesel. Therefore, the BTE of the A30 and P30 blends are found to be 6.3% and 6.7% lower than diesel. The performance of biodiesel blends operated engine improves by the addition of CeO_2 nanoparticles. Improved air-fuel mixing and enhanced fuel evaporation (due to the secondary atomization process) seem mainly responsible for improved performance by the CeO_2 nanoparticle. Nanoparticle addition provided better performance enhancement for the *Scenedesmus* biodiesel. At high load levels, the performance of *Scenedesmus* blend A30C100 is found to be almost equal to diesel. The NOx emissions of A30 and P30 blends are found to be 7.26% and 5.67% lower than diesel in the current study. However, improved combustion by nanoparticles has an adverse effect on NOx emissions. The emissions of NOx for P30C100 are even higher than diesel. A convincible reduction is found in smoke emissions of all the tested biodiesel blends with and without nanoparticles. A30 and P30 reduced smoke emissions by an average of 58.9% and 54.0% compared to diesel. Similarly, A30C100 and

P30C100 lowered average smoke emissions by 70.4% and 60.4% compared to diesel. *Scenedesmus* sp. biodiesel blends are found to be slightly superior to Pongamia biodiesel blends in terms of performance and emissions. More such studies will help to identify the potential microalgae biodiesel-nanoparticle combinations for catering to the demand for transportation fuel on a national and global level.

7 ASSESSMENT OF MICROALGAE AND PONGAMIA BIODIESEL MIX-FUEL BLEND

7.1 Introduction

Biodiesel is basically a mixture of fatty acid methyl esters having carbon chain length of 12 to 24 carbon atoms with or without double bonds [188,189]. As explained earlier, if there is no double bond, the fatty acid is called as saturated fatty acid (SFA); whereas one or more double bonds containing fatty acid is called as monounsaturated (MUFA) or polyunsaturated fatty acid (PUFA). The proportion of these fatty acids in the biodiesel govern the properties important for engine operation and storage stability as the individual fatty acids have their own values of properties [65,190,191]. Therefore, biodiesel obtained from different sources have dissimilar properties as the fatty acid composition differs accordingly. Ultimately, the engine performance and emission output is influenced by the proportion of fatty acids present in the biodiesel. In this view, the effect of saturation-unsaturation content and chain length of fatty acids has also been investigated by researchers [67,68,70,192]. A proper mixture of SFA, MUFA and PUFA should be present in the biodiesel to have properties suitable for optimum engine output characteristics.

Microalgae biodiesel, even though regarded as a promising new source of biodiesel, typically contains long-chain PUFA like linolenic acid and, to some extent, EPA and DHA [188]. Second-generation biodiesel like pongamia (also calle7d karanja) contains lower PUFA and sufficient SFA and MUFA. Therefore, mixing these two biodiesels and using them as a fuel for diesel engines will be interesting. The current investigation used biodiesel from microalgae *Scenedesmus* sp. and second-generation pongamia biodiesel to prepare a mix-fuel blend for a four-cylinder four-stroke diesel engine. The study was conducted in a

constant-speed varying-load operating condition, and performance and emission output parameters were reported and compared. The blends tested were 20% microalgae biodiesel in diesel (A20), 20% pongamia biodiesel in diesel (P20), and 10% each of microalgae and pongamia biodiesel in diesel (A10P10).

7.2 Results and discussion

7.2.1 Performance characteristics

Figure 7.1 represents the variation of brake thermal efficiency (BTE) of an engine with a load of different fuels. As seen from the figure, the BTE of an engine increases with an increase in load. More fuel is injected inside the engine as the load increases to keep the speed constant. However, the rise in fuel intake is less compared to the increase in load; therefore, efficiency is higher at high loads. The BTE of the engine for microalgae and pongamia biodiesel blends (A20 and P20) is almost similar. However, the average BTE for A20 and P20 is approximately 3% lower than diesel. This is due to the lower calorific value, higher viscosity, and density of the biodiesel than diesel. High latent heat of vaporization also affects the evaporation rate of the fuel droplets in the combustion chamber and, thus, the air-fuel mixing. However, the extra oxygen content of the biodiesel may cancel out this negative effect to some extent. Therefore, the difference between the BTE of A20 and P20 with that of diesel is limited to around 3%. Mix-fuel A10P10 slightly improved BTE as compared to A20 and P20 blends, especially after mid-range. This may be because of the mixing of the two biodiesel blends, which compensate for the very high PUFA content and low MUFA content of *Scenedesmus* sp. biodiesel as well as the low SFA content of pongamia biodiesel.

Figure 7.2 represents the brake-specific fuel consumption (BSFC) variation of an engine with a load of different fuels. BSFC graph is complementary to the BTE graph as it represents inverse trends for fuels, as in the case of BTE. The lowest BSFC can be seen for diesel, indicating the superiority of diesel fuel in terms of properties and

engine combustion over other fuels. For most of the load range, the pure blends A20 and P20 showed the highest consumption compared to the other two fuels. This shows that blending microalgae and pongamia biodiesel in diesel caused some negative effects in terms of properties, so the fuel required for the same power generation was more. The mix-fuel A10P10 caused improvement in the BSFC compared to pure blends A20 and P20 by around 2% for both. This clearly illustrates that there is an improvement in performance, in terms of fuel consumption, of an engine by a biodiesel blend containing a mix of two different biodiesels. Even though the average difference in BSFC for pure blends and mix-fuel blends is not much, there can be an improvement with higher blends and other methods, such as nanoparticle addition. Due to the limited availability of microalgae biodiesel, only a 20% blend has been checked in this study.

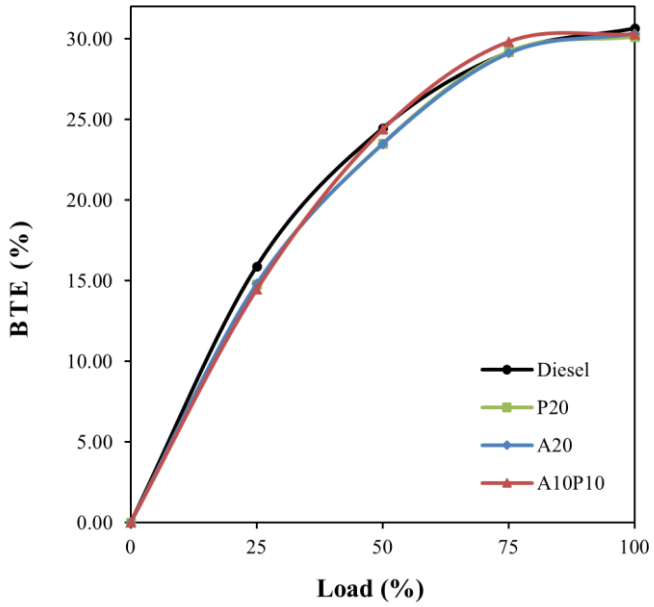

Figure 7.1 Variation of BTE with load for diesel and biodiesel blends

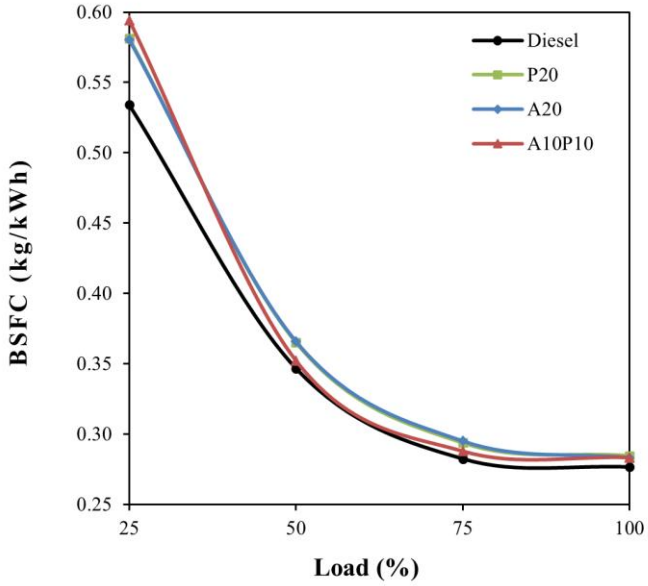

Figure 7.2 Variation of BSFC with load for diesel and biodiesel blends

7.2.2 Combustion characteristics

Figure 7.3 presents the in-cylinder pressure variation for diesel and biodiesel blends at 50% load. The developed cylinder pressure during the combustion is mainly governed by the rate of fuel burning in the premixed combustion phase. This, in turn, is affected by the ignition delay period and spray formation. The fuel properties such as viscosity, density, and latent heat of vaporization play crucial roles in ignition delay and spray behavior of the fuel. Slightly high pressure was observed for biodiesel blends as compared to diesel. A similar trend was observed in previous studies of IDI diesel engines [171–174]. The extra oxygen content of the biodiesel assisted the combustion of the blends and possibly increased the peak pressure developed during the combustion. Also, biodiesel blends had higher density as compared to diesel, which indicates a higher bulk modulus. This means that the biodiesel blends are more incompressible than pure diesel. Therefore, the pressure build-up will be quick in the injection pump, and fuel will be injected early. Moreover, high temperature during the injection causes higher molecular weight FAMEs to break down into smaller

molecules. The gasification of these compounds spreads the jets and causes early ignition [140,193]. This early injection and advanced combustion might have caused higher peak pressure for biodiesel blends [143]. The A20 blend showed marginally higher peak pressure than the P20 blend, whereas the highest peak pressure was observed for the A10P10 blend among all the tested fuels. This indicated better combustion characteristics for a mix-fuel blend, which in turn showed its potential to incorporate the positives of two biodiesels into one.

Figure 7.4 presents the heat release rate (HRR) variation for diesel and biodiesel blends at 50% load. As discussed in the previous paragraph, the early injection and shorter ignition delay of the biodiesel is evident from Figure 7.4 for biodiesel blends as the HRR curves moved towards TDC (left) as compared to diesel, indicating earlier completion of premixed combustion. The excess oxygen content of the biodiesel was also a responsible factor in the deviation from HRR trends for diesel and biodiesel blends [172]. The mixing of the two biodiesel fuels affected the HRR trends slightly as the highest peak HRR was observed for mix-fuel A10P10, evincing better combustion quality due to the mixing of two biodiesel blends. HRR trend for the mix-fuel blend also showed the lowest values during the later part of the combustion, indicating that most of the charge is burning at the premixed combustion stage. This result, along with performance values, further reinforced that mixing two biodiesel with different saturated and unsaturated fatty acid percentages helped in improving engine output characteristics.

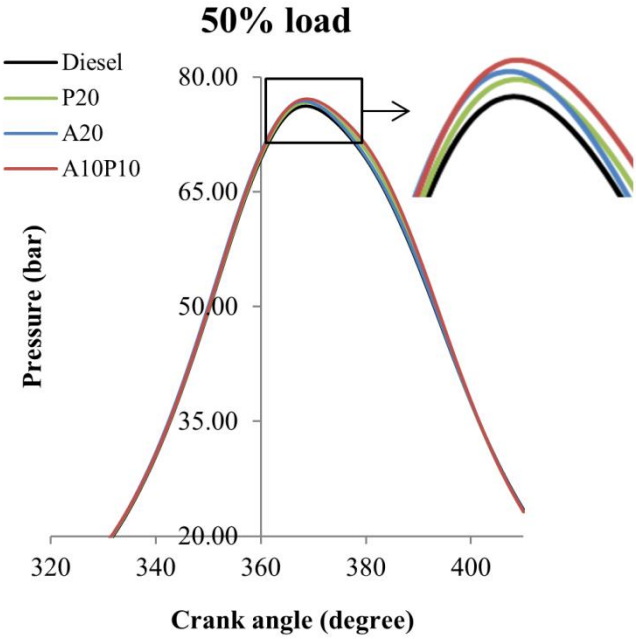

Figure 7.3 In-cylinder pressure variation with crank angle

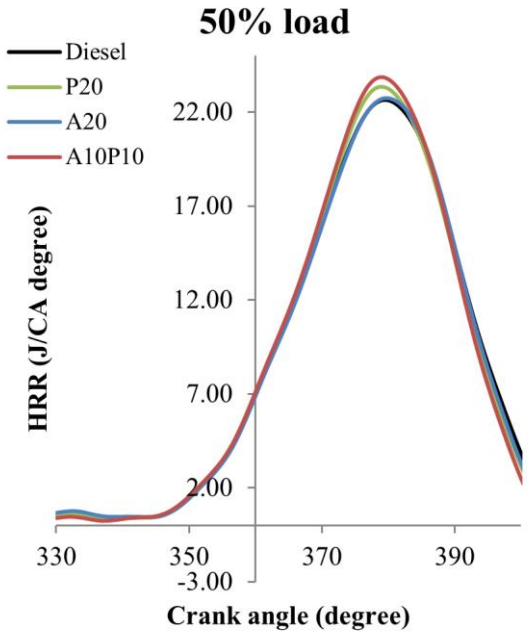

Figure 7.4 Net heat release rate (HRR) variation with crank angle

7.2.3 Emission characteristics

Figure 7.5 compares the NOx emissions of different fuels tested in this study under different loads. In the current study, biodiesel blends

produced lower NOx emissions than diesel by 4.43%, 13.14%, and 15.70% for P20, A20, and A10P10 blends, respectively. This was in agreement with previous studies for other biodiesel sources [86,183–185]. As discussed previously, even though some authors argued that the increase in cetane number and reduced ignition delay lead to increased NOx emissions, a counterargument claimed that high cetane number and short ignition delay, in fact, reduce the NOx emission[88,93,175]. This could be the possible reason for the reduced NOx emission of biodiesel blends in the current study. Out of the biodiesel blends, P20 blends produced the highest NOx emissions, and there was only a slight difference between the blends A20 and A10P10. This can be credited to the difference in the fatty acid composition of pongamia and microalgae biodiesel. NOx emissions decrease with higher saturated fatty acid content [194,195]. *Scenedesmus* sp. biodiesel has higher SFA content (38.43%) compared to pongamia biodiesel (18.54%). Therefore, A20 showed lower NOx emissions. The blending of the two biodiesel had a positive impact on average NOx emissions as it was further reduced by 3.07% as compared to A20. The negative effect of higher unsaturation content (MUFA and PUFA) of pongamia biodiesel was balanced by adding microalgae biodiesel having high Palmitic acid (C16:0).

Figure 7.6 compares the amount of smoke from exhaust for different fuels tested in this study under different loads. Smoke emission was highest at full load conditions as excess fuel was injected, creating fuel-rich zones at such high load conditions. The air deficiency at such zones causes more smoke because of a partially burnt charge. On average, the smoke emissions of biodiesel blends P20, A20, and A10P10 were lower than diesel by 21.19%, 30.66% and 26.49% respectively. This significant decrease in smoke emission was because of the low sulfur and aromatic content, low C/H proportion, and increased oxygen content of biodiesel blends. Diesel fuel had a longer ignition delay and more burning in the diffusion combustion phase. Therefore, it showed the highest smoke emissions. Among the

biodiesel blends, P20 showed the highest smoke emissions, whereas the lowest smoke emissions were observed for the A20 blend. Higher unsaturation content (number of double bonds) in the biodiesel leads to increased smoke emissions [69,187]. Pongamia biodiesel contains more unsaturated FAs (MUFA+PUFA); therefore, the P20 blend showed increased smoke. Smoke emissions are also proportional to the carbon chain length of the fatty acids. Microalgae biodiesel had high Palmitic acid (C16:0) content, whereas pongamia biodiesel contains higher carbon fatty acids (C18 and C20). The mix-fuel blend showed smoke values in between P20 and A20 blends as it compensated for the negative effect of the FA content of pongamia biodiesel. Even though mix-fuel A10P10 did not produce the lowest smoke emissions, it was quite lower as compared to diesel, as mentioned earlier.

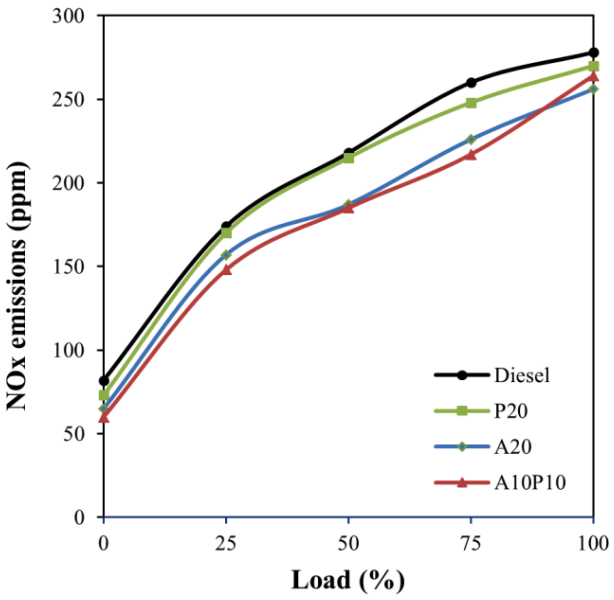

Figure 7.5 Variation of NOx emissions with load for diesel and biodiesel blends

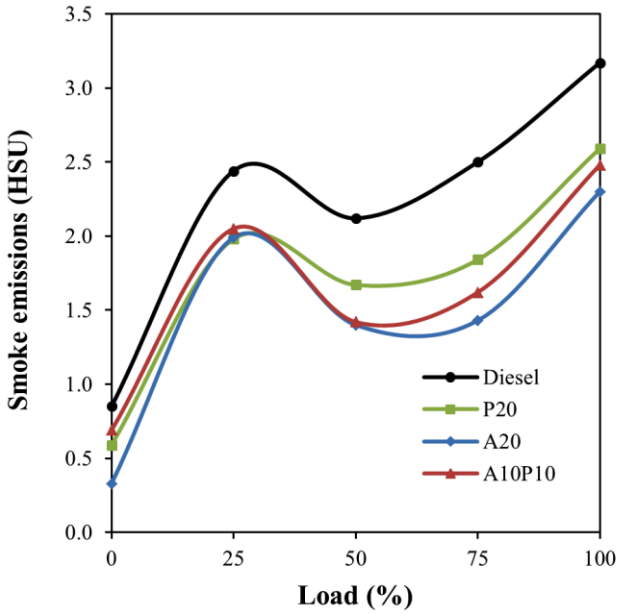

Figure 7.6 Variation of smoke emissions with load for diesel and biodiesel blends

7.3 Conclusions

Microalgae biodiesel has high PUFA content but also has high Palmitic acid. Pongamia biodiesel has very high MUFA content in the form of Oleic acid. Mixing of these two biodiesel has the potential to produce a good mix of saturated and unsaturated fatty acids. Mix-fuel blend A10P10 improved BTE by around 1% and BSFC by around 2% compared to the blends A20 and P20. The combustion characteristics showed that the A10P10 blend produced the highest pressure and heat release rate. The mix-fuel blend also showed the lowest NOx emissions among all the fuels. The smoke emissions of A10P10 were slightly higher than A20, but they were still lower than diesel by 26.4%. Therefore, mixing the two biodiesels with dissimilar fatty acid contents can be a good strategy to improve engine performance and emissions.

8 OVERALL CONCLUSIONS AND PLAN FOR FUTURE WORK

8.1 Conclusions

The present study's objective is to identify suitable microalgae for biodiesel production based on fatty acid profile and lipid content. The selected species were cultivated in outdoor raceway ponds for large-scale biomass production. Harvested biomass was subjected to oil extraction and biodiesel production through transesterification. Eventually, experiments were carried out to evaluate the possibility of microalgae biodiesel as a blend in a diesel engine. Additionally, to overcome the poor performance level of the microalgae biodiesel blend, the addition of nanoparticles and fuel mixing were studied as methods of improving diesel engine performance and emissions.

Following are the outcomes of the current research work.

1. The species selection methodology was found to be useful in screening microalgae for large-scale biofuel production. Even under the same growth conditions, the studied species show significant variation in their SFA, MUFA, and PUFA percentages. Green unicellular species *Chlorella* and *Scenedesmus* showed relatively higher PUFA with around 30% lipids. Compared to this, cyanobacterial species *Lyngya* and *Calothrix* had higher SFA, MUFA, and only 10 to 20% lipids.
2. Based on the FAME profile and lipid content analysis, *Scenedesmus* sp. and *Calothrix* sp. were found to be the top two preferred species. Extended temperature-dependent property analysis of these two species showed that the low viscosity of the former and higher vapor pressure of the latter was their decisive fuel characteristic. Density, latent heat of

vaporization, and vapor diffusivity were not too different for the two species. However, *Scenedesmus* sp. was considered superior based on lipid content and fast growth.

3. Growth in outdoor cultivation was found to be quite adequate in this research work with economical urea and DAP as nutrient media. However, implementing simple and economical methods for harvesting and oil extraction, such as gravity sedimentation and soxhlet apparatus, was found to yield a lower quantity of biodiesel. In this work, 14.2% oil/lipid yield was obtained from dried microalgae biomass.

4. The SFA, MUFA, and PUFA proportions in *Scenedesmus* sp. microalgae biodiesel were found to be 38.43%, 17.49%, and 29.75%, respectively. The higher presence of PUFA was because of high linolenic acid content.
5. Experimental analysis of the diesel engine found that the engine's performance slightly deteriorated with A20 and A30 blends of microalgae biodiesel with an average of 3.05% and 6.33% decrease in BTE (brake thermal efficiency) as compared to diesel. This difference at full load conditions was only 1.1% (for A20) and 3.6% (for A30) compared to diesel.
6. The use of *Scenedesmus* sp. biodiesel resulted in an adequate reduction of NOx and smoke emissions. The NOx emission reduction was found in the range of 7.9% to 20.7% for A20 blend and in the range of 5.0% to 21.9% for A30 blend compared to diesel. Similarly, A20 blend lowered smoke emissions by 18.4% to 61.1%, and A30 blend reduced smoke emissions by 50.0% to 61.3% at various loading conditions compared to diesel.
7. The cerium oxide nanoparticles improved the average BTE by 4.2% and 3.8% when added to *Scenedesmus* sp. and Pongamia biodiesel blends, but at the cost of a slight increase in NOx emissions. NOx emissions were 2.17% and 6.17% higher for nanoparticle-added blends than their plane biodiesel blends (A30 and P30). The blend's cost and stability are the two critical

concerns regarding the application of nanoparticles as a fuel additive.

8. Mix blend containing 10% each of *Scenedesmus* sp. and Pongamia biodiesel increased the performance by around 2.1 to 3.8% at the mid-load range compared to pure 20% blends (A20 and P20). It also decreased NOx emissions by 3.07% and 11.89% compared to A20 and P20. Smoke emissions were lower for all biodiesel blends as compared to diesel. Therefore, the mixing of two biodiesels, *Scenedesmus* sp., and Pongamia, was observed to be an economic strategy to increase the performance to some extent and reduce emissions at the same time.

Technological innovations hold the key to improving efficiency and cost competitiveness. Some techno-economic analysis carried out recently estimated the cost of microalgae biodiesel around 2.07 to 2.17 $/L with bio-refinery approach. It was also reported in one study that microalgae biodiesel cost should be less than 147 $/barrel to have biodiesel production business with heavy metal removal profitable. The regulatory support and consumer preferences will shape microalgae biodiesels market success. Continued research and investment are essential to harness its potential as a sustainable alternative to fossil fuels.

Overall, the major conclusions of the study that are useful for practical approach are

- Microalgae species selection based on FA composition is a cheap and easy method.
- After initial adaptation to the outdoor environment, single culture microalgae growth is possible in open raceway ponds.
- Urea-DAP can be successfully used for sufficient microalgae biomass growth.
- With year round cultivation and some improvement in biodiesel production process, it is possible to set up microalgae biodiesel plant.

8.2 Future scope

Following is the plan for future work:

1. Based on semi-outdoor cultivation experience, the development of efficient harvesting and oil extraction processes needs to be studied to increase the biodiesel output.
2. To increase the net energy output of the process, the possibility of production of other biofuels like ethanol and biohydrogen from microalgae biomass after lipid extraction can also be explored.
3. Integrated bio-refinery approach with life cycle analysis of microalgae biodiesel production can also be studied as a multi-objective strategy.
4. Detailed economic analysis of microalgae biodiesel production process where methods like possible water recycling, renewable sources for drying and paddlewheel operation etc. can be studied. The trade-off between nutrient cost and biomass generation can also be a useful study.
5. The effect of engine parameters, such as injection timing, compression ratio, etc., as well as spray characteristics in the case of *Scenedesmus* sp. biodiesel, can also be studied in detail.
6. Analysis of exhaust soot particles is crucial in case of diesel engine exhaust. For second generation biodiesel, the exhaust soot particles concentration was found to dominated by nucleation mode particles (<50 nm), which affect the human health. The similar study can be performed for microalgae biodiesel fuel, where thorough soot formation process and size of particles can be analyzed.

REFERENCES

[1] International Energy Agency, World Energy Outlook, 2016. https://doi.org/10.1787/weo-2016-en.

[2] A.E. Atabani, A.S. Silitonga, I.A. Badruddin, T.M.I. Mahlia, H.H. Masjuki, S. Mekhilef, A comprehensive review on biodiesel as an alternative energy resource and its characteristics, Renew. Sustain. Energy Rev. 16 (2012) 2070–2093. https://doi.org/10.1016/j.rser.2012.01.003.

[3] P. Tamilselvan, N. Nallusamy, S. Rajkumar, A comprehensive review on performance, combustion and emission characteristics of biodiesel fuelled diesel engines, Renew. Sustain. Energy Rev. 79 (2017) 1134–1159.

[4] L.C. Meher, V.S.S. Dharmagadda, S.N. Naik, Optimization of alkali-catalyzed transesterification of Pongamia pinnata oil for production of biodiesel, Bioresour. Technol. 97 (2006) 1392–1397. https://doi.org/10.1016/j.biortech.2005.07.003.

[5] A. Karmakar, S. Karmakar, S. Mukherjee, Properties of various plants and animals feedstocks for biodiesel production, Bioresour. Technol. 101 (2010) 7201–7210.

[6] J. Janaun, N. Ellis, Perspectives on biodiesel as a sustainable fuel, Renew. Sustain. Energy Rev. 14 (2010) 1312–1320. https://doi.org/10.1016/j.rser.2009.12.011.

[7] T.M. Mata, A.A. Martins, N.S. Caetano, Microalgae for biodiesel production and other applications: A review, Renew. Sustain. Energy Rev. 14 (2010) 217–232. https://doi.org/10.1016/j.rser.2009.07.020.

[8] Y. Chisti, Biodiesel from microalgae, Biotechnol. Adv. 25 (2007) 294–306. https://doi.org/10.1016/j.tibtech.2007.12.002.

[9] A. Demirbas, F.M. Demirbas, Importance of algae oil as a source of biodiesel, Energy Convers. Manag. 52 (2011) 163–170. https://doi.org/10.1016/j.enconman.2010.06.055.

[10] B. Kiran, K. Pathak, R. Kumar, D. Deshmukh, Cultivation of Chlorella sp. IM-01 in municipal wastewater for simultaneous nutrient removal and energy feedstock production, Ecol. Eng. 73 (2014) 326–330. https://doi.org/10.1016/j.ecoleng.2014.09.094.

[11] B. Kiran, A. Kaushik, Equilibrium sorption study of Cr (VI) from multimetal systems in aqueous solutions by Lyngbya putealis, Ecol. Eng. 38 (2012) 93–96. https://doi.org/10.1016/j.ecoleng.2011.11.001.

[12] B. Kiran, K. Thanasekaran, An indigenous cyanobacterium, Lyngbya putealis, as biosorbent: Optimization based on

statistical model, Ecol. Eng. 42 (2012) 232–236. https://doi.org/10.1016/j.ecoleng.2012.02.026.

[13] B. Kiran, K. Thanasekaran, Metal tolerance of an indigenous cyanobacterial strain, Lyngbya putealis, Int. Biodeterior. Biodegrad. 65 (2011) 1128–1132.

[14] V. Anand, R. Gautam, R. Vinu, Non-catalytic and catalytic fast pyrolysis of Schizochytrium limacinum microalga, Fuel. 205 (2017) 1–10. https://doi.org/10.1016/j.fuel.2017.05.049.

[15] Y. Guo, T. Yeh, W. Song, D. Xu, S. Wang, A review of bio-oil production from hydrothermal liquefaction of algae, Renew. Sustain. Energy Rev. 48 (2015) 776–790. https://doi.org/10.1016/j.rser.2015.04.049.

[16] S.K. Thangavelu, A.S. Ahmed, F.N. Ani, Review on bioethanol as alternative fuel for spark ignition engines, Renew. Sustain. Energy Rev. 56 (2016) 820–835. https://doi.org/10.1016/j.rser.2015.11.089.

[17] Y.M. Yun, K.W. Jung, D.H. Kim, Y.K. Oh, H.S. Shin, Microalgal biomass as a feedstock for bio-hydrogen production, Int. J. Hydrogen Energy. 37 (2012) 15533–15539. https://doi.org/10.1016/j.ijhydene.2012.02.017.

[18] J.R. Benemann, Hydrogen production by microalgae, J. Appl. Phycol. 12 (2000) 291–300.

[19] M. Dębowski, M. Zieliński, A. Grala, M. Dudek, Algae biomass as an alternative substrate in biogas production technologies - Review, Renew. Sustain. Energy Rev. 27 (2013) 596–604. https://doi.org/10.1016/j.rser.2013.07.029.

[20] P. Collet, A. Hélias Arnaud, L. Lardon, M. Ras, R.A. Goy, J.P. Steyer, Life-cycle assessment of microalgae culture coupled to biogas production, Bioresour. Technol. 102 (2011) 207–214. https://doi.org/10.1016/j.biortech.2010.06.154.

[21] A. Marcilla, L. Catalá, J.C. García-Quesada, F.J. Valdés, M.R. Hernández, A review of thermochemical conversion of microalgae, Renew. Sustain. Energy Rev. 27 (2013) 11–19. https://doi.org/10.1016/j.rser.2013.06.032.

[22] E.B. D'Alessandro, N.R. Antoniosi Filho, Concepts and studies on lipid and pigments of microalgae: A review, Renew. Sustain. Energy Rev. 58 (2016) 832–841.

[23] B. Kiran, R. Kumar, D. Deshmukh, Perspectives of microalgal biofuels as a renewable source of energy, Energy Convers. Manag. 88 (2014) 1228–1244.

[24] N. Pragya, K.K. Pandey, P.K. Sahoo, A review on harvesting,

oil extraction and biofuels production technologies from microalgae, Renew. Sustain. Energy Rev. 24 (2013) 159–171. https://doi.org/10.1016/j.rser.2013.03.034.

[25] R. Halim, M.K. Danquah, P.A. Webley, Extraction of oil from microalgae for biodiesel production: A review, Biotechnol. Adv. 30 (2012) 709–732.

[26] F.D. Gunston, J.L. Harwood, A.J. Dijkstra, The lipid handbook, 2007. https://doi.org/10.1016/0144-8617(88)90020-3.

[27] J. Sheehan, T. Dunahay, Jo. Benemann, P. Rooessler, A Look Back at the U.S. Department of Energy's Aquatic Species Program—Biodiesel from Algae, 2014. https://doi.org/10.1038/507528a.

[28] J. Pruvost, G. Van Vooren, G. Cogne, J. Legrand, Investigation of biomass and lipids production with Neochloris oleoabundans in photobioreactor, Bioresour. Technol. 100 (2009) 5988–5995. https://doi.org/10.1016/j.biortech.2009.06.004.

[29] M.J. Griffiths, R.P. van Hille, S.T.L. Harrison, Lipid productivity, settling potential and fatty acid profile of 11 microalgal species grown under nitrogen replete and limited conditions, J. Appl. Phycol. 24 (2012) 989–1001. https://doi.org/10.1007/s10811-011-9723-y.

[30] A. Converti, A.A. Casazza, E.Y. Ortiz, P. Perego, M. Del Borghi, M. Del Borghi, Effect of temperature and nitrogen concentration on the growth and lipid content of Nannochloropsis oculata and Chlorella vulgaris for biodiesel production, Chem. Eng. Process. Process Intensif. 48 (2009) 1146–1151. https://doi.org/10.1016/j.cep.2009.03.006.

[31] S. Ruangsomboon, Effect of light, nutrient, cultivation time and salinity on lipid production of newly isolated strain of the green microalga, Botryococcus braunii KMITL 2, Bioresour. Technol. 109 (2012) 261–265.

[32] P.R. Pandit, M.H. Fulekar, M.S.L. Karuna, Effect of salinity stress on growth, lipid productivity, fatty acid composition, and biodiesel properties in Acutodesmus obliquus and Chlorella vulgaris, Environ. Sci. Pollut. Res. 24 (2017) 13437–13451. https://doi.org/10.1007/s11356-017-8875-y.

[33] H.C. Fidalgo JP, Cid A, Torres E, Sukenik A, Effects of nitrogen source and growth phase on proximate biochemical composition, lipid classes and fatty acid profile of the marine microalga Isochrysis galbana., Aquaculture. 166 (1998) 105–116.

[34] G.A. Dunstan, J.K. Volkman, S.M. Barrett, C.D. Garland, Changes in the lipid composition and maximisation of the

polyunsaturated fatty acid content of three microalgae grown in mass culture, J. Appl. Phycol. 5 (1993) 71–83. https://doi.org/10.1007/BF02182424.

[35] M.P. Mansour, J.K. Volkman, S.I. Blackburn, The effect of growth phase on the lipid class, fatty acid and sterol composition in the marine dinoflagellate, Gymnodinium sp. in batch culture, Phytochemistry. 63 (2003) 145–153. https://doi.org/10.1016/S0031-9422(03)00052-9.

[36] R. Huerlimann, R. de Nys, K. Heimann, Growth, lipid content, productivity, and fatty acid composition of tropical microalgae for scale-up production, Biotechnol. Bioeng. 107 (2010) 245–257. https://doi.org/10.1002/bit.22809.

[37] S.K. Sinha, A. Gupta, R. Bharalee, Production of biodiesel from freshwater microalgae and evaluation of fuel properties based on fatty acid methyl ester profile, Biofuels. 7 (2016) 105–121. https://doi.org/10.1080/17597269.2015.1118781.

[38] C.D. Calixto, J.K. da Silva Santana, V.P. Tibúrcio, L. de F.B.L. de Pontes, C.F. da Costa Sassi, M.M. da Conceição, R. Sassi, Productivity and fuel quality parameters of lipids obtained from 12 species of microalgae from the northeastern region of Brazil, Renew. Energy. 115 (2018) 1144–1152. https://doi.org/10.1016/j.renene.2017.09.029.

[39] L. Rodolfi, G.C. Zittelli, N. Bassi, G. Padovani, N. Biondi, G. Bonini, M.R. Tredici, Microalgae for oil: Strain selection, induction of lipid synthesis and outdoor mass cultivation in a low-cost photobioreactor, Biotechnol. Bioeng. 102 (2009) 100–112. https://doi.org/10.1002/bit.22033.

[40] M. Cooney, G. Young, N. Nagle, Extraction of bio-oils from microalgae, Sep. Purif. Rev. 38 (2009) 291–325. https://doi.org/10.1080/15422110903327919.

[41] E. Martinez-Guerra, V.G. Gude, A. Mondala, W. Holmes, R. Hernandez, Microwave and ultrasound enhanced extractive-transesterification of algal lipids, Appl. Energy. 129 (2014) 354–363. https://doi.org/10.1016/j.apenergy.2014.04.112.

[42] E. Bligh, W. Dyer, A rapid method of total lipid extraction and purification, Can. J. Biochem. Physiol. 37 (1959) 911–917.

[43] J. Folch, M. Lees, G.H.S. Stanley, A simple method for the isolation and purification of total lipids from animal tissues, J Biol Chem. 226 (1957) 497–509. https://doi.org/10.1007/s10858-011-9570-9.

[44] K.S. Suslick, The Chemical Effects of Ultrasound, Sci. Am. 260 (1989) 80–86. https://doi.org/10.1038/scientificamerican0289-80.

[45] A. Ranjan, C. Patil, V.S. Moholkar, Mechanistic assessment of microalgal lipid extraction, Ind. Eng. Chem. Res. 49 (2010) 2979–2985. https://doi.org/10.1021/ie9016557.

[46] S.D. Ríos, J. Castañeda, C. Torras, X. Farriol, J. Salvadó, Lipid extraction methods from microalgal biomass harvested by two different paths: Screening studies toward biodiesel production, Bioresour. Technol. 133 (2013) 378–388. https://doi.org/10.1016/j.biortech.2013.01.093.

[47] M. Mubarak, A. Shaija, T.V. Suchithra, A review on the extraction of lipid from microalgae for biodiesel production, Algal Res. 7 (2015) 117–123. https://doi.org/10.1016/j.algal.2014.10.008.

[48] S. Saka, D. Kusdiana, Biodiesel fuel from rapeseed oil as prepared in supercritical methanol, Fuel. 80 (2001) 225–231. https://doi.org/10.1016/S0016-2361(00)00083-1.

[49] C.H. Cheng, T.B. Du, H.C. Pi, S.M. Jang, Y.H. Lin, H.T. Lee, Comparative study of lipid extraction from microalgae by organic solvent and supercritical CO2, Bioresour. Technol. 102 (2011) 10151–10153.

[50] R. Halim, B. Gladman, M.K. Danquah, P.A. Webley, Oil extraction from microalgae for biodiesel production, Bioresour. Technol. 102 (2011) 178–185. https://doi.org/10.1016/j.biortech.2010.06.136.

[51] P.D. Patil, V.G. Gude, A. Mannarswamy, P. Cooke, N. Nirmalakhandan, P. Lammers, S. Deng, Comparison of direct transesterification of algal biomass under supercritical methanol and microwave irradiation conditions, Fuel. 97 (2012) 822–831. https://doi.org/10.1016/j.fuel.2012.02.037.

[52] H. Zhao, G.A. Baker, Ionic liquids and deep eutectic solvents for biodiesel synthesis: A review, J. Chem. Technol. Biotechnol. 88 (2013) 3–12. https://doi.org/10.1002/jctb.3935.

[53] W.M.A. Wan Mahmood, C. Theodoropoulos, M. Gonzalez-Miquel, Enhanced microalgal lipid extraction using bio-based solvents for sustainable biofuel production, Green Chem. 19 (2017) 5723–5733. https://doi.org/10.1039/c7gc02735d.

[54] H.Y. Yang, W.J. Lu, Y.C. Chen, K.T. Chen, J.C. Teng, H.P. Wan, New algal lipid extraction procedure using an amphiphilic amine solvent and ionic liquid, Biomass and Bioenergy. 100 (2017) 108–115.

[55] C. Wu, Y. Xiao, W. Lin, J. Zhu, H. De la Hoz Siegler, M. Zong, J. Rong, Surfactants assist in lipid extraction from wet Nannochloropsis sp, Bioresour. Technol. 243 (2017) 793–799. https://doi.org/10.1016/j.biortech.2017.07.010.

[56] M.B. Johnson, Z. Wen, Production of biodiesel fuel from the microalga schizochytrium limacinum by direct transesterification of algal biomass, Energy and Fuels. 23 (2009) 5179–5183. https://doi.org/10.1021/ef900704h.

[57] C.Z. Liu, S. Zheng, L. Xu, F. Wang, C. Guo, Algal oil extraction from wet biomass of Botryococcus braunii by 1,2-dimethoxyethane, Appl. Energy. 102 (2013) 971–974. https://doi.org/10.1016/j.apenergy.2012.08.016.

[58] L. Lardon, A. Helias, B. Sialve, J.-P. Steyer, O. Bernard, Life-Cycle Assessment of Biodiesel Production from Microalgae, Environ. Sci. Technol. 43 (2009) 6475–6481. https://doi.org/10.1021/es900705j.

[59] V. Kumar, M. Muthuraj, B. Palabhanvi, A.K. Ghoshal, D. Das, Evaluation and optimization of two stage sequential in situ transesterification process for fatty acid methyl ester quantification from microalgae, Renew. Energy. 68 (2014) 560–569. https://doi.org/10.1016/j.renene.2014.02.037.

[60] E.A. Ehimen, Z.F. Sun, C.G. Carrington, Variables affecting the in situ transesterification of microalgae lipids, Fuel. 89 (2010) 677–684. https://doi.org/10.1016/j.fuel.2009.10.011.

[61] E.A. Ehimen, Z. Sun, G.C. Carrington, Use of ultrasound and co-solvents to improve the in-situ transesterification of microalgae biomass, in: 1st Asia-Oceania Algae Innov. Summit, 2012: pp. 47–55. https://doi.org/10.1016/j.proenv.2012.05.009.

[62] G. Yoo, W. Park, C. Woong, Y. Choi, J. Yang, Bioresource Technology Direct lipid extraction from wet Chlamydomonas reinhardtii biomass using osmotic shock, Bioresour. Technol. 123 (2012) 717–722.

[63] S.P. Singh, D. Singh, Biodiesel production through the use of different sources and characterization of oils and their esters as the substitute of diesel: A review, Renew. Sustain. Energy Rev. 14 (2010) 200–216. https://doi.org/10.1016/j.rser.2009.07.017.

[64] A. Demirbas, Progress and recent trends in biodiesel fuels, Energy Convers. Manag. 50 (2009) 14–34. https://doi.org/10.1016/j.enconman.2008.09.001.

[65] G. Knothe, Dependence of biodiesel fuel properties on the structure of fatty acid alkyl esters, Fuel Process. Technol. 86 (2005) 1059–1070.

[66] R.D. Lanjekar, D. Deshmukh, A review of the effect of the composition of biodiesel on NOx emission, oxidative stability and cold flow properties, Renew. Sustain. Energy Rev. 54 (2016) 1401–1411. https://doi.org/10.1016/j.rser.2015.10.034.

[67] S. Pinzi, P. Rounce, J.M. Herreros, A. Tsolakis, M.P. Dorado, The effect of biodiesel fatty acid composition on combustion and diesel engine exhaust emissions, Fuel. 104 (2012) 170–182. https://doi.org/10.1016/j.fuel.2012.08.056.

[68] P. Hellier, N. Ladommatos, T. Yusaf, The influence of straight vegetable oil fatty acid composition on compression ignition combustion and emissions, Fuel. 143 (2015) 131–143. https://doi.org/10.1016/j.fuel.2014.11.021.

[69] L. Zhu, C.S. Cheung, Z. Huang, Impact of chemical structure of individual fatty acid esters on combustion and emission characteristics of diesel engine, Energy. 107 (2016) 305–320. https://doi.org/10.1016/j.energy.2016.04.030.

[70] A. Schönborn, N. Ladommatos, J. Williams, R. Allan, J. Rogerson, The influence of molecular structure of fatty acid monoalkyl esters on diesel combustion, Combust. Flame. 156 (2009) 1396–1412.

[71] B. Mohan, W. Yang, K.L. Tay, W. Yu, Experimental study of spray characteristics of biodiesel derived from waste cooking oil, Energy Convers. Manag. 88 (2014) 622–632. https://doi.org/10.1016/j.enconman.2014.09.013.

[72] C. a. W. Allen, K.C. Watts, R.G. Ackman, Predicting the surface tension of biodiesel fuels from their fatty acid composition, J. Am. Oil Chem. Soc. 76 (1999) 317–323. https://doi.org/10.1007/s11746-999-0238-5.

[73] M. Lapuerta, J. Rodríguez-Fernández, O. Armas, Correlation for the estimation of the density of fatty acid esters fuels and its implications. A proposed Biodiesel Cetane Index, Chem. Phys. Lipids. 163 (2010) 720–727. https://doi.org/10.1016/j.chemphyslip.2010.06.004.

[74] L.F. Ramírez-Verduzco, J.E. Rodríguez-Rodríguez, A.D.R. Jaramillo-Jacob, Predicting cetane number, kinematic viscosity, density and higher heating value of biodiesel from its fatty acid methyl ester composition, Fuel. 91 (2012) 102–111. https://doi.org/10.1016/j.fuel.2011.06.070.

[75] I.A. Nascimento, S.S.I. Marques, I.T.D. Cabanelas, S.A. Pereira, J.I. Druzian, C.O. de Souza, D.V. Vich, G.C. de Carvalho, M.A. Nascimento, Screening microalgae strains for biodiesel production: lipid productivity and estimation of fuel quality based on fatty acids profiles as selective criteria, Bioenergy Res. 6 (2013) 1–13. https://doi.org/10.1007/s12155-012-9222-2.

[76] A.F. Talebi, S.K. Mohtashami, M. Tabatabaei, M. Tohidfar, A. Bagheri, M. Zeinalabedini, H. Hadavand Mirzaei, M. Mirzajanzadeh, S. Malekzadeh Shafaroudi, S. Bakhtiari, Fatty acids profiling: A selective criterion for screening microalgae

strains for biodiesel production, Algal Res. 2 (2013) 258–267. https://doi.org/10.1016/j.algal.2013.04.003.

[77] M.A. Islam, M. Magnusson, R.J. Brown, G.A. Ayoko, M.N. Nabi, K. Heimann, Microalgal species selection for biodiesel production based on fuel properties derived from fatty acid profiles, Energies. 6 (2013) 5676–5702. https://doi.org/10.3390/en6115676.

[78] M. El-Sheekh, A.E.F. Abomohra, H. Eladel, M. Battah, S. Mohammed, Screening of different species of Scenedesmus isolated from Egyptian freshwater habitats for biodiesel production, Renew. Energy. 129 (2018) 114–120. https://doi.org/10.1016/j.renene.2018.05.099.

[79] W. Xiong, X. Li, J. Xiang, Q. Wu, High-density fermentation of microalga Chlorella protothecoides in bioreactor for microbio-diesel production, Appl. Microbiol. Biotechnol. 78 (2008) 29–36. https://doi.org/10.1007/s00253-007-1285-1.

[80] S.B. Velasquez-Orta, J.G.M. Lee, A. Harvey, Alkaline in situ transesterification of Chlorella vulgaris, Fuel. 94 (2012) 544–550. https://doi.org/10.1016/j.fuel.2011.11.045.

[81] S. Devi, P. Santhanam, V. Rekha, S. Ananth, B.B. Prasath, R. Nandakumar, S. Jeyanthi, S.D. Kumar, Culture and biofuel producing efficacy of marine microalgae Dunaliella salina and, J. Algal Biomass Util. 3 (2012) 38–44. http://jalgalbiomass.com/paper7vol3no4.pdf.

[82] N. Zhukova, N.A. Aizdaicher, Fatty acid composition of 15 species of marine microalgae, Phytochemistry. 39 (1995) 351–356. https://doi.org/10.1016/0031-9422(94)00913-E.

[83] K. Becker, H.P.S. Makkar, Jatropha curcas: A potential source for tomorrow's oil and biodiesel, Lipid Technol. 20 (2008) 104–107. https://doi.org/10.1002/lite.200800023.

[84] F. Goembira, S. Saka, Advanced supercritical Methyl acetate method for biodiesel production from Pongamia pinnata oil, Renew. Energy. 83 (2015) 1245–1249. https://doi.org/10.1016/j.renene.2015.06.022.

[85] E. Crabbe, C. Nolasco-Hipolito, G. Kobayashi, K. Sonomoto, A. Ishizaki, Biodiesel production from crude palm oil and evaluation of butanol extraction and fuel properties, Process Biochem. 37 (2001) 65–71. https://doi.org/10.1016/S0032-9592(01)00178-9.

[86] N. Saravanan, G. Nagarajan, S. Puhan, Experimental investigation on a DI diesel engine fuelled with Madhuca Indica ester and diesel blend, Biomass and Bioenergy. 34 (2010) 838–843. https://doi.org/10.1016/j.biombioe.2010.01.028.

[87] A.S. Ramadhas, C. Muraleedharan, S. Jayaraj, Performance and emission evaluation of a diesel engine fueled with methyl esters of rubber seed oil, Renew. Energy. 30 (2005) 1789–1800. https://doi.org/10.1016/j.renene.2005.01.009.

[88] J. Xue, T.E. Grift, A.C. Hansen, Effect of biodiesel on engine performances and emissions, Renew. Sustain. Energy Rev. 15 (2011) 1098–1116. https://doi.org/10.1016/j.rser.2010.11.016.

[89] A.M. Ashraful, H.H. Masjuki, M.A. Kalam, I.M. Rizwanul Fattah, S. Imtenan, S.A. Shahir, H.M. Mobarak, Production and comparison of fuel properties, engine performance, and emission characteristics of biodiesel from various non-edible vegetable oils: A review, Energy Convers. Manag. 80 (2014) 202–228. https://doi.org/10.1016/j.enconman.2014.01.037.

[90] M.A. Islam, M.M. Rahman, K. Heimann, M.N. Nabi, Z.D. Ristovski, A. Dowell, G. Thomas, B. Feng, N. Von Alvensleben, R.J. Brown, Combustion analysis of microalgae methyl ester in a common rail direct injection diesel engine, Fuel. 143 (2015) 351–360. https://doi.org/10.1016/j.fuel.2014.11.063.

[91] V. Makarevičienė, S. Lebedevas, P. Rapalis, M. Gumbyte, V. Skorupskaite, J. Žaglinskis, Performance and emission characteristics of diesel fuel containing microalgae oil methyl esters, Fuel. 120 (2014) 233–239. https://doi.org/10.1016/j.fuel.2013.11.049.

[92] Y. Haik, M.Y.E. Selim, T. Abdulrehman, Combustion of algae oil methyl ester in an indirect injection diesel engine, Energy. 36 (2011) 1827–1835.

[93] S.H. Al-lwayzy, T. Yusaf, Diesel engine performance and exhaust gas emissions using Microalgae Chlorella protothecoides biodiesel, Renew. Energy. 101 (2017) 690–701. https://doi.org/10.1016/j.renene.2016.09.035.

[94] P. Nautiyal, K.A. Subramanian, M.G. Dastidar, Production and characterization of biodiesel from algae, Fuel Process. Technol. 120 (2014) 79–88. https://doi.org/10.1016/j.fuproc.2013.12.003.

[95] E. Martinez-Guerra, M.S. Howlader, S. Shields-Menard, W.T. French, V.G. Gude, Optimization of wet microalgal FAME production from Nannochloropsis sp. under the synergistic microwave and ultrasound effect, Int. J. Energy Res. 42 (2018) 1934–1949. https://doi.org/10.1002/er.3989.

[96] R. Sarin, M. Sharma, S. Sinharay, R.K. Malhotra, Jatropha-Palm biodiesel blends: An optimum mix for Asia, Fuel. 86 (2007) 1365–1371. https://doi.org/10.1016/j.fuel.2006.11.040.

[97] P. Benjumea, J. Agudelo, A. Agudelo, Basic properties of palm

oil biodiesel-diesel blends, Fuel. 87 (2008) 2069–2075. https://doi.org/10.1016/j.fuel.2007.11.004.

[98] G. Labeckas, S. Slavinskas, The effect of rapeseed oil methyl ester on direct injection Diesel engine performance and exhaust emissions, Energy Convers. Manag. 47 (2006) 1954–1967. https://doi.org/10.1016/j.enconman.2005.09.003.

[99] J. Jayaprabakar, A. Karthikeyan, Performance and emission characteristics of rice bran and alga biodiesel blends in a CI engine, Mater. Today Proc. 3 (2016) 2468–2474. https://doi.org/10.1016/j.matpr.2016.04.164.

[100] S. Tayari, R. Abedi, A. Rahi, Comparative assessment of engine performance and emissions fueled with three different biodiesel generations, Renew. Energy. 147 (2020) 1058–1069. https://doi.org/10.1016/j.renene.2019.09.068.

[101] J. Jayaraman, K. Alagu, P. Appavu, N. Joy, A. Mariadhas, Impact of Methyl, Ethyl, and Butyl Ester Blends of Freshwater Algae Oil on the Combustion, Performance, and Emissions of a CI Engine, Energy and Fuels. 34 (2020) 9763–9770. https://doi.org/10.1021/acs.energyfuels.0c02058.

[102] P. Nautiyal, K.A. Subramanian, M.G. Dastidar, A. Kumar, Experimental assessment of performance, combustion and emissions of a compression ignition engine fuelled with Spirulina platensis biodiesel, Energy. 193 (2020) 116861. https://doi.org/10.1016/j.energy.2019.116861.

[103] H. Venu, V.D. Raju, L. Subramani, P. Appavu, Experimental assessment on the regulated and unregulated emissions of DI diesel engine fuelled with Chlorella emersonii methyl ester (CEME), Renew. Energy. 151 (2020) 88–102. https://doi.org/10.1016/j.renene.2019.11.010.

[104] U. Rajak, P. Nashine, T.N. Verma, Effect of spirulina microalgae biodiesel enriched with diesel fuel on performance and emission characteristics of CI engine, Fuel. 268 (2020) 117305. https://doi.org/10.1016/j.fuel.2020.117305.

[105] U. Rajak, P. Nashine, T.N. Verma, A. Pugazhendhi, Performance, combustion and emission analysis of microalgae Spirulina in a common rail direct injection diesel engine, Fuel. 255 (2019) 115855. https://doi.org/10.1016/j.fuel.2019.115855.

[106] A.I. El-Seesy, A.M.A. Attia, H.M. El-Batsh, The effect of Aluminum oxide nanoparticles addition with Jojoba methyl ester-diesel fuel blend on a diesel engine performance, combustion and emission characteristics, Fuel. 224 (2018) 147–166. https://doi.org/10.1016/j.fuel.2018.03.076.

[107] P. Appavu, M. Venkata Ramanan, Study of emission

characteristics of a diesel engine using cerium oxide nanoparticle blended pongamia methyl ester, Int. J. Ambient Energy. 41 (2020) 524–527. https://doi.org/10.1080/01430750.2018.1477063.

[108] N. Kumar, H. Raheman, Thermal and environmental performance of CI engine using CeO2 nanoparticles as additive in water–diesel–biodiesel fuel blend, Int. J. Environ. Sci. Technol. (2021). https://doi.org/10.1007/s13762-021-03262-w.

[109] I. Örs, S. Sarıkoç, A.E. Atabani, S. Ünalan, S.O. Akansu, The effects on performance, combustion and emission characteristics of DICI engine fuelled with TiO2 nanoparticles addition in diesel/biodiesel/n-butanol blends, Fuel. 234 (2018) 177–188. https://doi.org/10.1016/j.fuel.2018.07.024.

[110] V. Perumal, M. Ilangkumaran, The influence of copper oxide nano particle added pongamia methyl ester biodiesel on the performance, combustion and emission of a diesel engine, Fuel. 232 (2018) 791–802. https://doi.org/10.1016/j.fuel.2018.04.129.

[111] S. Ge, K. Brindhadevi, C. Xia, A. Salah Khalifa, A. Elfasakhany, Y. Unpaprom, H. Van Doan, Enhancement of the combustion, performance and emission characteristics of spirulina microalgae biodiesel blends using nanoparticles, Fuel. 308 (2022) 121822. https://doi.org/10.1016/j.fuel.2021.121822.

[112] S. Karthikeyan, A. Prathima, Microalgae biofuel with CeO2 nano additives as an eco-friendly fuel for CI engine, Energy Sources, Part A Recover. Util. Environ. Eff. 39 (2017) 1332–1338. https://doi.org/10.1080/15567036.2017.1328002.

[113] S. Karthikeyan, A. Prathima, Environmental effect of CI engine using microalgae methyl ester with doped nano additives, Transp. Res. Part D Transp. Environ. 50 (2017) 385–396. https://doi.org/10.1016/j.trd.2016.11.028.

[114] S. Karthikeyan, T. Dharma Prabhakaran, Emission analysis of Botryococcus braunii algal biofuel using Ni-Doped ZnO nano additives for IC engines, Energy Sources, Part A Recover. Util. Environ. Eff. 40 (2018) 1060–1067. https://doi.org/10.1080/15567036.2018.1468517.

[115] K. Kalaimurugan, S. Karthikeyan, M. Periyasamy, G. Mahendran, T. Dharmaprabhakaran, Performance, emission and combustion characteristics of RuO2 nanoparticles addition with neochloris oleoabundans algae biodiesel on CI engine, Energy Sources, Part A Recover. Util. Environ. Eff. 00 (2019) 1–15. https://doi.org/10.1080/15567036.2019.1694102.

[116] K. Kalaimurugan, S. Karthikeyan, M. Periyasamy, G. Mahendran, T. Dharmaprabhakaran, Experimental studies on the influence of copper oxide nanoparticle on biodiesel-diesel

fuel blend in CI engine, Energy Sources, Part A Recover. Util. Environ. Eff. 00 (2019) 1–16. https://doi.org/10.1080/15567036.2019.1679290.

[117] V. Venkatraman, S. Sugumar, S. Sekar, S. Viswanathan, Environmental effect of CI engine using microalgae biofuel with nano-additives, Energy Sources, Part A Recover. Util. Environ. Eff. 41 (2019) 2429–2438.

[118] P.M. Rastogi, A. Sharma, N. Kumar, Effect of CuO nanoparticles concentration on the performance and emission characteristics of the diesel engine running on jojoba (Simmondsia Chinensis) biodiesel, Fuel. 286 (2021) 119358. https://doi.org/10.1016/j.fuel.2020.119358.

[119] S.S. Kumar, K. Rajan, V. Mohanavel, M. Ravichandran, P. Rajendran, A. Rashedi, A. Sharma, S.A. Khan, A. Afzal, Combustion, performance, and emission behaviors of biodiesel fueled diesel engine with the impact of alumina nanoparticle as an additive, Sustainability. 13 (2021) 12103. https://doi.org/10.3390/su132112103.

[120] J. Arunprasad, R. Thirugnanasambantham, T. Jayakumar, R. Rajesh, S. Sugumar, T. Elango, Experimental investigation of performance and emission characteristics of jojoba biodiesel with La2O3 nanoparticles, Mater. Today Proc. (2021). https://doi.org/10.1016/j.matpr.2021.01.793.

[121] R. Sridhar, V.S. Shaisundaram, S. Baskar, S. Ramasubramanian, G. Sathiskumar, S. Sivabalan, Investigation of grape seed oil biodiesel with cerium oxide nanoparticle in CI engine, Mater. Today Proc. 37 (2020) 1399–1402. https://doi.org/10.1016/j.matpr.2020.06.595.

[122] M.A. Mujtaba, M.A. Kalam, H.H. Masjuki, M. Gul, M.E.M. Soudagar, H.C. Ong, W. Ahmed, A.E. Atabani, L. Razzaq, M. Yusoff, Comparative study of nanoparticles and alcoholic fuel additives-biodiesel-diesel blend for performance and emission improvements, Fuel. 279 (2020) 118434. https://doi.org/10.1016/j.fuel.2020.118434.

[123] Ü. Ağbulut, M. Karagöz, S. Sarıdemir, A. Öztürk, Impact of various metal-oxide based nanoparticles and biodiesel blends on the combustion, performance, emission, vibration and noise characteristics of a CI engine, Fuel. 270 (2020) 117521. https://doi.org/10.1016/j.fuel.2020.117521.

[124] Y. Devarajan, B. Nagappan, G. Subbiah, A comprehensive study on emission and performance characteristics of a diesel engine fueled with nanoparticle-blended biodiesel, Environ. Sci. Pollut. Res. 26 (2019) 10662–10672. https://doi.org/10.1007/s11356-019-04446-1.

[125] M.E.M. Soudagar, N.N. Nik-Ghazali, M.A. Kalam, I.A. Badruddin, N.R. Banapurmath, T.M. Yunus Khan, M.N. Bashir, N. Akram, R. Farade, A. Afzal, The effects of graphene oxide nanoparticle additive stably dispersed in dairy scum oil biodiesel-diesel fuel blend on CI engine: performance, emission and combustion characteristics, Fuel. 257 (2019) 116015. https://doi.org/10.1016/j.fuel.2019.116015.

[126] A. Ranjan, S.S. Dawn, J. Jayaprabakar, N. Nirmala, K. Saikiran, S. Sai Sriram, Experimental investigation on effect of MgO nanoparticles on cold flow properties, performance, emission and combustion characteristics of waste cooking oil biodiesel, Fuel. 220 (2018) 780–791.

[127] S. Mendonca, R. Prabhu, T. Bhat, Influence of Aluminium Oxide Nanoparticles in a Compression Ignition Engine with Simarouba Biodiesel, IOP Conf. Ser. Mater. Sci. Eng. 376 (2018) 012080. https://doi.org/10.1088/1757-899X/376/1/012080.

[128] E. Jiaqiang, Z. Zhang, J. Chen, M.H. Pham, X. Zhao, Q. Peng, B. Zhang, Z. Yin, Performance and emission evaluation of a marine diesel engine fueled by water biodiesel-diesel emulsion blends with a fuel additive of a cerium oxide nanoparticle, Energy Convers. Manag. 169 (2018) 194–205. https://doi.org/10.1016/j.enconman.2018.05.073.

[129] A.I. El-Seesy, H. Hassan, S. Ookawara, Effects of graphene nanoplatelet addition to jatropha Biodiesel–Diesel mixture on the performance and emission characteristics of a diesel engine, Energy. 147 (2018) 1129–1152. https://doi.org/10.1016/j.energy.2018.01.108.

[130] M. Sivakumar, N. Shanmuga Sundaram, R. Ramesh kumar, M.H. Syed Thasthagir, Effect of aluminium oxide nanoparticles blended pongamia methyl ester on performance, combustion and emission characteristics of diesel engine, Renew. Energy. 116 (2018) 518–526. https://doi.org/10.1016/j.renene.2017.10.002.

[131] Y. Devarajan, D.B. Munuswamy, A. Mahalingam, Influence of nano-additive on performance and emission characteristics of a diesel engine running on neat neem oil biodiesel, Environ. Sci. Pollut. Res. 25 (2018) 26167–26172. https://doi.org/10.1007/s11356-018-2618-6.

[132] A. Keskin, A. Yaşar, Ş. Yıldızhan, E. Uludamar, F.M. Emen, N. Külcü, Evaluation of diesel fuel-biodiesel blends with palladium and acetylferrocene based additives in a diesel engine, Fuel. 216 (2018) 349–355. https://doi.org/10.1016/j.fuel.2017.11.154.

[133] M. Mehregan, M. Moghiman, Effects of nano-additives on pollutants emission and engine performance in a urea-SCR

equipped diesel engine fueled with blended-biodiesel, Fuel. 222 (2018) 402–406. https://doi.org/10.1016/j.fuel.2018.02.172.

[134] P. Anchupogu, L.N. Rao, B. Banavathu, Effect of alumina nano additives into biodiesel-diesel blends on the combustion performance and emission characteristics of a diesel engine with exhaust gas recirculation, Environ. Sci. Pollut. Res. 25 (2018) 23294–23306. https://doi.org/10.1007/s11356-018-2366-7.

[135] S.H. Hosseini, A. Taghizadeh-Alisaraei, B. Ghobadian, A. Abbaszadeh-Mayvan, Performance and emission characteristics of a CI engine fuelled with carbon nanotubes and diesel-biodiesel blends, Renew. Energy. 111 (2017) 201–213. https://doi.org/10.1016/j.renene.2017.04.013.

[136] B. Ashok, K. Nanthagopal, R. Subbarao, A. Johny, A. Mohan, A. Tamilarasu, Experimental studies on the effect of metal oxide and antioxidant additives with Calophyllum Inophyllum Methyl ester in compression ignition engine, J. Clean. Prod. 166 (2017) 474–484. https://doi.org/10.1016/j.jclepro.2017.08.050.

[137] H. Raheman, P.C. Jena, S.S. Jadav, Performance of a diesel engine with blends of biodiesel (from a mixture of oils) and high-speed diesel, Int. J. Energy Environ. Eng. 4 (2013) 1–9. https://doi.org/10.1186/2251-6832-4-6.

[138] M. Habibullah, H.H. Masjuki, M.A. Kalam, I.M. Rizwanul Fattah, A.M. Ashraful, H.M. Mobarak, Biodiesel production and performance evaluation of coconut, palm and their combined blend with diesel in a single-cylinder diesel engine, Energy Convers. Manag. 87 (2014) 250–257.

[139] A. Sanjid, H.H. Masjuki, M.A. Kalam, S.M.A. Rahman, M.J. Abedin, S.M. Palash, Production of palm and jatropha based biodiesel and investigation of palm-jatropha combined blend properties, performance, exhaust emission and noise in an unmodified diesel engine, J. Clean. Prod. 65 (2014) 295–303. https://doi.org/10.1016/j.jclepro.2013.09.026.

[140] A. Sanjid, M.A. Kalam, H.H. Masjuki, M. Varman, N.W.B.M. Zulkifli, M.J. Abedin, Performance and emission of multi-cylinder diesel engine using biodiesel blends obtained from mixed inedible feedstocks, J. Clean. Prod. 112 (2016) 4114–4122. https://doi.org/10.1016/j.jclepro.2015.07.154.

[141] A.M. Ruhul, M.A. Kalam, H.H. Masjuki, A. Alabdulkarem, A.E. Atabani, I.M.R. Fattah, M.J. Abedin, Production, characterization, engine performance and emission characteristics of Croton megalocarpus and Ceiba pentandra complementary blends in a single-cylinder diesel engine, RSC Adv. 6 (2016) 24584–24595.

[142] K. Srithar, K. Arun Balasubramanian, V. Pavendan, B. Ashok

Kumar, Experimental investigations on mixing of two biodiesels blended with diesel as alternative fuel for diesel engines, J. King Saud Univ. - Eng. Sci. 29 (2017) 50–56. https://doi.org/10.1016/j.jksues.2014.04.008.

[143] B.R. Hosamani, V. V. Katti, Experimental analysis of combustion characteristics of CI DI VCR engine using mixture of two biodiesel blend with diesel, Eng. Sci. Technol. an Int. J. 21 (2018) 769–777.

[144] K. Khan, G. Kumar, A.K. Sharma, P.S. Kumar, C. Mandal, V. Chintala, Performance and emission characteristics of a diesel engine using complementary blending of castor and karanja biodiesel, Biofuels. 9 (2018) 53–60. https://doi.org/10.1080/17597269.2016.1256552.

[145] V. Sharma, G. Duraisamy, Production and characterization of bio-mix fuel produced from the mixture of raw oil feedstock, and its effects on performance and emission analysis in DICI diesel engine, Environ. Sci. Pollut. Res. 26 (2019) 16742–16761. https://doi.org/10.1007/s11356-019-04958-w.

[146] S. Kumar, S. Jain, H. Kumar, Experimental Study on Biodiesel Production Parameter Optimization of Jatropha-Algae Oil Mixtures and Performance and Emission Analysis of a Diesel Engine Coupled with a Generator Fueled with Diesel/Biodiesel Blends, ACS Omega. 5 (2020) 17033–17041. https://doi.org/10.1021/acsomega.9b04372.

[147] K. Sudalaiyandi, K. Alagar, R. Vignesh Kumar, V. Manoj Praveen, P. Madhu, Performance and emission characteristics of diesel engine fueled with ternary blends of linseed and rubber seed oil biodiesel, Fuel. 285 (2021) 119255. https://doi.org/10.1016/j.fuel.2020.119255.

[148] S. Swarna, M.T. Swamy, T.R. Divakara, K.N. Krishnamurthy, S. Shashidhar, Experimental assessment of ternary fuel blends of diesel, hybrid biodiesel and alcohol in naturally aspirated CI engine, Int. J. Environ. Sci. Technol. (2021). https://doi.org/10.1007/s13762-021-03586-7.

[149] G. Tüccar, K. Aydın, Evaluation of methyl ester of microalgae oil as fuel in a diesel engine, Fuel. 112 (2013) 203–207. https://doi.org/10.1016/j.fuel.2013.05.016.

[150] J.S. Patel, N. Kumar, A. Deep, A. Sharma, D. Gupta, Evaluation of Emission Characteristics of Blend of Algae Oil Methyl Ester with Diesel in a Medium Capacity Diesel Engine, SAE Tech. Pap. (2014). https://doi.org/10.4271/2014-01-1378.Copyright.

[151] S. Mishra, K. Anand, P.S. Mehta, Predicting the Cetane Number of Biodiesel Fuels from Their Fatty Acid Methyl Ester Composition, Energy and Fuels. 30 (2016) 10425–10434.

https://doi.org/10.1021/acs.energyfuels.6b01343.

[152] M.J. Ramos, C.M. Fernández, A. Casas, L. Rodríguez, Á. Pérez, Influence of fatty acid composition of raw materials on biodiesel properties, Bioresour. Technol. 100 (2009) 261–268. https://doi.org/10.1016/j.biortech.2008.06.039.

[153] J.Y. Park, D.K. Kim, J.P. Lee, S.C. Park, Y.J. Kim, J.S. Lee, Blending effects of biodiesels on oxidation stability and low temperature flow properties, Bioresour. Technol. 99 (2008) 1196–1203. https://doi.org/10.1016/j.biortech.2007.02.017.

[154] W. Yuan, A.C. Hansen, Q. Zhang, Predicting the physical properties of biodiesel for combustion modeling, Trans. Am. Soc. Agric. Eng. 46 (2003) 1487–1493. https://doi.org/10.13031/2013.15631.

[155] K. Anand, R.P. Sharma, P.S. Mehta, A comprehensive approach for estimating thermo-physical properties of biodiesel fuels, Appl. Therm. Eng. 31 (2011) 235–242. https://doi.org/10.1016/j.applthermaleng.2010.09.003.

[156] H.M. Ismail, H.K. Ng, X. Cheng, S. Gan, T. Lucchini, G. D'Errico, Development of thermophysical and transport properties for the CFD simulations of in-cylinder biodiesel spray combustion, Energy and Fuels. 26 (2012) 4857–4870. https://doi.org/10.1021/ef300862u.

[157] S.K. Mishra, W.I. Suh, W. Farooq, M. Moon, A. Shrivastav, M.S. Park, J.W. Yang, Rapid quantification of microalgal lipids in aqueous medium by a simple colorimetric method, Bioresour. Technol. 155 (2014) 330–333.

[158] M.M.A. Shirazi, A. Kargari, M. Tabatabaei, B. Mostafaeid, M. Akia, M. Barkhi, M.J.A. Shirazi, Acceleration of biodiesel-glycerol decantation through NaCl-assisted gravitational settling: A strategy to economize biodiesel production, Bioresour. Technol. 134 (2013) 401–406. https://doi.org/10.1016/j.biortech.2013.02.026.

[159] K. Krisnangkura, A simple method for estimation of cetane index of vegetable oil methyl esters, J. Am. Oil Chem. Soc. 63 (1986) 552–553. https://doi.org/10.1007/BF02645752.

[160] B. Mareschal, Y. De Smet, Visual PROMETHEE: Developments of the PROMETHEE & GAIA multicriteria decision aid methods, IEEM 2009 - IEEE Int. Conf. Ind. Eng. Eng. Manag. (2009) 1646–1649.

[161] R.C. Reid, T.K. Sherwood, R.E. Street, The properties of gases and liquids, 4th ed., McGraw-Hill, New York, 1959. https://doi.org/10.1063/1.3060771.

[162] M.S. Graboski, R.L. McCormick, Combustion of fat and vegetable oil derived fuels in diesel engines, Prog. Energy Combust. Sci. 24 (1998) 125–164. https://doi.org/10.1016/S0360-1285(97)00034-8.

[163] M.J. Pratas, S. Freitas, M.B. Oliveira, S.C. Monteiro, A.S. Lima, J. Ao, A.P. Coutinho, Densities and Viscosities of Minority Fatty Acid Methyl and Ethyl Esters Present in Biodiesel, J. Chem. Eng. Data. 56 (2011) 2175–2180. https://doi.org/10.1021/je1012235.

[164] M.J. Pratas, S. Freitas, M.B. Oliveira, S.C. Monteiro, A.S. Lima, J.A.P. Coutinho, Densities and Viscosities of Fatty Acid Methyl and Ethyl Esters, J. Chem. Eng. Data. 55 (2010) 3983–3990. https://doi.org/10.1021/je100042c.

[165] Y. Ra, R.D. Reitz, J. McFarlane, C.S. Daw, Effects of fuel physical properties on diesel engine combustion using diesel and bio-diesel fuels, SAE Int. J. Fuels Lubr. 1 (2009) 703–718. https://doi.org/10.4271/2008-01-1379.

[166] V. Anand, M. Kashyap, K. Samadhiya, A. Ghosh, B. Kiran, Salinity driven stress to enhance lipid production in Scenedesmus vacuolatus: A biodiesel trigger?, Biomass and Bioenergy. 127 (2019) 105252.

[167] C. Hu, M. Li, J. Li, Q. Zhu, Z. Liu, Variation of lipid and fatty acid compositions of the marine microalga Pavlova viridis (Prymnesiophyceae) under laboratory and outdoor culture conditions, World J. Microbiol. Biotechnol. 24 (2008) 1209–1214. https://doi.org/10.1007/s11274-007-9595-0.

[168] M. Olofsson, T. Lamela, E. Nilsson, J.P. Bergé, V. del Pino, P. Uronen, C. Legrand, Seasonal variation of lipids and fatty acids of the microalgae Nannochloropsis oculata grown in outdoor large-scale photobioreactors, Energies. 5 (2012) 1577–1592. https://doi.org/10.3390/en5051577.

[169] J. P. Holman, Experimental Methods for Engineers, 8th ed., 2011.

[170] A. Dhar, A.K. Agarwal, Performance, emissions and combustion characteristics of Karanja biodiesel in a transportation engine, Fuel. 119 (2014) 70–80. https://doi.org/10.1016/j.fuel.2013.11.002.

[171] A.N. Ozsezen, M. Canakci, C. Sayin, Effects of biodiesel from used frying palm oil on the exhaust emissions of an indirect injection (IDI) diesel engine, Energy and Fuels. 22 (2008) 2796–2804. https://doi.org/10.1021/ef800174p.

[172] A.N. Ozsezen, M. Canakci, C. Sayin, Effects of biodiesel from used frying palm oil on the performance, injection, and

combustion characteristics of an indirect injection diesel engine, Energy and Fuels. 22 (2008) 1297–1305. https://doi.org/10.1021/ef700447z.

[173] K. Ryu, Effect of antioxidants on the oxidative stability and combustion characteristics of biodiesel fuels in an indirect-injection (IDI) diesel engine, J. Mech. Sci. Technol. 23 (2009) 3105–3113. https://doi.org/10.1007/s12206-009-0902-6.

[174] V. Soloiu, J. Weaver, H. Ochieng, B. Vlcek, C. Butts, M. Jansons, Evaluation of peanut fatty acid methyl ester sprays, combustion, and emissions, for use in an indirect injection diesel engine, Energy and Fuels. 27 (2013) 2608–2618. https://doi.org/10.1021/ef302069d.

[175] F. Wu, J. Wang, W. Chen, S. Shuai, A study on emission performance of a diesel engine fueled with five typical methyl ester biodiesels, Atmos. Environ. 43 (2009) 1481–1485. https://doi.org/10.1016/j.atmosenv.2008.12.007.

[176] M. Vinayagam, S.S. Kumar, M.M. Ravikumar, S. Mahendiran, T. Raja, Feasibility and emission study on employing MgO nanoparticle as oxygenated additive in neat biodiesel, Int. J. Ambient Energy. 0 (2019) 1–6. https://doi.org/10.1080/01430750.2019.1611659.

[177] M. Karthick, S. Ganesan, T. Raja, Study on emission characteristics of a methanol–biodiesel blends fuelled diesel engine, Int. J. Ambient Energy. 42 (2021) 314–318. https://doi.org/10.1080/01430750.2018.1550014.

[178] A. Anbarasu, A. Karthikeyan, M. Balaji, Performance and Emission Characteristics of Diesel Engine Using Alumina Nanoparticle Blended Biodiesel Emulsion Fuel, J. Energy Resour. Technol. 138 (2015) 022203. https://doi.org/10.1115/1.4031834.

[179] Ş. Altun, C. Öner, Gaseous emission comparison of a compression-ignition engine fueled with different biodiesels, Int. J. Environ. Sci. Technol. 10 (2013) 371–376. https://doi.org/10.1007/s13762-012-0142-7.

[180] P. Purushothaman, V. Gnanamoorthi, A. Gurusamy, Performance combustion and emission characteristics of novel biofuel peppermint oil in diesel engine, Int. J. Environ. Sci. Technol. 16 (2019) 8547–8556. https://doi.org/10.1007/s13762-019-02270-1.

[181] A. Uyaroğlu, A. Uyumaz, İ. Çelikten, Comparison of the combustion, performance, and emission characteristics of inedible Crambe abyssinica biodiesel and edible hazelnut, corn, soybean, sunflower, and canola biodiesels, Environ. Prog. Sustain. Energy. 37 (2018) 1438–1447.

https://doi.org/10.1002/ep.12794.

[182] D. Singh, A. Deep, S.S. Sandhu, A.K. Sarma, Experimental Assessment of Combustion, Performance and Emission Characteristics of a CI Engine Fueled with Biodiesel and Hybrid Fuel Derived from Waste Cooking Oil, Environ. Prog. Sustain. Energy. 38 (2019). https://doi.org/10.1002/ep.13112.

[183] J. Huang, Y. Wang, J. Qin, A.P. Roskilly, Comparative study of performance and emissions of a diesel engine using Chinese pistache and jatropha biodiesel, Fuel Process. Technol. 91 (2010)1761–1767. https://doi.org/10.1016/j.fuproc.2010.07.017.

[184] C. Boubahri, E. Ridha, S. Rachid, B. Jamel, Experimental study of a diesel engine performance running on waste vegetable oil biodiesel blend, J. Energy Resour. Technol. Trans. ASME. 134 (2012) 1–6. https://doi.org/10.1115/1.4006655.

[185] T. Daho, G. Vaitilingom, S.K. Ouiminga, B. Piriou, A.S. Zongo, S. Ouoba, J. Koulidiati, Influence of engine load and fuel droplet size on performance of a CI engine fueled with cottonseed oil and its blends with diesel fuel, Appl. Energy. 111 (2013) 1046–1053.

[186] H. Mohamed Ismail, H.K. Ng, S. Gan, T. Lucchini, Computational study of biodiesel-diesel fuel blends on emission characteristics for a light-duty diesel engine using OpenFOAM, Appl. Energy. 111 (2013) 827–841.

[187] M. Salamanca, F. Mondragón, J.R. Agudelo, P. Benjumea, A. Santamaría, Variations in the chemical composition and morphology of soot induced by the unsaturation degree of biodiesel and a biodiesel blend, Combust. Flame. 159 (2012) 1100–1108.
https://doi.org/10.1016/j.combustflame.2011.10.011.

[188] S. Deshmukh, R. Kumar, K. Bala, Microalgae biodiesel: A review on oil extraction, fatty acid composition, properties and effect on engine performance and emissions, Fuel Process. Technol. 191 (2019) 232–247.

[189] B. Sajjadi, A.A.A. Raman, H. Arandiyan, A comprehensive review on properties of edible and non-edible vegetable oil-based biodiesel: Composition, specifications and prediction models, Renew. Sustain. Energy Rev. 63 (2016) 62–92. https://doi.org/10.1016/j.rser.2016.05.035.

[190] A.A. Refaat, Correlation between the chemical structure of biodiesel and its physical properties, Int. J. Environ. Sci. Technol. 6 (2009) 677–694.

[191] G.R. Stansell, V.M. Gray, S.D. Sym, Microalgal fatty acid composition: Implications for biodiesel quality, J. Appl. Phycol.

24 (2012) 791–801. https://doi.org/10.1007/s10811-011-9696-x.

[192] E. Jiaqiang, L. Teng, W.M. Yang, J. Li, J. Gong, Y. Deng, Effects of fatty acid methyl esters proportion on combustion and emission characteristics of a biodiesel fueled diesel engine, Energy Convers. Manag. 117 (2016) 410–419. https://doi.org/10.1016/j.enconman.2016.03.021.

[193] A.K. Agarwal, D. Khurana, Long-term storage oxidation stability of Karanja biodiesel with the use of antioxidants, Fuel Process. Technol. 106 (2013) 447–452. https://doi.org/10.1016/j.fuproc.2012.09.011.

[194] S.K. Hoekman, A. Broch, C. Robbins, E. Ceniceros, M. Natarajan, Review of biodiesel composition, properties, and specifications, Renew. Sustain. Energy Rev. 16 (2012) 143–169. https://doi.org/10.1016/j.rser.2011.07.143.

[195] E.G. Giakoumis, A statistical investigation of biodiesel physical and chemical properties, and their correlation with the degree of unsaturation, Renew. Energy. 50 (2013) 858–878. https://doi.org/10.1016/j.renene.2012.07.040.